Functional analysis of the mouse histamine H_4 receptor in myeloid cells

Dissertation

zur Erlangung des Doktorgrades der Naturwissenschaften

- Dr. rer. nat. -

an der Fakultät für Chemie und Pharmazie

der Universität Regensburg

vorgelegt von

Louay Jouma aus Damaskus, Syrien

2009

Die vorliegende Arbeit entstand im Zeitraum von Oktober 2006 bis Oktober 2009 am Institut für Immunologie des Klinikums der Universität Regensburg unter der Anleitung von Prof. Dr. Daniela Männel und Prof. Dr. Roland Seifert.

Promotionsgesuch eingereicht am:

11.08.2009

Tag des Kolloquiums:

02.10.2009

Prüfungsausschuss:

Prof. Dr. Prof. Dr. Sigurd Elz	(Vorsitz)
Prof. Dr. Roland Seifert	(Erstgutachter)
Prof. Dr. Daniela N. Männel	(Zweitgutachter)
Prof. Dr. Jens Schlossmann	(Drittprüfer)

Erklärung

Hiermit versichere ich, dass ich die vorliegende Arbeit selbständig angefertigt und keine anderen als die hier angegebenen Quellen und Hilfsmittel verwendet habe.

.....

Louay Jouma

To my mother and father

who I am today is because of them

The whole of science is nothing more than a refinement of everyday thinking."

Albert Einstein (1879 – 1955)

Acknowledgements

First of all I would like to express my sincere gratitude to my advisor Prof. Dr. Daniela Männel for her guidance, patience and immense knowledge. Her support and valuable advice helped me in all the time of my work as well as during writing of this thesis.

I owe my deepest gratitude to Prof. Dr. Roland Seifert for introducing me to this field of research, and for his continuous advices and support during my Ph.D study and research.

Beside my supervisors, my sincere thanks go to:

Graduiertenkolleg 760 and Deutsche Forschungsgemeinschaft (DFG) for the financial and scientific support,

Prof. Dr. Jens Schlossman for his insightful comments, and hard questions during my seminars,

PD. Dr. Uwe Ritter for his helpful scientific ideas and constructive comments during my work,

Prof. Dr. Thomas Hehlgans, Dr. Bernd Echtenacher, Dr. Anja Lechner, and Dr. Anja Wege, for their stimulating discussions which widened my knowledge in the field of immunology,

Prof. Dr. Werner Falk for providing the chemotaxis chambers and his help in establishing the assay, and for Susanne Brüggemann who counted some of the chemotaxis assays in a blind fashion,

Dr. Barbara Daller and Karin Holz for their numerous help and daily atmosphere, without which my work would have been more difficult,

Sabine Laberer for helping me genotyping the mice and Catherine Botteron for her help with the cell sorter, and to the other hardworking technicians Veronika Hochleitner and Dorothea Weber-Steffens,

All my colleagues in the institute of immunology and in the Department of Pharmacology and Toxicology, especially Christian Florian, Johannes Polz, David Schnell and Dr. Erich Schneider, Dr. Michaela Windbichler, and Dr. Alex Sigrüner with all of them I have shared the good and the bad moments of my work,

Last but not least I would like to thank the most important persons in my life my parents, brother and sister for their unlimited spiritual and financial support in all the stages of my life, as well as the beauty of my life Laura.

شُكراً

Contents

Abbreviations

4MEH	**4-methylhistamine**
ANOVA	**Analysis of variance**
AP	**Alkaline phosphatase**
APC	**Allophycocyanin / antigen-presenting cells**
BMDC	**Bone marrow-derived dendritic cells**
BMDM	**Bone marrow-derived macrophages**
BSA	**Bovine serum albumin**
cAMP	**Cyclic adenosine monophosphate**
CD	**Cluster of differentiation**
cDNA	**Complementary deoxyribonucleic acid**
CFSE	**Carboxyfluorescein succinimidyl ester**
CNS	**Central nervous system**
CFA	**Complete Freund's adjuvant**
CpG	**Cytosine-phosphate-guanine**
C_t	**Threshold cycle**
DAO	**Diamine oxidase**
DC	**Dendritic cells**
DMSO	**Dimethyl sulfoxide**
DNA	**Deoxyribonucleic acid**
dNTP	**Deoxyribonucleotide triphosphate**
E. coli	**Escherichia coli**
ECD	**Extracellular domain**
EDTA	**Ethylenediaminetetraacetic acid**

ELISA	**Enzyme-linked immunosorbent assay**
ERK	**Extracellular-signal-regulated kinase**
FACS	**Fluorescent-activated cell sorting**
FCS	**Fetal calf serum**
FcγR	**Fragment crystallizable gamma receptor**
FITC	**Fluorescein isothiocyanate**
fMLP	**N-Formyl-methionyl-leucyl-phenylalanine**
GAPDH	**Glyceraldehyde 3-phosphate dehydrogenase**
GM-CFU	**Granulocyte/macrophage colony-forming units**
GM-CSF	**Granulocytes monocytes colony stimulating factor**
GPCR	**G-protein-coupled receptor**
h	**Hour**
$H_4R^{-/-}$	**Histamine H_4 receptor knock-out**
$H_4R^{-/-}$ BMDM	**Bone marrow-derived macrophages from $H_4R^{-/-}$ mice**
HDC	**L-histidine decarboxylase**
Histamine receptor	**HR**
HNMT	**Histamine-N-methyltransferase**
HRP	**Horse Radish Peroxidase**
IFN	**Interferon**
IgE	**Immunoglobulin E**
IgG	**Immunogobulin G**

IgM	**Immunogobulin M**
IL-6	**Interleukin-6**
IFA	**Incomplete Freund's adjuvant**
IP	**Intra-peritoneal**
KLH	**Keyhole Limpet Hemocyanin**
L. major	**Leishmania major**
LPS	**Lipopolysaccharide**
MAPK	**Mitogen-activated protein kinase**
MCP1	**Monocyte chemoattractant protein 1 or CCL2**
M-CSF	**Macrophages colony stimulating factor**
MFI (arbitrary unit)	**Mean fluorescence intensity**
mH_1R	**Mouse histamie H_1 receptor**
mH_2R	**Mouse histamie H_2 receptor**
mH_3R	**Mouse histamie H_3 receptor**
mH_4R	**Mouse histamie H_4 receptor**
MHC II	**Major histocompatibility class 2**
M-MLV RT	**Moloney murine leukemia virus reverse transcriptase**
mRNA	**Messenger ribonucleic acid**
MyD88	**Molecule myeloid differentiation primary-response gene 88**
NFκB	**Nuclear factor kappa-light-chain-enhancer of activated B cells**
NK	**Natural killer**

NO	**Nitric oxide**
NOD	**Nucleotide oligomerization domain**
O.D.	**Optical density**
Oligo dT	**Oligomere desoxy-Thymidin**
SDS-PAGE	**Polyacrylamide gel electrophoresis-sodium dodecyl sulfate**
PAMP	**Pathogen associated molecular pattern**
PBS	**Phosphate buffered saline**
PCR	**Polymerase chain reaction**
PE	**Phycoerythrin**
PEC	**Peritoneal exudate cells**
PI3K	**Phosphatidylinositol-3-OH kinase**
PTEN	**Phosphatase and tensin homolog**
PVP	**Polyvinylpirrolidone**
RNA	**Ribonucleic acid**
RPMI	**Roswell park memorial institute**
RT	**Room temperature**
RT-PCR	**Reverse transcription polymerase chain reaction**
SD	**Standard deviation**
TAE	**Tris-acetate-EDTA**
Taq polymerase	**Thermus aquaticus polymerase**
TBS	**Tris Buffered Saline**
TGF-β	**Transforming growth factor-beta**
T_H	**T-Helper cells**

T_H1	**T-helper 1**
T_H2	**T-helper 2**
TLR	**Toll-like receptor**
TNBS	**Trinitrobenzene sulphonic acid**
TNF	**Tumor necrosis factor**
UV	**Ultraviolet**
WT	**Wild-type**
WT-BMDM	**Bone marrow-derived macrophages from WT mice**

1. Introduction

1.1 Histamine

Histamine is a low molecular mass biogenic amine found in many animal tissues with a wide spectrum of physiological as well as pathological effects. Its effect is mediated by four receptors variably expressed in various tissues with different functions. This made histamine one of the most intensively studied molecules in medicine [1].

1.1.1. History

Almost a hundred years ago histamine or 2-(1-h-imidazo-4-lyl)ethylamine was discovered by Sir Dale from the mould ergot, which was later characterized as a smooth muscle stimulator in gut and respiratory tract, as well as vasodepressor. Histamine was then isolated from liver and lung, and was found to be a natural constituent of the body with a physiological role. Further investigation reported that histamine injection in animals leads to a shock-like syndrome which identified histamine as a mediator of anaphylactic reactions in 1932 [2;3].

1.1.2. Histamine synthesis and storage

Histamine is synthesized from the amino acid L-histidine by L-histidine decarboxylase (HDC). Histamine production was detected in various cells like central nervous system (CNS) neurons and gastric mucosa parietal cells, but the main sources of histamine are the immune cells including eosinophils, basophils, and mast cells. In these cells histamine is stored intracellularly in vesicles and released upon stimulation. Remarkably, other immune cells also show high HDC activity and are capable to produce large amounts of histamine. These cells include monocytes/macrophages, dendritic cells (DC), neutrophils and T and B cells [4;5].

These cells do not store histamine, and therefore, it is released as soon as it is synthesized [6]. HDC activity is easily modulated both *in vitro*, in response to cytokines such as IL-3, GM-CSF, IL-1, IL-18, IL-12, M-CSF and TNF, and *in vivo*, during allograft rejection, infection, inflammation and stimulation with LPS.

1.1.3. Histamine metabolism

Histamine can be metabolized by two pathways: oxidation or methylation. The oxidation pathway by diamine oxidase (DAO) is mainly responsible for extracellular histamine degradation. This includes histamine released upon stimulation and histamine-rich food ingestion [7;8], because DAO is stored in plasma membrane–associated vesicular structures in epithelial cells. Conversely, the histamine methylation pathway by histamine-N-methyltransferase (HNMT) is capable of degrading histamine only in the intracellular space of cells, because of the cytosolic localization of HMNT [9]. HNMT is considered the key enzyme for histamine degradation in the bronchial epithelium as well as some other tissues, based on its wide expression in human tissues [10;11]. In contrast, DAO expression is restricted to specific tissues like small bowel, colon ascendens, placenta and kidney [12].

1.1.4. Histamine receptors

Four histamine receptors (HRs) that belong to the G-protein-coupled receptor (GPCR) family mediate the wide variety of histamine effects.

The histamine H_1 receptor (H_1R) is responsible for most of the acute allergic responses. Based on that, several drugs were designed to antagonize the histamine effect, and the term “anti-histamines” was used to describe the anti-H_1R effect. Among a long list of H_1R antagonists, diphenhydramine and cetirizine as H_1R inverse agonists are effective in the allergic inflammatory treatment.

The histamine H_2 receptor (H_2R) is mainly known for its role as a modulator of gastric acid secretion, and its antagonists such as famotidine and ranitidine are successfully used for the treatment of peptic ulcer, and gastroesophageal reflux disease.

The histamine H_3 receptor (H_3R) is highly expressed in the nervous system and modulates the neurotransmitter levels. Antagonists for H_3R are still under development, where its potential use is in sleep and cognition disorder treatment.

In contrast to H_1R and H_2R, H_4R has a more selective expression pattern, being expressed mainly in cells of haematopoietic origin, in particular DC, mast cells, eosinophils, monocytes, basophils and T cells, giving rise to an immune modulatory role. H_4R is encoded by a gene containing three exons separated by two large introns. The sequence homology between human and mouse receptor is 68% with 390 and 391 amino acids, respectively. A considerable sequence homology is also observed in different species between H_4R and H_3R which is 34-35%. Therefore, many H_3R ligands like clobenpropit and thioperamide bind to H_4R as an agonist and antagonist, respectively [13-16]. The affinity of histamine binding to different HRs varies significantly, with K_i values ranging from 5-10 nM for H_3R and H_4R, to 2-10 µM for H_1R and H_2R [17;18]. 4-Methyl histamine (4MEH) was considered as a human H_2R agonist, but the discovery of H_4R revealed that it possesses a 100-fold higher selectivity for human H_4R than human H_2R. Some other data show similar results for the mouse H_4R *in vitro* as well as *in vivo* [19;20]. In 2004 Thurmond *et al.* reported the first H_4R selective antagonist with anti-inflammatory effect, 1-(5-chloro-1*H*-indol-2-yl)carbonyl-4-methylpiperazine or JNJ 7777120. JNJ 7777120 was repeatedly used since then by several groups to antagonize H_4R in human, mouse and rats [18;21-23]. Therefore, 4MEH and JNJ 7777120 were used in the following experiments as selective agonist and antagonist in mouse cells. Recently, and based on the frequent reports about the immunological role of H_4R, an increasing number of reports appeared with the focus on the specific effect of H_4R on the immune system. This was associated with numerous agonists and antagonists designed by several research groups and pharmaceutical companies [24-32].

1.1.4.1. Histamine receptor-mediated signalling

HRs are coupled to different Gα subunits as intracellular mediators. Histamine binding to H_1R generates an intracellular signal through $G\alpha_q$, which leads to allergy symptoms in the skin, nose and airway. This is associated with phospholipase C activation, inositol phosphate production and Ca^{2+} influx as well as activation of the transcription factor $NF_\kappa B$. H_2R signaling leads to $G\alpha_s$ activation, which activates

adenylate cyclase and increases the intracellular cAMP levels. H_3R and H_4R signals are mediated by $G\alpha_{i/o}$ proteins, leading to activation of mitogen-activated protein kinases (MAPKs) and inhibition of cAMP formation, as well as modulation of ion channels and increases Ca^{2+} influx. In addition H_4R activation also leads to activation of the transcription factor AP-1 [1;33;34].

1.1.4.2. Histamine receptors constitutive activity

The expression of GPCR in a recombinant system revealed a constitutive spontaneous receptor activity, which occurred in the absence of an agonist. This basal activity can be modulated upon binding of an agonist or an inverse agonist to the receptor. The two state model hypothesis assumes that GPCR isomerize from an inactive (R) state to an active (R*) state [35]. Agonist binding to the receptor increases the basal activity and maximally stabilizes the R* state which can couple to, and activate, G-proteins, by promoting the GDP/GTP exchange at G-proteins. Conversely, binding of an inverse agonist to the receptor decreases the basal activity and maximally stabilizes the R state, where GPCR are uncoupled from G-proteins. Antagonists can bind to both states with the same affinity without altering the equilibrium between R and R* or the basal activity, but they block both the inhibitory effects of inverse agonists and the stimulatory effects of agonists (Fig. 1.1) [21;35;36].

Like other GPCR, constitutive activity has been observed in all human histamine receptors [21;28;37-39]. This phenomenon is most commonly seen in systems with a high expression level of the receptor [40-42].

A

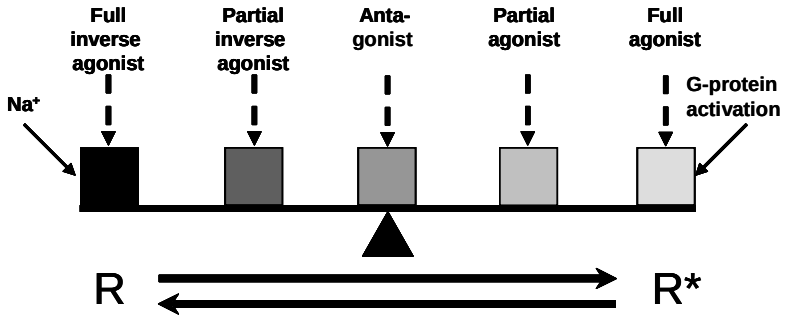

B

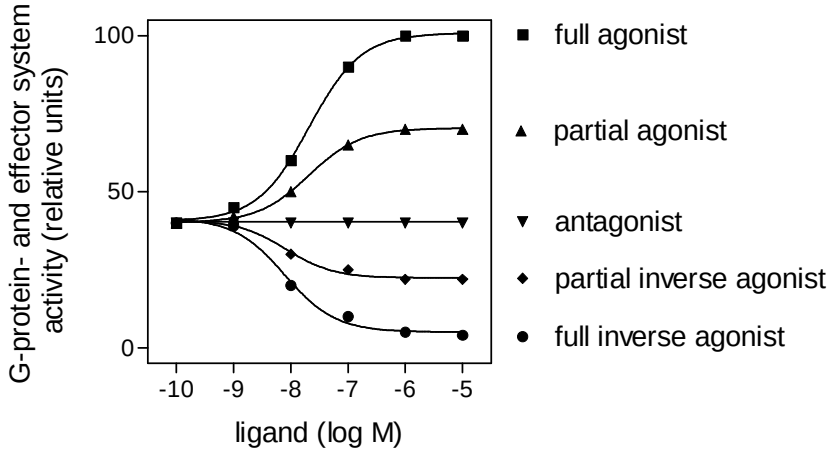

Fig. 1.1: Two-state model of GPCR activation. A: The agonist binding to the receptor leads to the active state of the receptor (R*), which promotes the GDP/GTP exchange at G-proteins and mediates the intracellular signal. Na^+ acts as an allosteric inverse agonist which stabilizes the inactive state (R) and reduces the basal G-protein activity. B: Partial agonists and partial inverse agonists have lower efficacies than full agonists and full inverse agonists, respectively. Adapted from Seifert *et al*.[35]

1.2. The role of histamine in the immune system

The effect of histamine as immune modulator has been reported frequently [5;43-45]. However, the co-expression of HRs on the same cell types, and the histamine concentrations used to mimic the *in vivo* conditions, complicate the recognition of the specific role of each receptor [33;46]. It has been long recognized that the interaction of histamine with H_1R mediates an allergic effect with additional immune and inflammatory functions. However, the discovery of H_4R and its functions revealed that there is an overlap in the histamine effect through H_1R and H_4R [34].

1.2.1 The role of histamine in monocytes and macrophages

Several reports have examined the expression of HRs in monocytes and macrophages in different species. The expression of H_1R is up-regulated during the differentiation of human monocytes to macrophages *in vitro* [47], whereas inflammatory stimuli such as IFN-γ alone or with TNF up-regulate H_4R in human monocyte [48]. In the same report, Dijkstra *et al.* state that H_4R stimulation induces Ca^{2+} influx and inhibits the production of CCL2 (monocytes chemoattractant protein 1 or MCP1). The functional expression of H_4R in human monocytes was also reported in THP-1 clone 15 by Damaj *et al.* in 2007. These cells exhibit a chemotactic response towards histamine, this response is inhibited by thioperamide, but not with diphenhydramine (H_1R antagonist) nor cimetidine (H_2R antagonist) [49]. Histamine effect through H_2R inhibits TNF, IL-12 and IL-18 production from LPS-activated human monocytes. It can also down-regulate CD14 expression on human monocytes [50]. There is one report on the role of H_1R in human lung macrophage activation which leads to IL-6 and β-glucuronidase production within 2-6 hours. Notably, no other confirmation of the role of histamine in macrophage activation has been reported [50-57]. In a single report about rat peritoneal macrophages, histamine was claimed to inhibit chemotaxis, phagocytosis, superoxide anion production, and the production of TNF and IL-12 [58].

HDC activity and histamine production was also reported in human precursor macrophages and macrophages. Furthermore, macrophages and precursor macrophages generate histamine upon exposure to LPS and IL-1 or M-CSF, respectively [59]. HDC activity is also induced in mouse macrophages after *Yersinia enterocolitica* infection, and the treatment of infected mice with the H_2R agonist dimaprit increased mice survival [60]. Another report relating histamine to macrophage function revealed that macrophages migrated in the human atherosclerosis lesion express HDC, and the regional histamine derived from macrophages may be relatively low in concentration but longer lasting in duration [61;62].

1.2.2. The role of histamine in DC

The expression profile of HRs on DC reveals co-expression of H_1R, H_2R and H_4R [34;49]. In other reports, H_3R in addition to H_4R expression has been observed

in human and mouse immature DC [63-65]. Histamine induces chemotaxis in human DC mainly through H_4R and H_1R [66]. IL-12p70 production from human DC can be also inhibited by histamine through H_4R [64]. In addition, cytokine production can also be modulated by histamine, this includes induction of IL-6 and IL-10 production. The inhibition of IL-12 and the induction of IL-6 and IL-10 from DC can drive T-helper 2 (T_H2) cell polarization in human and mouse cells by H_1R and H_4R [64;67].

1.2.3. The role of histamine in T-lymphocytes

The role of histamine in driving the immune response in towards T_H1 (anti-microbial and cellular immunity) and T_H2 (allergic response) has been intensively investigated. In the last 20 years, several reports of histamine effects on the production of IFN-γ, IL-4 and IL-13 have been published. These cytokines are essential in driving the naïve T cell differentiation into T_H1 or T_H2 [68]. In a recent report, functional expression of H_4R in human T_H2 cells as well as T_H1 cells was reported, in which H_4R stimulation increases IL-31 production in T_H2 cells. The role of IL-31 is associated with inflammatory bowel disease and airway hypersensitivity [23].

The expression of H_4R in $CD4^+$ T cells and $CD8^+$ T cells has been shown in human cells but not in the mouse. However, there is considerable evidence that histamine can act on mouse $CD4^+$ T cells, and regulate the immune response in asthma model through H_4R [69;70]. Histamine can also induce a chemotactic effect in human T cells *in vitro*, with evidence of H_1R and H_4R involvement [71;72].

1.2.4. The role of histamine in mast cells

Previously, H_4R was considered to be exclusively expressed in mast cells and eosinophils in addition to H_1R and H_2R. Furthermore, the histamine effect through H_4R was reported to induce chemotaxis in mouse mast cells. In response to histamine, there was redistribution of mast cells to the tracheal epithelium that could be blocked by systemic administration of the H_4R antagonist. This change in tissue localization of mast cells *in vivo* may mimic what happens in allergic conditions, where the presence of allergens in the airways leads to release of histamine either by the resident mast cells or by other cells [18;18;73].

1.2.5. The role of histamine in eosinophils

The chemotactic role of H_4R in human eosinophils was the first function assigned to H_4R. Histamine at low concentrations can induce chemotaxis in human eosinophils through H_4R, but at higher concentrations, chemotaxis is inhibited *via* H_2R activation [74-78].

1.3. The role of H_4R in the development of several pathological mechanisms

1.3.1. Asthma

The expression of H_4R in most of the immune cells contributing to the asthma inflammation mechanism, and the early observation about the anti-inflammatory role of H_4R antagonist suggest that this receptor may play a role in asthma development. In addition, the histamine contribution in driving the asthmatic response, and the limited effect of the traditional H_1R antagonist in asthma treatment, increase the evidence of possible role of H_4R in the development and treatment of the disease [34].

In the mouse asthma model, H_4R-deficient mice ($H_4R^{-/-}$) or those given H_4R antagonists during sensitization, show reduced lung inflammation and T_H2 inflammatory cytokines [69]. The effect was similar in mast cell-deficient mice, suggesting that mast cells were not the main source of histamine, and histamine produced by DC and other leukocytes can stimulate H_4R and induce inflammation. The preventive effect of JNJ 7777120 in asthma reaction was confirmed in a guinea pig model [79].

1.3.2. Pruritus

Histamine is an important mediator of itching in the periphery, and might also function as a transmitter of pruritic signals in the CNS. In the mouse model, $H_1R^{-/-}$ mice and mice treated with H_1R antagonists show a partial inhibition of itching induced by mast cells degranulation with compound 48/80. A similar effect was also found in an IgE-mediated-mast-cell activation model. In $H_4R^{-/-}$ mice as well as in mice treated with JNJ 7777120 the itching behaviour was notably diminished,

suggesting that a combination between H_1R and H_4R antagonists could completely eliminate histamine-induced itching [80]. Blocking H_4R with JNJ 7777120 has a remarkable effect on reducing the itch in allergic contact dermatitis in mice [81].

1.3.3. Other pathological mechanisms

The role of H_4R was investigated in several animal models by examining the effect of JNJ 7777120 in these models. In a rat model, JNJ 7777120 shows a promising effect in treating experimental colitis induced by trinitrobenzene sulphonic acid (TNBS) [22]. A similar effect was observed in treating rats with carrageenan-induced inflammation [82]. JNJ 7777120 also reduced the nasal symptoms in mice with allergic rhinitis [83]. Furthermore, the investigation of an allergic conjunctivitis model in the mouse, revealed that JNJ 7777120 can inhibit eye scratching behaviour induced by histamine and 4MEH, and the combination with levocabastine (H_1R antagonist) could inhibit both eye scratching and the allergic-like symptoms score [84].

1.4. Macrophages

1.4.1. Historical background

Macrophages are the first cells to be assigned a function in host defence. They were first recognized by their size and phagocytic properties. 100 years ago Elie Metchnikoff had discovered the phagocytic activity protecting the host from infection through a process he called ‘innate immunity’. This was awarded with the Nobel Price in Physiology and Medicine in 1908, simultaneously to Paul Ehrlich who in contrast described what is now called ‘adaptive immunity’. Macrophages remain a hot topic in immunity based on their dual role in innate and adaptive immunity [85].

1.4.2. Monocyte-derived macrophages in tissues

Macrophages are present in virtually all tissues. They differentiate from circulating peripheral blood monocytes, which migrate into tissue in the steady state or in response to inflammation. In humans, monocyte development starts from a

common myeloid progenitor cell in the bone marrow that is the precursor of many other immune cells including neutrophils, eosinophils, basophils, macrophages, DC and mast cells [86]. During monocyte development, myeloid progenitor cells or granulocyte/macrophage colony-forming units (GM-CFU) sequentially give rise to monoblasts, pro-monocytes and finally monocytes, which proceed to the bloodstream. Once monocytes migrate and settle in tissues, they mature and become macrophages which exist in all organs and connective tissues, and have been given special names to designate a specific location (Fig. 1.2). Each type of those macrophages plays a key role in the homeostasis and immune reaction in their organs, and initiates the immune response at all sites where microbes may exist.

Mouse monocytes in general have different cell-surface markers than human monocytes. This seems to give rise to distinct physiology between human and mouse [86-90].

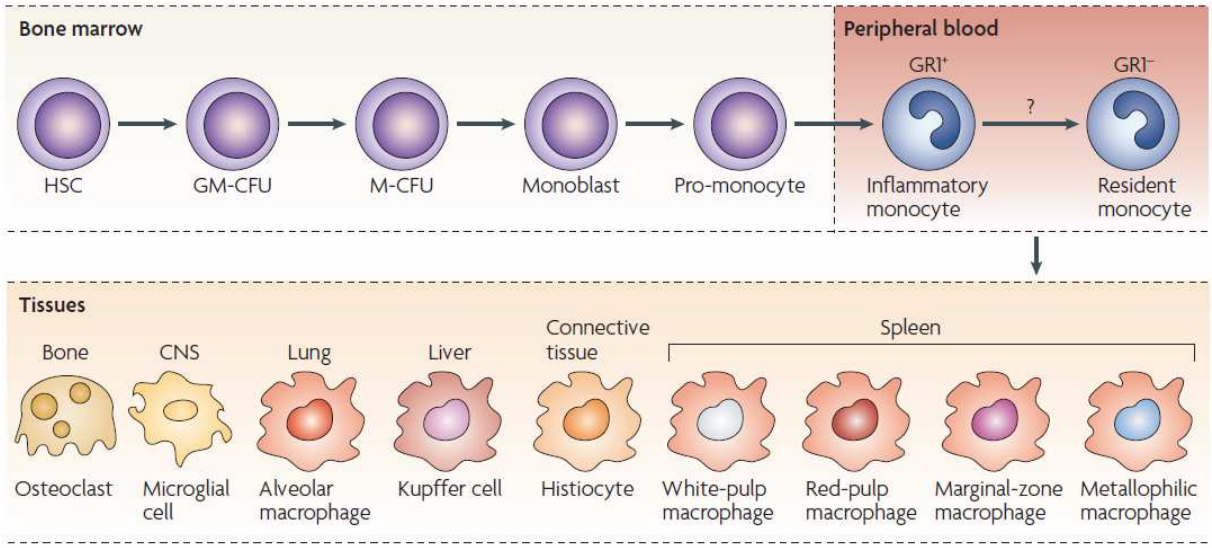

Fig. 1.2: Monocytes differentiation from bone marrow and tissue-specific-macrophages. Adapted from Mosser *et al.* [91]

Human macrophages are obtained *in vitro* by incubating isolated blood monocytes with macrophages-colony stimulating factor (M-CSF) for 4 days [92;93]. In contrast, in mouse and due to the low number of circulating monocytes, macrophage differentiation starts from bone marrow cells to generate bone marrow-derived macrophages (BMDM) [93]. BMDM represent a suitable cell model to generate non-activated macrophages *in vitro* that mimic the tissue-residing macrophages in their cell-surface markers and functions [94].

1.4.3. Recognition of microbes by macrophages

Macrophages express surface receptors that recognize microbes and stimulate phagocytosis and killing mechanisms. These receptors can detect the danger signals that are present in the debris of necrotic cells, injury or infection. Specifically, these receptors are capable of recognizing '*pathogen associated molecular patterns*' (PAMPs) that exist in the targets. Among these receptors, the Toll-like receptors (TLRs) represent one of the main receptors required for macrophage functions. The intracellular signal of these TLR goes through an adaptor molecule called *molecule myeloid differentiation primary-response gene 88* (MyD88). The best example of the TLR response in macrophages is lipopolysaccharide (LPS) recognition by TLR4, which leads to distinct macrophage activation. Macrophages also respond to signals produced by immune cells, which may activate them. In addition macrophages also produce several factors that influence their own physiology [91;95-97].

1.4.4. Macrophage activation

The term "activated macrophages" was used previously to describe inflammatory macrophages which phagocytose and kill microorganisms. Thereafter, this term defined a heterogeneous group of cells derived from different activation conditions with different physiology and immune functions (Fig. 1.3).

1.4.4.1. Classically activated macrophages

Classically activated macrophages are also known as M1 macrophages. The classical activation mechanism was the first discovered mechanism of macrophage activation. Two signals mediate the activation; Interferon-γ (IFN-γ) and tumor-necrosis factor (TNF) resulted in macrophages that had enhanced microbicidal or tumoricidal capacity and secreted high levels of pro-inflammatory cytokines and mediators. IFN-γ can be produced by innate or adaptive immune cells including natural killer (NK) cells and T_H1 cells [98]. TNF is the second stimulus required for the classical activation. Its production is induced by TLR ligands from antigen-presenting cells as well as macrophages. This cooperates with IFN-γ and leads to an exogenous/autocrine manner of macrophage activation. Therefore, the term of

classicaly activated macrophages includes the IFN-γ- and LPS-activated cells. Macrophages can also be activated by direct TLR stimuli (*e.g.* LPS, CpG, flagellin) or by stimulating *nucleotide oligomerization domain* (NOD) receptors. This activation phenotype resembles to a certain extent the classical activation, especially in the rapid TNF production.

The classically activated macrophages are mainly involved in host defence to bacterial infections and intracellular pathogens. This effect is mediated by several pro-inflammatory cytokines; for example, IL-1, IL-6, TNF and nitric oxide (NO), that are produced by classically activated macrophages. However, these macrophages with their killing capability can cause extensive damage to the host. Therefore their activation must be tightly controlled [86;99;100].

1.4.4.2. Wound-healing macrophages

Wound-healing macrophages were previously called alternatively activated macrophages or M2 macrophages. The name alternative implies that this is the only other (alternative) way that macrophages can be activated, and this is certainly not the case. The activation is mediated by IL-4 or IL-13, in which basophils and mast cells as well as other granulocytes are important sources of innate IL-4 production. In addition to injury, these cells can also produce IL-4 in response to chitin, a structural biopolymer that is found in some fungi and parasites. IL-4 stimulates arginase activity in macrophages, allowing them to convert arginine to ornithine, a precursor of polyamines and collagen, thereby contributing to the production of the extracellular matrix. Their primary function seems to be related to wound healing [91;101;102].

1.4.4.3. Regulatory macrophages

Recently, the regulatory macrophage population was identified as a distinct population generated in response to both innate and adaptive immunity. The primary role of regulatory macrophages is to dampen the immune response and limit inflammation. Regulatory T cells (T-reg) can drive regulatory macrophage differentiation by IL-10 production. Moreover, the production of the anti-inflammatory cytokine *Transforming growth factor-beta* (TGF-β) by macrophages following the phagocytosis of apoptotic cells in the presence of pro-inflammatory stimuli can also contribute to the immunoregulatory function of these macrophages [103-105]. Other

inducers of regulatory macrophages are ligands of GPCRs including histamine and adenosine [106;107]. The exact mechanisms mediating the switch to regulatory functions remains unknown with some evidence for MAPK extracellular-signal-regulated kinase (ERK) involvement [106;108].

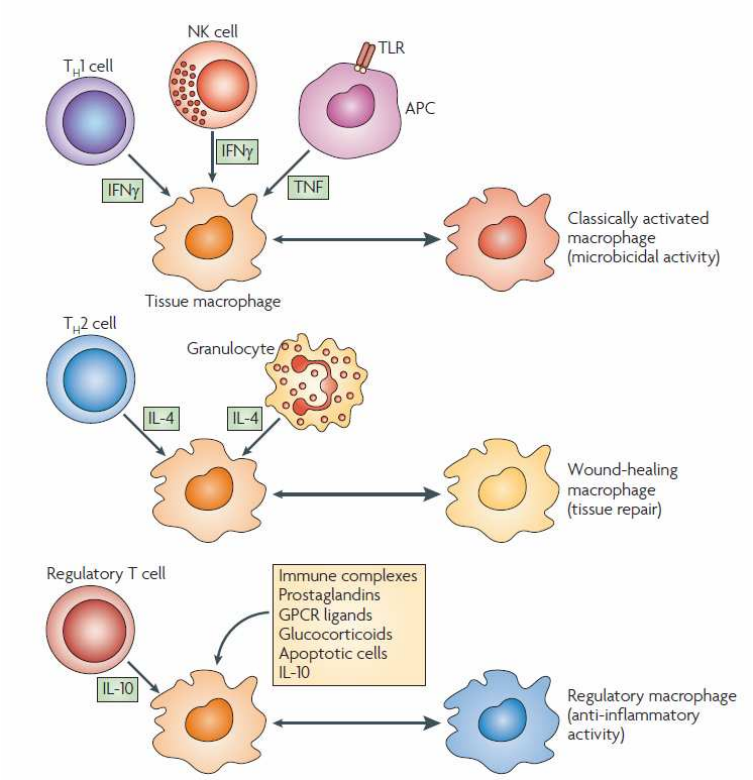

Mosser *et al*; *Nat. Rev. Immunol.* (2008)

Fig. 1.3: The different population of activated macrophages. Adapted from Mosser *et al*. [91]

1.4.5. Macrophage phagocytosis mechanism

Macrophages have the ability to clear infectious agents and apoptotic cells by phagocytosis, in which the discrimination between self and non-self is a key factor. The specificity of the phagocytic activity is achieved by a restricted number of phagocytosis receptors. This multi-step mechanism is initiated by particle recognition, which is mediated by a wide variety of surface receptors that bind directly or indirectly through opsonins (complement fragments, IgG) to the particle. FcγR is an example of phagocytosis receptors that require IgG opsonization to initiate phagocytosis. CD44 can also internalize hyaluronan-coated particles in mouse macrophages in a process that involves complement receptor 3 (CR3).

The phagocytosis mechanisms vary depending on the phagocytosed elements. Therefore, there is no single pathway by which phagocytosed elements can be internalized, but the recognition of PAMPs remains as a common initiator of the process. These PAMPs include mannans in the yeast cell wall, formylated peptides in bacteria, and LPS and lipoteichoic acids on the surface of Gram negative and Gram positive bacteria. Several receptors can recognize PAMPs such as integrins (CD11b/CD18), mannose receptors and scavenger receptors. In addition, many of the phagocytic receptors have dual functions, often mediating both adhesion and particle internalization.

In general, the uptake of large particles occurs by an actin-dependent mechanism, including rearrangements in the actin cytoskeleton that lead to the formation of the phagocytic cup. Once the phagocytic cup is closed the maturation process begins and phagosomes become increasingly more acidic and hydrolytically active. They transiently fuse with the recycling endosomal system, the secretory system (including secretory lysosomes), multi-vesicular bodies such as the MHC class II compartment and even the endoplasmic reticulum (Fig. 1.4) [95;109-114].

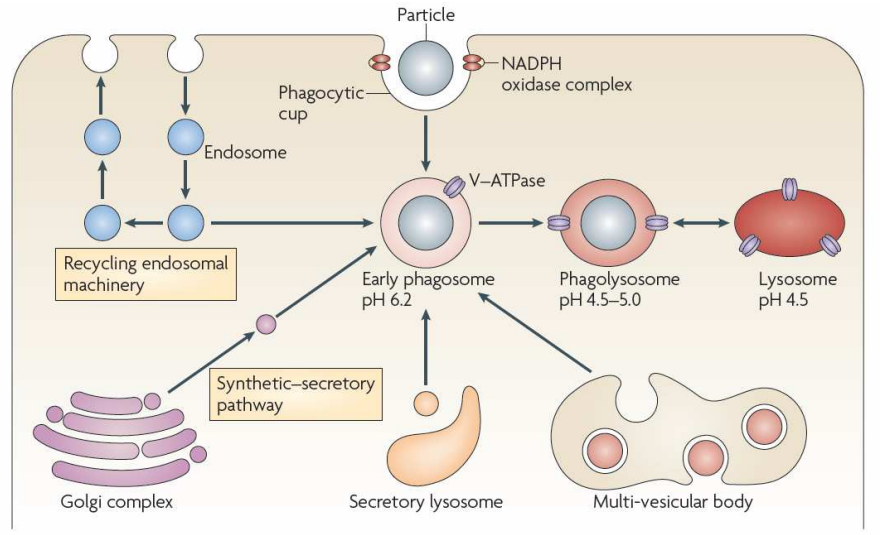

Fig. 1.4: Phagocytic cup formation and phagosome maturation. Following engagement of phagocytic receptors, an area of the cell surface is remodelled around the particle, forming the phagocytic cup. Finally, the phagosome fuses with pre-existing, dense lysosomal bodies and equilibrates to a pH of 4.5–5.0. Adapted from Russell *et al.* [112]

1.4.6. Chemotaxis mechanism

Chemotaxis is the function in which the cells sense a chemical compound (chemoattractant) and migrate towards its higher concentration. It is an essential process in embryogenesis, angiogenesis, metastasis, and the immune response. Immune cells chemotaxis is considered as one of the essential properties of the cells to defend against pathogens and to migrate into tissues and ensure the cell to cell interactions [115;116].

In general, eukaryotic cells detect these chemical signals through GPCRs, which activate the chemotaxis mechanism only in the continuous presence of the external signal gradient [117]. It has previously been shown that $G\alpha_i$ signaling is generally important for cell migration, and pertussis toxin (PTX) from *Bordetella pertussis*, a specific inhibitor for the $G\alpha_i$ unit, completely blocks cell migration induced by most chemokines. Interestingly, $G\alpha_i$ itself does not seem to be required for cell migration. Instead, the free $G_{\beta\gamma}$ subunit released from the G_i complex is necessary for the transduction of migratory signals [118-120]. The downstream signal of the GPCR-mediated chemotaxis in neutrophils goes to the phosphatidylinositol-3-OH kinase (PI3K) phosphatase and tensin homolog (PTEN) pathway, and the p38 mitogen-activated protein kinase pathway, with the p38 pathway dominating over the PI3K pathway [121].

1.5. Dendritic cells (DC)

DC are potent antigen presenting cells (APCs) that possess the ability to uptake, transport, process and present antigens to naïve T cells and activate them. This step is the initiator of the adaptive immune response. DC are widely distributed in all tissues, especially in those that provide an environmental interface [122].

1.5.1. The development of DC

It is important to mention that DC are not a single cell type, but a heterogeneous collection of cells, each cell type develops from unique progenitors. The development is driven by cytokine combinations, and the developed cells within a particular pathway exhibit distinct specialized functions [123]. Human and mouse

monocytes can undergo several differentiation steps and generate DC residing in the tissues. Myeloid DC are another mouse DC subtype differentiated from bone marrow cells. The cells are differentiated from bone marrow cells in the presence of granulocyte macrophages-colony stimulating factor (GM-CSF) for 8 days. The resulting cells are immature DC which express CD11c as a specific marker for mouse DC. The immature DC can be driven into maturation state by stimulation with antigen or TLR ligands such as LPS or CpG, this leads to mature DC which expresses CD80, CD86 and MHC class II [90;124;125].

1.6. Leishmania major *(L. major)*

L. major is a one of 15 different species of the protozoan parasite genus Leishmania, responsible for the human disease Leishmaniasis. Leishmaniasis severity ranges from self-limiting cutaneous infections to disseminating diffuse cutaneous, mucocutaneous and visceral Leishmaniasis. The infection affects more than 20 million people worldwide. Furthermore, the absence of vaccination and effective treatment, in addition to the co-infection with HIV, made Leishmaniasis as complex disease [126].

1.6.1. Pathopysiology

L. major exists in two morphological forms, Promastigotes, amastigotes as an extracelluar and intracellular forms respectively. Promastigotes can subcutaneously infect the host by the bite of an infected sandfly. Leishmania are obligate intracellular pathogens, preferring phagocytes as host cells. Neutrophils are the first phagocytic cells that infiltrate to the subcutaneous site of infection. Upon phagocytosis, neutrophils serve as intermediate host cells, where *L. major* remain in the promastigote stage without multiplication. In the mean time neutrophils produce IL-8 which attracts macrophages to the infected region. Subsequently, and because of the short lifespan of neutrophils, promastigotes use apoptotic neutrophils as a Trojan horse to infect their final host, the macrophages [127]. In the macrophages, the parasites loose their flagella and become amastigotes, where they survive and multiply by inhibiting the antimicrobial defense by several mechanisms [127;128].

1.6.2. The experimental model of Leishmaniasis in the mouse

Infecting mice with *L. major* comprises a valuable tool on the way to understand the cell-mediated response to intracellular pathogens. One of the early benefits of this model, is the observation that T_H1 immune response is a key factor in controlling the parasite replication. This includes the generation of IFN-γ activated macrophages that are able to release nitric oxide (NO) and kill the parasites. Interestingly, Leishmaniasis prognosis varies basically in between the mouse strains. Leishmaniasis development in C57BL/6 is limited to local subcutaneous inflammation; and the mice survive and heal after a few weeks, because of their capability of generating a T_H1 responses, whereas the T_H2 immune responses associated with BALB/c mice make Leishmaniasis infection a lethal disease for these mice [129;130].

Aim of the thesis

This thesis intended to functionally characterize mH_4R. Therefore, the expression of this receptor was examined on different cells of the immune system such as DC, macrophages, T and B cells. Furthermore, it was investigated, whether regulatory factors influence the receptor expression in different cell states. To achieve this several techniques were used, including bone marrow differentiation to macrophages and DC, FACS analysis, RNA isolation, RT-PCR and real-time PCR.

The main topic of this thesis was the functional analysis of mH_4R in DC and macrophages. Several, functional assays were established such as chemotaxis, phagocytosis and cytokine production in response to histamine and other stimuli. These functional assays were also used to compare macrophage derived from WT mice with those derived from $H_4R^{-/-}$ mice, to characterize the functions are affected by the absence of mH_4R.

Another aim of this thesis was the generation of specific antibodies against mH_4R in order to analyze mH_4R on the protein level to obtain further insight on its function.

2. Materials and methods

2.1. Materials

2.1.1. Mice

Wild type mice C57BL/6 at the age of 12-16 weeks were obtained from Charles River breeding Laboratories and Elevage-Janvier. H_4R-knockout mice were generated by Lexicon Genetics (Woodlands, TX, USA) and kindly provided by Johnson & Johnson Pharmaceutical Research and Development (San Diego, CA, USA). $H_4R^{-/-}$ mice. A 9-kb mouse genomic fragment containing the mouse H_4 receptor gene was obtained from the embryonic stem cell line 2G9 and used as a template to prepare the knockout construct. A 0.5-kb region covering most of exon 1 and part of intron 1 of the H_4R gene was deleted from this genomic fragment and replaced with a neomycin-resistant gene cassette. The mice were crossed on C57BL/6J background for 10 generations then have been bred between brother/sister pairs. The founding breeding pair provided from Johnson & Johnson were genotyped and found to be homozygous for the knock-out. All the knock-out mice in the study were derived from that breeding pair.

Both mouse line were used for organ isolations (bone-marrow cells, lymph-nodes, peritoneal exudates cells and splenocytes) and examine *in-vivo Leishmaniasis* model as well as generating mouse anti-mH_4R. The isolated organs were subjected either to RNA isolation and gene expression determination, or cultured to generate *in-vitro* cells such as bone-marrow derived macrophages or DC. The mice breeding and raising conditions were approved by the Central Animal Laboratories (ZTL) department of the University of Regensburg.

2.1.2 Cell lines

The cell lines used in the experiments were RAW 264.7, J774.1 and Pu5-1.8 (mouse macrophages cell line), WEHI 164H, L929 and X6310 (mouse fibroblast), LA-4 (mouse lung epithelial), P815 (mouse mastocytoma cell line) and HEK 293 (human embryo kidney).

2.1.3. Chemicals

4-methylhistamine (4MEH)	Biotrend (Tocris), Zurich
5-nitrophenyl phosphate disodium salt hexahydrate 20 mg substrate tablets	Sigma-Aldrich, Taufkirchen
Acrylamide solution	Roth, Karlsruhe
Agarose	Peqlab, Erlangen
Bovine serum albumine (BSA) fraction V	PAN Biotech, Aidenbach
CFSE	Sigma-Aldrich, Taufkirchen
Dimethyl sulfoxide (DMSO)	Merck, Darmstadt
DNA 100 bp ladder	New England Biolabs, Ipswich
dNTP mix	Promega, Mannheim
Elisa tablets (AP Sustrate)	Sigma-Aldrich, Taufkirchen
Ethanol, absolute	J.T. Baker, Deventer
Ethidium bromide 10 mg/ml	Promega, Mannheim
Famotidine	Sigma-Aldrich, Taufkirchen
Fetal calf serum (FCS)	PAN Biotech, Aidenbach
Fluoresbrite microparticles 0,75 µm (FITC-beads) (1.08×10^{11} beads/ml)	Polysciences, Eppelheim
fMLP (N-Formy-methionyl-leucyl-phenylalanine)	Sigma-Aldrich, Taufkirchen
Histamine (2-(imidazol-4-yl) ethylamine)	Sigma-Aldrich, Taufkirchen
IFN-α	Abd Serotec, UK

IFN-γ	Abd Serotec, UK
IL-4	Immunotools, Friesoythe
Isopropanol	Merck, Darmstadt
JNJ 7777120 (1-(5-chloro-1H-indol-2-yl)carbonyl-4-methylpiperazine)	Johnson & Johnson, San Diego, USA
Lipopolysaccharide (LPS) from *E. coli* (0127:38)	Sigma-Aldrich, Taufkirchen
Mepyramine	Sigma-Aldrich, Taufkirchen
N,N,N′,N′-Tetramethylethylenediamine (TEMED)	Sigma-Aldrich, Taufkirchen
Naphtyl-ethylenediamine dihydrochloride (NEDD)	Sigma-Aldrich, Taufkirchen
NOWA solution A and B	MoBioTec, Heidelberg
Nuclease free water	Promega, Mannheim
Oligo(dt)	Promega, Mannheim
Penicillin/streptomycin (10000 Units/ml and 10 mg/ml respectively)	PAA Laboratories, Cölbe
Pep.89064,1 - BSA conjugate (2nd ECD of mH_4R)	Biogenes, Berlin
Pep.89064,1 - KLH conjugate (2nd ECD of mH_4R)	Biogenes, Berlin
Pep.89065,2 - BSA conjugate (3rd ECD of mH_4R)	Biogenes, Berlin
Pep.89065,2 - KLH conjugate (3rd ECD of mH_4R)	Biogenes, Berlin
Phosphoric acid, H_3PO_4	Sigma-Aldrich, Taufkirchen
Precision plus protein all blue standards	Bio-Rad Laboratories, München
RPMI 1640 medium	PAN Biotech, Aidenbach
Sodium nitrite	Sigma-Aldrich, Taufkirchen
Sulfanilamide	Sigma-Aldrich, Taufkirchen
Sulforic acid 2N	Sigma-Aldrich, Taufkirchen
TMB substrate solution for ELISA (A and B	BD Biosciences, Heidelberg

substrates)	
TNF	Peprotech, Hamburg
Trypan blue	Sigma-Aldrich, Taufkirchen
Türk's solution	Merck, Darmstadt
Tween 20	Sigma-Aldrich, Taufkirchen
β-Mercaptoethanol	Sigma-Aldrich, Taufkirchen

2.1.4. Enzymes

DNase	Macherey-Nagel, Düren
goTaq green polymerase	Promega, Mannheim
iQ™ SYBR® Green Supermix	Bio-Rad Laboratories, München
M-MLV reverse transcriptase	Promega, Mannheim
Pronase E	Sigma-Aldrich, Taufkirchen
Proteinase K	Sigma-Aldrich, Taufkirchen
Taq polymerase	Institute of Immunology, Regensburg

2.1.5. Kits

Diff-Quick® staining set	DAED Behring, Marburg
IL-6 ELISA	R&D Systems, Wiesbaden
Nucleospin RNA II (RNA isolation)	Macherey-Nagel, Düren
TNF ELISA	R&D Systems, Wiesbaden

2.1.6. Antibodies

antibody	source	clone	conjugate	dilution	provider
anti-B220	Rat	RA3-6B2	PE	1:400	BD
anti-CD11b	Rat	M/170	FITC	1:200	AbD Serotec
anti-CD11c	Hamster	N418	PE	1:100	AbD Serotec
anti-CD3	Rat	17A2	APC	1:200	BD
anti-CD4	Rat	RM4-5	PE	1:400	BD
anti-CD8	Rat	53-6.7	PE	1:400	BD
anti-CD86	Rat	GL-1	FITC	1:200	BD
anti-F4/80	Rat	BM-8	PeCy5	1:200	AbD Serotec
anti-FcγR	Rat	2.4G	-	1:500	BD
anti-MHC II	Rat	M5/114.15	APC	1:150	Miltenyi
anti-mouse H_4R	Goat	Polyclonal	-	1:100	Santa Cruz (sc-3397)
anti-mouse IgG (whole molecule)	Goat	Polyclonal	AP	1:10000	Sigma-Aldrich
anti-mouse IgG (whole molecule)	Goat	Polyclonal	HRP	1:10000	Sigma-Aldrich

2.1.7. Oligonucleotides

All oligonucleotides used for PCR and RT-PCR were purchased lyophilized from Metabion, and stored in -20 °C at a concentra tion of 100 µM. The primers were used at the concentration of 0.3 µM in the PCR.

Primer	Sequence
H_1R_fwd	5’ ATGGGAAAACTGCTGTGGAG 3’
H_1R_rv	5’ TACAGCACCAGCAGGTTGAG 3’
H_2R_fwd	5’ GCAAGCCACAACTCTCACAA 3’
H_2R_rv	5’ GCTCAGGCTCAGGAGACAAC 3’

H_3R_fwd	5’ AGCTGTGGCTGGTGGTAGAC 3’
H_3R_rv	5’ CGGACAGGTACTCCCAACTC 3’
H_4R_fwd	5’ TTCCTCGTGGGTTTGATTTC 3’
H_4R_rv	5’ GCCAGTGTGTTGAGCCCTAT 3’
β-actin_fwd	5’ TGACGGGGTCACCCACACTGT 3’
β-actin_rv	5’ CTAGAAGCATTTGCGGTGGAC 3’
18S_fwd	5’ GTAACCCGTTGAACCCCATT 3’
18S_rv	5’ CCATCCAATCGGTAGTAGCG 3’
JNJ11-31	5’ GGAAATTGCCACCACAAGTTG 3’
JNJ11-32	5’ GCAGACACATGATTCTTATTAC 3’
Neo3b	5’ TTCTATCGCCTTCTTGACGA 3’

2.1.8. Instruments

Bioimaging system, Genius	Syngene, Darmstadt
Biophotometer, 6131	Eppendorf, Hamburg
Cellsafe Cells incubators	Integra bioscience, Fernwald
Centrifuge 5417R	Eppendorf, Hamburg
Centrifuge 5810R	Eppendorf, Hamburg
Emax Microplate Reader	Molecular Devices, München
FACSAria system	BD Biosciences, Heidelberg
Fastblot B34	Biometra, Göttingen
Film developer Optimax Typ TR	MS Labordevices, Heidelberg
Hera safe Safety cabinet	Heraeus, Berlin
iQ™5 Multicolor Real-Time PCR Detection System	Bio-Rad Laboratories, München
LSR II FACS system	BD Biosciences, Heidelberg

Microscope Leitz Diaplan	Ernst Leitz Wetzlar, Wetzlar
My Cycler™ thermal cycler	Bio-Rad Laboratories, München
Neubauer cell chamber	Brand, Gießen
pH-Meter Inolab	WTW, Weilheim
ThermoShaker TS-100	Biometra, Göttingen
Vortex MS2 Minishaker	IKA®, Staufen

2.1.9. Laboratory materials

100 mm square Petri dishes	Sterilin Ltd, Stone, Staffs, UK
96 well PCR plate	Peqlab, Erlangen
Amersham hyperfilm ECL	GE Healthcare, München
Cell culture flasks 75 cm^2	BD Biosciences, Heidelberg
Cell culture multi-wells plates (6 and 96 well plates)	Nunc, Langenselbold
Cell scraper (rubber policeman)	Sarstedt, Nümbrecht
Cell Strainer 40 µm (Nylon) BD Falcon	BD Biosciences, Heidelberg
FACS tubes	Sarstedt, Nümbrecht
Film cassette	Siemens, München
Gel-Blotting-Paper Whatman®	A. Hartenstein, Würzburg
Immersion oil for microscopy (immersol)	Zeiss, Oberkochen
Microscope slide 76 x 26 x 1 mm	Paul Marienfeld GmbH, Königshofen
Mechanical external measuring gauge Measuring range 0 - 10 mm, Scale interval 0.010 mm	Kröplin, Schluechtern
Multiwell chemotaxis chamber 48 well (AP48) with its accessories	Neuro probes, Gaithersburg MD, USA
Petri dishes 100 mm (Polystyrene)	Greiner, Frickenhausen

Poly carbonate membrane 5.0 µm PVP surface treatment 25 x 80 mm stock# PRB5	Neuro Probes, Gaithersburg MD, USA
Poly carbonate membrane Sandard 5.0 µm (PVP surface treatment) 25 x 80 mm Cat# 10468	Osmonics, Minnetonka MN, USA
Serological pipepette (5, 10 and 25 ml)	Sarstedt, Nümbrecht
Sterile filter 0.2 µm	Sartorius, Göttingen

2.1.10. Buffers and Reagents

Trypanblue solution

Trypan-blue 0.16 % (w/v)
150 mM NaCl
pH 7.4

FACS buffer

2 % FCS in PBS

2.1.10.1. ELISA buffers

TBS buffer (10x):

(1x: 150 mM NaCl, 10 mM Tris pH 8.0)
87.6 g NaCl
12.1 g Tris
~ 4 ml HCl to pH
Add dd H_2O to 1L

TBS-T:

TBS with 0.05 % (V/V) Tween 20

PBS buffer (pH 7.3) Ca^{2+} and Mg^{2+}-free:

137 mM NaCl

6.5 mM Na_2HPO_4 x H_2O

1.5 mM NH_2PO_4

2.7 mM KCl

2.1.10.2. Western-blot buffers

RIPA buffer:

50 mM Tris-base

150 mM NaCl

1 mM EDTA

1 % Triton X-100 (V/V)

0.1 % SDS (W/V)

1 % sodium-desoxycholat (W/V)

1.5 M Tris Buffer pH 8.8:

90.83 g Tris-base

Add 400 ml H_2O

Adjust pH to 8.8 with HCl

Add ddH_2O to 500 ml

0.5 M Tris buffer pH 6.8:

30 g Tris-base

Add 400 ml H_2O

Adjust pH to 6.8 with HCl

Add ddH_2O to 500 ml

4x Lämmli buffer:

3.04 g Tris-base

40 ml H_2O

4 g SDS

2 mg Bromphenolblue

Adjust pH to 6.8 with HCl

Add ddH_2O to 100 ml

Add 4 ml β-mercaptoethanol

5x Running buffer:

15.1 g Tris-base

72 g glycine

5 g SDS

Add ddH_2O to 1 L.

Transfer buffer A:

36.35 g Tris-base

800 ml ddH_2O

100 ml methanol

Adjust pH to 10.4 with HCl

Add ddH_2O to 1 L

Transfer buffer B:

30.03 g Tris base

800 ml ddH_2O

100 ml methanol

Adjust pH to 10.4 with HCl

Add ddH_2O to 1 L

Transfer buffer C:

30.03 g Tris base

3.25 g ε-amino capronic acid

800 ml ddH_2O

100 ml methanol

Adjust pH to 9.4 with HCl

Add ddH_2O to 1 L

2.1.10.3. DNA electrophoresis buffers and solutions

TAE DNA electrophoresis buffer (50x):

(2 M Tris 50 nM EDTA)

484 g Tris-base

114.2 ml glacial acetic acid

200 ml 0.5 M EDTA pH 8.0

Add ddH_2O to 2 L

0.5 M EDTA pH 8.0:

148 g EDTA

Adjust pH by NaOH (30-40g)

Add ddH_2O to 1 L

Loading Dye 6 x

40 g Saccharose

250 mg Bromphenolblue

250 mg Xylencyanol

Add ddH_2O to 1 L

2.1.10.4. Griess reagent

(1:1 mixture of the following two solution) mix directly before use:

1) 1% sulfanilamide 5% H_3PO_4 (W/V)

   10 g sulfanilamide

   50 ml H_3PO_4

   Add ddH_2O to 1 L

   Store at 4°C

2) 0.1% naphtyl-ethylenamine dihydrochloride (NEDD) (W/V):

   1 g NEDD

   Add ddH_2O to 1 L

   Store at 4°C for a few weeks, as long as the the c olor has not turned to pink

2.1.10.5. Genomic DNA isolation solutions and buffers

NaCl 6M:

351 g NaCl

Add ddH_2O to 1 L

Pronase E solution:

100 mg Pronase

10 mM Tris-HCl pH 8.0

10 mM NaCl

Add ddH_2O to 10 ml

Activation for 1 h at 37°C before use

Proteinase K solution:

10 µg Proteinase K

10 mM Tris pH 8.0

10 mM NaCl

1% Triton X-100 (V/V)

10 mM EDTA

1% SDS (W/V)

in 500 µl ddH_2O

2.1.11. Cell culture media

2.1.11.1. BMDM medium

In 500 ml RPMI 1640 medium bottle:

50 ml FCS

5 ml Penicillin and streptomycin solution (contains 10.000 Units/ml and 10 mg/ml respectively)

50 ml of L-929 cells supernatant medium (sterile filtered)

2.1.11.2. BMDC medium

In 500 ml RPMI 1640 medium bottle:

50 ml FCS

5 ml Penicillin and streptomycin solution (contains 10000 Units/ml and 10 mg/ml respectively)

50 ml of X6310 cells supernatant medium (sterile filtered)

2.1.11.3. General cell culture medium

In 500 ml RPMI 1640 medium bottle:

50 ml FCS

5 ml Penicillin and Streptomycin solution (contains 10000 Units/ml and 10 mg/ml respectively)

2.1.12. Synthesized peptides

Two peptides were synthesized representing two different epitopes of the mH_4R sequence. The first peptide is a 19 amino acids peptide second extra-cellular domain (2nd-ECD), and the second peptide is 10 amino acids third extra-cellular domain (3rd-ECD) (Table 2.1). The peptides were coupled either to KLH to be used for immunizing the mice, or to BSA to screen the mice sera for antibody generation. All peptides were provided by (BioGenes, Berlin) at concentration of 5 mg/ml potassium-phosphate buffer.

Peptide	Sequence
2^{nd}-ECD	DSWKNSTNTKDCEPGFVTE
3^{rd}-ECD	YPRTERPKSV

Table 2.1: The sequences of peptides used to immunize $H_4R^{-/-}$ mice and generate antibodies.

2.1.13. Software

The figures as well as the statistical analyses were performed by Microsoft Office 2003® and GraphPad Prism 4®. The agarose photos were taken by GeneSnap 6® software. Analyses of the FACS data were performed by BD FACSDiva™ 5.0.3 and FlowJo 8.7.1 softwares.

2.2. Methods

2.2.1. Cell culture techniques

2.2.1.1. Cell lines

2.2.1.1.1. Macrophages like cell lines

RAW 264.7, J774A.1, and Pu5-1.8 were cultured in general cell culture medium (see 2.1.11.3.). The cells were incubated in incubators with 95% humidity and 5% CO_2 at 37° C. The cells grow as adherent monolayer cells, and were split twice per week by mechanically scraping the cells using a rubber cell scraper before full confluently grow. Some morphological changes were observed after multiple passages for RAW 264.7 cells. These were associated with a different expression pattern of the histamine receptors (mainly H_4R). Therefore, those cells were replaced every 8-10 weeks with a new aliquot from liquid nitrogen-frozen cells.

2.2.1.1.2. Supernatant isolation of L-929 and X6310 cells

The supernatants of L-929 and X6310 were used as a source of M-CSF and GM-CSF, respectively. The cells grow as adherent monolayer cells with the general cell culture medium. The cells were split twice per week and the supernatant medium was collected from the 3-4 day old cultures and filtered with 0.2 µm sterile filter, and stored at -20° C to be used as a supplementary medium in BMDM and BMDC medium.

2.2.1.1.3. Other mouse cell lines

WEHI 164H, LA-4, and P815 were cultured with the general cell culture medium. The non-adherent cells P815 were split twice per week, and kept below $1x10^6$ cells/ml, whereas the adherent WEHI 164H and LA-4 cells were split twice per

week before fully confluent grow by mechanically scraping the cells using a rubber scraper.

2.2.1.2. Mouse primary cell isolation and in-vitro generated cells

2.2.1.2.1. BMDM differentiation

The protocol used to generate BMDM was obtained from several reports with minor modifications [131;132]. In order to isolate bone marrow cells from C57BL/6 or $H_4R^{-/-}$ mice were euthanized by cervical dislocation. The tibias and femurs were removed, cleaned from the muscle with a napkin, and incubated in Petri dishes containing ice-cold PBS. The bones were then sterilized by short incubation for 15 seconds in 70% ethanol, and then moved to sterile chilled PBS. Bone marrow cells were obtained by cutting the ends of the bones under sterile conditions, and flushing the bone marrow cells out with chilled PBS using a 27G needle, the cells were counted with Türk's solution to exclude the erythrocytes, and $10x10^6$ cells were seeded in 20 ml BMDM medium (see 2.1.11.1.) in 10 x 10 cm Sterilin square dishes, and incubated in humid incubator at 37° C with 5% CO_2 for 7 days. On day 5, the non-adherent cells were discarded with the old medium and replaced by fresh 20 ml BMDM medium. BMDM cells were also generated in 6-well plates similar to the previous protocol, but bone marrow cells were seeded at $1x10^6$ cells in 4 ml BMDM medium. Macrophage markers were analyzed on day 7 by FACS to ensure the successful differentiation (see 2.2.3.1.).

2.2.1.2.2. Isolation of mouse peritoneal macrophages

In order to enhance yield of peritoneal exudates cells (PEC) and macrophages harvested from the peritoneal cavity, sub-inflammation induction prior to the harvest is essential. Such inflammatory induction was generated by injecting 1 ml sterile PBS with a 25 G needle in the peritoneal cavity; 14 hours later the mouse was euthanized by decapitation. After sterilizing the abdomen with 70% ethanol, 10 ml of chilled PBS containing 10% FCS were used for peritoneal lavage, the procedure was to use 20 ml syringe attached to 19 G needle, and inject the medium in the intact peritoneal cavity, with the beveled end of needle facing up without hitting the intestine. After gently removing it, the same needle was reinserted in the upper part of the

peritoneum, with the beveled end of needle facing down, and the peritoneal fluid was withdrawn slowly. The peritoneal exudates cells were amounted to be around $2x10^6$ cells per mouse, and were seeded at $1x10^6$ in 60 mm cell culture dishes for 2 hours to ensure macrophages adherence. Non-adherent cells were discarded, and only adherent cells were used for RNA isolation or phagocytosis assays. The samples with PEC above $2x10^6$ were discarded because this might indicate a bacterial infection in the peritoneal cavity.

2.2.1.2.3. BMDC differentiation

Bone marrow cells were obtained as mentioned before (see BMDM differentiation). $2x10^6$ cells were seeded in 10 ml BMDC medium (see 2.1.11.2.) in 10 cm Petri dishes, or $2x10^5$ cells in 1 ml BMDC medium in 24 well plate. On day three the cells were supplied with additional (10 or 1) ml fresh medium, respectively. On day six 10 or 1 ml respectively from the supernatant were centrifuged and the pellet was resuspended in a fresh (10 or 1) ml medium and added to the original dish. On day eight, the same step as in day six was repeated. The cells on day 8 were considered as immature DC which express CD11c, the specific mouse DC marker. The cells could be incubated for longer time up to day 10 when new medium is frequently supplied. BMDC were detached from the dishes by vigorously aspiring the medium with the pipette [133].

2.2.1.2.4. Spleen and lymph-nodes cells

C57BL/6 mice were euthanized by cervical dislocation. Spleen, axillary and brachial lymph-nodes were immediately isolated and incubated on chilled PBS. Organs homogenization was performed by pressing them through a cellular strainer (40 µm) with a syringe plunger. The cells and the strainer were washed with 10 ml of chilled PBS and resuspended to ensure the cell separation and formation of single cell suspension. Afterwards, spleen and lymph node cells were used for RNA isolation, or stained by specific antibodies for FACS experiments (spleen only).

2.2.1.2.5. Spleen macrophage preparation

In order to study the macrophages residing in spleen, the spleen single cell suspension was prepared and the cells were left for 2 hours in 10 cm Petri dishes to adhere. After that, the non-adherent cells were washed away, and the adherent cells were washed by PBS and gently scraped by rubber scraper and analyzed by FACS, after staining the cellular markers with labeled-antibodies (see 2.2.3.1.).

2.2.1.3. Cell stimulation, maturation and activation

2.2.1.3.1. Classical and alternative activation of BMDM

In order to generate M1 macrophages by classical activation, LPS (*E. coli*) was used at a concentration of 100 ng/ml for 24 h, or IFN-γ at a concentration of 50 IU/ml for 24 h. The activation was performed with BMDM generated in 6 wells plates. BMDM alternative activation to generate M2 macrophages was performed by incubating BMDM with IL-4 for 24 h at a concentration of 50 ng/ml. M1 and M2 macrophages were later subjected to RNA isolation and real-time PCR experiments to quantify the mH_4R expression.

2.2.1.3.2. RAW 264.7 cells stimulation

RAW 264.7 cells were seeded in 6 well plates for 24 hours at a concentration of 2×10^5 in 3 ml medium. Later, medium was substituted with medium alone or medium containing IFN-α (120 IU/ml), IFN-γ (50 IU/ml), and TNF (50 ng/ml) separately for 3, 6 and 24 hours. At each time point, the stimulated and non-stimulated cells were harvested to isolate RNA for real-time PCR.

2.2.1.3.3. BMDC maturation

BMDC were incubated on day 8 with 100 ng/ml LPS for 24 hours in order to induce the maturation. The maturation was examined by FACS to inspect the expression of CD86 and MHC II (mature DC markers) among the CD11c positive population.

2.2.1.3.4. BMDC maturation with histamine and 4MEH in the presence or absence of LPS

BMDC generated in 24 well plates were incubated on day 8 with 10 µM histamine or 10 µM 4MEH. As positive control, cells were incubated with 10 ng/ml, or 50 ng/ml LPS alone or with histamine and 4MEH separately (10 µM). As negative control, cells were incubated with 10 µl/well sterile H_2O. The experiment was performed in duplicate for each incubation condition, and the cells were analyzed by FACS on the next day for maturation markers (CD86 and MHC class II).

2.2.2. Molecular biology techniques

2.2.2.1. RNA isolation and quantification

Nucleospin RNA II kit from Macherey-Nagel was used to isolate total RNA from different cells according to the supplier's instructions. The principle of the method is to lyse the cells using the provided lysis buffer plus β-mercaptoethanol, and then RNA and genomic DNA were precipitated with 70% (V/V) ethanol which adsorb on the provided silica column. Contaminating genomic DNA was digested with DNase, followed by several washing steps to remove salts and protein lysate, and finally the total RNA was eluted with RNase and DNase free water.
The RNA was quantified by measuring the absorbance of diluted solutions (1:25) with spectrophotometer at 260 nm, and the purity was determined by absorbance ratio at 260/280 to be 1.6 - 2.0.

2.2.2.2. cDNA synthesis

1 µg total RNA was later subjected to synthesize cDNA (Promega two-step RT- PCR) with 0.5 µg Oligo(dt), 10 mM dNTP mix, and 100 unit M-MLV RT using the supplied reaction buffer. The mixture was incubated at 48° C for 50 min for the first strand cDNA synthesis, then the reaction was inactivated by incubation at 70° C for 15 min.

2.2.2.3. Polymerase chain reaction (PCR) using cDNA

The expression of histamine receptors H_1, H_2, H_3, H_4, and β-actin (positive control) were determined by PCR technology using specific primers (see 2.1.7). The amplification was performed with 160 ng cDNA, 0.5 µM of each primer (forward and reverse) and *GoTaq* polimerse (Promega). The following PCR program was used:

(First step 1 cycle)	94°C	3 min
(Second step 35 cycle)	94°C	30 sec
	57°C	30 sec
	72°C	1 min
(Third step 1 cycle)	72°C	5 min
(Forth step 1 cycle)	16°C	∞

2.2.2.4. Genomic DNA isolation

Genomic DNA was isolated from all $H_4R^{-/-}$ mice tails to perform genotyping. Mouse tail (0.6 cm) was incubated overnight with 500 µl lysis buffer (QIAGEN), 10 µl Proteinase K and 25 µl activated Pronase E (pre-incubation for 1 hour at 37°C). The proteins was precipitated with 6M NaCl by shacking it for 10 min at room temperature. The undesired protein and unlysed debris were centrifuged and the supernatant was collected in a new cup. The DNA content was precipitated with isopropanol, and the pellet was washed with ethanol 70% (V/V) and left to dry out in room temperature for at least 15 min. The pellet was dissolved in 75 µl RNase and DNase free water, and stored at -20°C.

2.2.2.5. DNA quantification

The DNA was quantified by measuring the absorbance of diluted solutions (1:25) with spectrophotometer at 260 nm, and the purity was measured by absorbance ratio at 260/280. The purity of all samples was between 1.6 - 2.0.

2.2.2.6. Agarose gel electrophoresis

PCR products were separated in 1% (W/V) agarose gel in TAE buffer with 0.4 µg/ml ethidium bromide. PCR samples were mixed with 6x loading dye (see 2.1.10.3.), and 20 µl were applied per well with the appropriate DNA ladder. Electrophoresis was performed at 90 volts for 50 min. The gel was visualized by UV light and photographed.

2.2.2.7. $H_4R^{-/-}$ mice genotyping

The mice were genotyped was performed by PCR according to the instructions fro Johnson & Johnson with two sets of primers (Fig. 2.1). Primers (JNJ11-31 forward primer located 166 bp upstream of exon 1, and JNJ11-32 reverse primer located 314 bp downstream to exon 1) should give a PCR product of 722 bp band only with WT genomic DNA. The other primer set is Neo3b (forward primer located at the 3' of the selection Neomycin cassette) and JNJ11-32. These primers should give a PCR product of 410 bp only with $H_4R^{-/-}$ genomic DNA. Therefore, all genomic DNA from $H_4R^{-/-}$ mice were tested with both primer pairs.

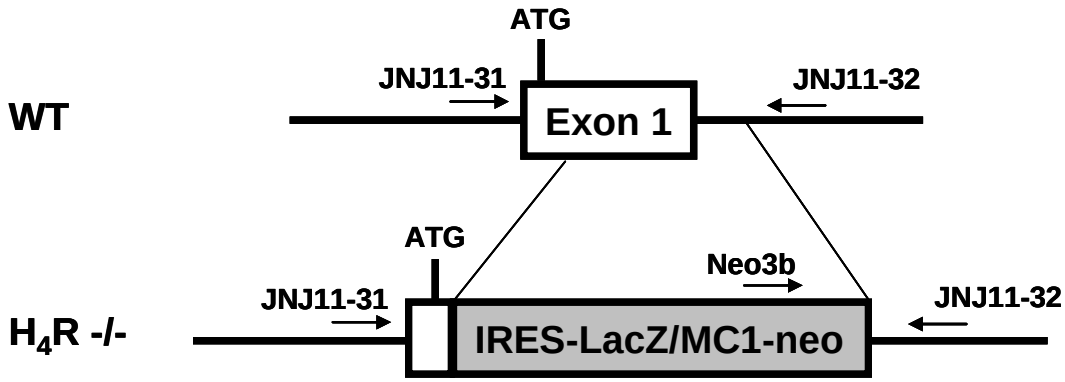

Fig. 2.1: the localization of primers in the gene map of WT and $H_4R^{-/-}$ mice.

Genotyping PCR was performed as follow:

200 ng	genomic DNA
1 µl	dNTP mix
5 µl (of 10 mM solution)	forward primer

5 µl (of 10 mM solution)	reverse primer
5 µl	5x *Taq* polymerase buffer
1 µl	*Taq* polymerase
H_2O to 50 µl.	

The PCR cycle details is:

(First step 1 cycle)	94°C	3 min
(Second step 35 cycle)	94°C	30 sec
	57°C	30 sec
	72°C	1 min
(Third step 1 cycle)	72°C	5 min
	16°C	∞

2.2.2.8. Real-time PCR

The real-time PCR was performed in IQ5 real-time PCR detection system (Biorad) with 0.25 µM of each primers, 50 ng of cDNA per well, and Sybergreen (iQ SYBR-Green supermix) as fluophore. The detailed reagents and volumes were:

12.5 µl	iQ SYBR-Green supermix
1 µl	5` primer (5 µM)
1 µl	3` primer (5 µM)
5.5 µl	Nuclease free H_2O
5 µl	cDNA

18S RNA was used as an endogenous house keeper to assess relative changes in mRNA amounts between samples. In the experiment setup, the target gene (mH_4R) and the house keeper were done in duplicate for each cDNA sample. The PCR protocol program was:

(First step 1 cycle)	95°C	3 min
(Second step 50 cycles)	94°C	10 sec
	57°C	30 sec
	60°C	30 sec
Melting curve step:	95°C	1 min
	57°C	10min
	57°C	30 sec (77x)
	16°C	∞

Sybergreen binds to the double-stranded DNA. This binding is detected by fluorescence of 521 nm emission wavelength after excitation at 494 nm. Real-time assay determine the time during cycles when amplification of PCR product is first detected, that cycle is referred as threshold cycle (C_t). Therefore, the higher starting copy number of the gene the faster the PCR product appears which mean lower C_t value. ΔC_t is calculated as follow:

$$\Delta C_t = \text{average } C_t \text{ (18s)} - \text{average } C_t \text{ (m}H_4\text{R)}$$

This value was used to calculate ($2^{-\Delta Ct}$) or the comparative quantification, this calculation is important in order to normalize differences in the mRNA extractions and efficiency of the reverse transcription. The relative mRNA expression or -fold changes of H_4R gene in each sample was compared to the control sample which was referred as a value of one [134;135].

2.2.3. Fluorescence activated cell sorter (FACS) technique

2.2.3.1. Examine the cellular markers of macrophages

BMDM on day 7 were gently scraped with rubber scraper and counted with trypan blue to visualize the dead cells. Around $5x10^5$ living cells were and resuspended in 100 µl FACS buffer and blocked with anti-FCγR (1:500) antibodies for 20 min on ice to avoid the unspecific binding of the labeled-antibodies on FcγR. FITC-labeled anti-CD11b antibodies and PeCy5-labeled anti-F4/80 antibodies were added to the cells and incubated for 20 min on ice in the dark. The cells were washed twice with FACS buffer, resuspended in 500 µl FACS buffer and analyzed in BD LSR II FACS® system according to the manufacturer's instructions. One tube containing unlabeled cells was used to set the auto-fluorescence value of the cells, in order to define the positive cells. Macrophage population was characterized as CD11b and F4/80 double positive cells. Bone marrow cells were analyzed in a similar procedure to determine the percentage of macrophages in bone marrow cells before differentiation to BMDM.

2.2.3.2. Examination of the cellular markers of BMDC

BMDC on day 8 were collected by vigorously aspiring the medium. The cell count, blocking, as well as washing steps were performed similar to BMDM. The cells were later stained with PE-labeled anti-CD11c antibodies as a specific marker of mouse DC, FITC-labeled anti-CD86 and APC-labeled anti-MHC II antibodies as markers of the DC maturation. Cells stained with each antibody separately were used to set the compensation of FACS system, this step is necessary to avoid the overlap between the fluorophore emission wavelength. Unstained cells were used to set the auto-fluorescence range.

2.2.3.3. Sorting mature and immature BMDC with cell sorter

BMDC stimulated with LPS for 24 h were subjected to staining with PE-labeled anti-CD11c antibodies, FITC-labeled anti-CD86 antibodies and APC-labeled anti-MHC II antibodies. After blocking with anti-FcγR, single staining with each of the previous antibody was performed to adjust the compensation of cell sorter. After a washing step, the cells were analyzed by BD FACS Aria cell sorter, and separated into two populations: ($CD11c^+$, $CD8^-$, and MHC II^-) and ($CD11c^+$, $CD8^-$, and MHC II^-). Sorting was performed by first gating the CD11c positive cells, and among this cell population sort the cells to immature BMDC (CD86-/MHC II-) and mature BMDC ($CD86^+$/MHC II^+). The sorted cells were collected in FACS tubes containing 1 ml FCS; the cells were kept on ice and proceeded to RNA isolation.

2.2.3.4. Sorting $CD4^+$ T cells, $CD8^+$ T cells and B cells from mouse spleen

Splenocytes from 13 week-old female C57BL/6 mouse (see 3.1.2.4.) were divided into three parts and stained with labeled-antibodies as follow: APC-labeled anti-CD3 antibodies and PE-labeled anti-CD4 antibodies to stain $CD4^+$ T cells, or with APC-labeled anti-CD3 antibodies and PE-labeled anti-CD8 antibodies to stain $CD8^+$ T cells, or with PE-labeled anti-B220 to stain B cells. After washing with FACS buffer, $CD4^+$ T cells ($CD3^+$ and $CD4^+$), $CD8^+$ T cells ($CD3^+$ and $CD8^+$) and B cells ($B220^+$) cells were collected in FACS tubes containing 1 ml FCS; the cells were kept on ice and proceeded to RNA isolation.

2.2.4. Cellular functional assays

2.2.4.1. BMDM chemotaxis assay

Chemotaxis assay was performed in a Neuro Probe 48-Well Micro Chemotaxis Chamber ® according to the provider instructions, the protocol was reported by Falk *et al.* in 1981 with minor modifications [136]. Chemotaxis medium used in the assay was RPMI containing 1% BSA (W/V). Six bottom wells for each concentration were filled either with 27 µl (has to form a slight meniscus to prevent air bubbles when the filter is applied) of pre-warmed medium alone as negative control, or with chemoattractant (4MEH or fMLP as a positive control) diluted with the previous medium. fMLP was used as positive control at concentration of 10 nM. Poycarbonate PVP-coated filter with 5 µm pore size was used to separate the bottom wells from the upper wells. The chamber was incubated at 37° C wit h 5% CO_2 for 25 min to ensure the gas equilibration before filling the upper chamber with cells. BMDM cells were gently scraped and resuspended in medium. Fifty µl medium containing 2 x 10^4 cells were added into the upper wells; the chamber were incubated for 1.45 h. Thereafter, the chamber was disassembled, and the upper side of the filter was carefully wiped to remove all remaining non-migrated cells. Cells adherent to the other side of the filter were stained with Diff-Quick staining kit and were counted on the microscopy. The counting procedure was to count the cells in 4 vertical frames which form the middle line of the each well. The obtained number was considered the number of migrated cells in the well. To test the chemotaxis activity of H_4R, 4MEH was used as a selective agonist of H_4R. To test the role of other histamine receptors in the chemotaxis activity, BMDM were incubated with 1 µM of each one of the antagonists (mepyramine as H_1R antagonist, famotidine as H_2R antagonist and JNJ 7777120 the selective H_4R antagonist) for 10 min at 37° C before starting t he assay. All three antagonists were dissolved in DMSO at a concentration of 10 mM and diluted in medium to a final concentration of 1 µM. In order to exclude the solvent effect, cells incubated with 0.01% (V/V) DMSO were used as a control.

2.2.4.2. Phagocytosis

2.2.4.2.1. BMDM phagocytosis of FITC-micro beads

Phagocytosis assay was performed with BMDM on day 7 generated in 6 well plates. The cells were incubated with 0.75 µm FITC-labeled polystyrene-based spheres (Fluoresbrite microbeads) at concentration of 5 x 10^7 /ml from which 0.5 µl/ml were taken. The cells were later incubated in a humid incubator at 37° C with 5% CO_2 for 2 hours. Thereafter, the cells were washed twice with 4 ml chilled FACS buffer to remove free beads, before gently scraping the cells and washing them twice with 5 ml chilled FACS buffer. Thereafter, the cells were resuspended in 1% (W/V) trypan blue to quench the extracellular FITC-beads. This step is essential in order to distinguish between the ingested beads and the beads attached to the external cellular compartments [137]. Cells were later analyzed in BD LSR II FACS system to determine the percentage of FITC-positive cells, the cells were considered positive with at least one ingested bead. From the FITC-positive population the mean fluorescent intensity (MFI) was inspected from 3x10^5 cells per each sample.

2.2.4.2.2. Peritoneal macrophage phagocytosis of FITC-micro beads

After isolating the peritoneal macrophages, the cells were incubated similar to the BMDM phagocytosis protocol. After 2 h, similar washing step was performed and 5x10^5 cells were collected and blocked with anti-FcγR for 15 min and then stained with anti-F4/80 (PeCy5 labeled) for 15 min. After washing step, the cells were re-suspended in 1 % (W/V) trypan blue and proceeded to FACS analysis. The cells were gated for F4/80 +/- cell populations, among the F4/80-positive cells the FITC signal was investigated, MFI values were measured from 3x10^5 cells per each sample.

2.2.4.2.3. BMDM phagocytosis of CFSE-labeled *L. major*

L. major promastigotes were cultured on blood-agar medium in 96 well plate, and were split once per week. To recover the virulence activity, parasites were injected in the footpad of BALB/c mouse after 11 passages, and isolated and cultured again on blood-agar medium. Promastigotes after passage 2 were isolated from the culture plate and washed twice with PBS. The promastigotes pellet was incubated

with 1 µM of carboxyfluorescein succinimidyl ester (CFSE) (1 ml for 10^7 promastigotes) in the incubator at 37° C for 10 min . Thereafter, the cells were washed twice with PBS 5% FCS.

From the CFSE-labeled promastigotes ~ 6 promastigotes / macrophage (5-10) were added to BMDM on day 7 generated in 6 well plates. After 6h, the supernatant medium was discarded and the cells were washed twice on the plate, and then gently scraped with rubber cell scraper and washed twice on the tube with PBS 5% FCS. Finally the cells were fixed with PBS containing 2% (V/V) FCS and 2 % para-formaldehyde for 15 min. The cells were later used in FACS system to investigate the percentage of CFSE positive cells. To setup the auto-fluorescence value, macrophages without CFSE-labeled promastigotes were used.

2.2.4.3. Nitric oxide production

The nitric oxide (NO) production was determined using Griess reagent (see 2.1.9.4.) the reagent was prepared directly before performing the assay. NO production was determined in the supernatant of LPS and IFN-γ activated BMDM for at least 48 hours (NO accumulation). In 96 well plate, 100 µM sodium nitrite was used to prepare six points standard curve, by serial diluting till 3.125 µM with normal cells medium as an assay diluent. Final volume was 100 µl per well in duplicates. Another 100 µl of Griess reagent were added to the wells, and then optical density was determined using a microplate ELISA reader set to 550 nm, after using the assay diluent as a blank.

2.2.4.4. IL-6 and TNF ELISA

IL-6 and TNF were measured using commercially available kits (R&D Systems). The principle is to coat 96 well plate with the specific capture antibody in PBS overnight at 4° C. The wells were later blocked with 1% BSA (W/V) in PBS (reagent diluent) for 2 hours to inhibit the unspecific binding. In the next step, 100 µl of samples were added, and the standard was prepared by 1:1 serial dilution of the standard stock solution (1000 and 2000 pg/ml for IL-6 and TNF respectively). After 2 hours at RT the biotinylated-detection-antibodies were added for 2 hours at RT, then 1:200 diluted streptavidin-HRP were added for 20 min. A washing step was performed after each step previously mentioned by aspirate the wells with 200 µl of

0.05% (V/V) tween 20 in PBS for 3 times. After that 100 µl of HRP-substrate (TMB substrate solution for ELISA, 1:1 mixture of solution A and B) were added for 20 min and then the reaction was stopped with 50 µl of 2N H_2SO_4, the optical density was determined using a microplate ELISA reader set to 450 nm, after using the assay diluent as a blank.

2.2.5. Antibody generation technique

2.2.5.1. Mouse immunization

Two synthesized peptides (2.1.12) were used to immunize two female $mH_4R^{-/-}$ mice (9 weeks old) separately. The immunization plan is shown in (Fig 2.2.2.), which aims to increase the antibody production against the target peptide. Two days before the immunization, pre-serum was collected from both mice, in order to be used as negative control for the screening. The mice were immunized as follow:

- On day 1: 100 µg peptide diluted with PBS were mixed with complete Freund's adjuvant (1:1) to form emulsion using 2 syringes connected to each other *via* a metal connector. The mixture was pressed in between the two syringes 10 time every 10 min and kept on ice for 30 min. Thereafter, 300 µl of the previous mixture containing 100 µg were injected in each mouse intra-peritonealy.
- On day 21: the same previous procedure was performed but with incomplete Freund adjuvant.
- On day 25: Serum was collected from both mice in order to inspect the antibody production in serum.
- On day 42: another immunization step was performed with 100 µg peptide without any adjuvant as a boost.
- On day 45: serum was collected from both mice, and their splenocytes were isolated and frozen in liquid nitrogen.

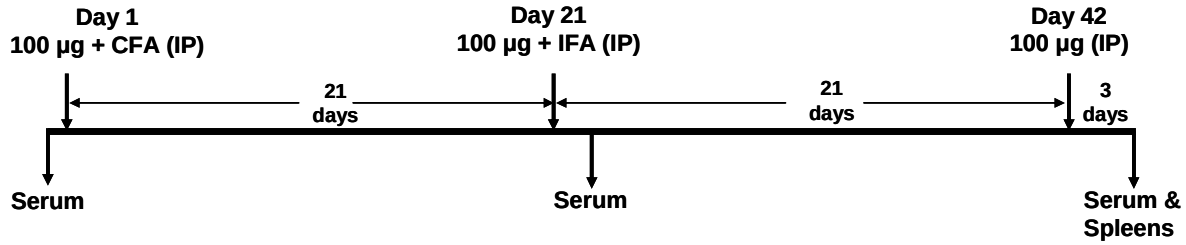

Fig. 2.2.: Immunization plan to generate mouse anti-mH_4R antibodies in mH_4R $^{-/-}$ mice.

2.2.5.2. Serum isolation from mouse blood

Mouse blood was incubated at RT for 1h and then at 4° C overnight. The next day, the blood was centrifuged at 1400 g for 7 min to separate the serum, sera was stored at -20 °C

2.2.5.3. ELISA test to determine the antibodies titer in mouse serum after immunization

ELISA test was used to screen antibody production in the immunized mice. In order to avoid the unspecific antibodies against KLH, the two peptides coupled to BSA were used in the ELISA screening test. A 96 well plate was coated with 100 µl containing 200 ng peptide and incubated overnight at 4° C. Washing step was performed three times by rinsing with TBS-T, and then the plate was blocked with 1% BSA (W/V) in TBS for 2 hours. From the mice serum 1:100 serum dilutions (triplicate) was used in 1:1 serial dilution to 1:25600, the plate was incubated at room temperature for 2 hours. Serum from the same mouse before immunization was used as negative control at the dilution 1:100. Washing step was performed as before to remove the unspecific binding, and then 1:10.000 detection antibody (goat anti-mouse IgG (whole molecule) AP conjugated) were incubated for 2 hours at room temperature. Thereafter, washing step as before was performed and 100 µl of the AP substrate were added (20 mg of 4-nitrophenyl phosphate disodium salt hexahydrate as tablet) dissolved in 10 ml AP buffer (diethanolamine buffer). To stop the reaction 50 µl of H_2SO_4 were added and the yellow color density was determined at 405 nm in ELISA plate reader. Optical density (OD) values were used to determine the serum titer, which was the dilution with double OD value of the negative control.

2.2.5.4. Freezing mouse spleen cells in liqud nitrogen

Both spleens were isolated and homogenized to prepare a single cell suspension. Each spleen was split in three parts and mixed (1:1) with freezing medium (80% FCS and 20% DMSO) at a density of $3x10^7$ cell per tube. The cells were frozen at -80 °C and then transferred in the liquid nitrogen tank.

2.2.6. Protein techniques

2.2.6.1. Cell protein lysate preparation

To prepare the protein lysate from the cells, 1 ml RIPA buffer per 10^7 cells was used. After mixing, the cells were centrifuged at 13000 g for 10 min at 4° C, and the supernatant was collected and stored in -80° C for further experiments.

2.2.6.2. SDS-PAGE

The gel was prepared with Mini-PROTEAN 3 system from Biorad. To form the separation gel, a 12 % (W/V) polyacrylamide gel was prepared and left to polymerize at RT in the system. Thereafter, the collection gel (4% (W/V) polyacrylamide) was poured on the top of the separation gel and left to polymerize at RT. Sixteen µl containing 20 µg protein lysate + 4 µl H_2O and 4 µl 4x Lämmli buffer were incubated for 5 min at 95° C, and then loaded in the well. A protein standard (Biorad) was used as molecular weight marker. The gel running step was performed with 60 mA for 45 min.

2.2.6.3. Western Blot

The previously separated protein lysates were blotted on PVDF membrane. The blotting was performed in three-buffer semi-dry blotting system. First the membrane was rehydrated in methanol for 1 min before soaking it in transfer buffer B. Whatman papers soaked with transfer buffers A, B and C were used to form the layers as follow (from cathode to anode):

3 layers Whatman paper (transfer buffer A)

3 layers Whatman paper (transfer buffer B)

Membrane (transfer buffer B)

Separating gel (transfer buffer C)

3 layers Whatman paper (transfer buffer C)

The layers were formed without air bubbles and bloting was preformed at 1 mA/cm^2 for 1 h. The membrane was blocked after that with 2% low-fat milk powder solution in TBS for 2 h, and then incubated with the primary antibodies solution (1:100 in the same blocking solution) over night at 4° C with sha king. The membrane was washed with TBS-T three times (5 min each) and then incubated with HRP-labeled secondary antibodies depending on the isotype of the first antibody for 1 h at RT. After washing (3 times 5 min each), the HRP substrate (Nowa A and B solutions) was added directly on the membrane in the dark before incubating the membrane with Amersham hyperfilm ECL in the film cassette. The film was developed in the film developer system.

2.2.7. High-dose infection model of *L. major* in C57BL/6 WT and $H_4R^{-/-}$ mice

L. major promastigotes were cultured on blood agar medium and isolated after three passage and washed twice with PBS. Thirty µl containing 3x10^6 promastigotes were injected subcutaneously in the right footpad to generate the high-dose infection in the mice paws. The infected and non-infected footpad thicknesses were weekly measured after infection by mechanical external measuring gauge, and the percentage of footpad swelling was calculated as the difference of feet thickness between the infected and non-infected paws as follow:

(infected foot [mm] – non-infected [mm] / non-infected [mm]) x 100.

3. Results

3.1. The role of mH_4R in DC

3.1.1. BMDC expression of mH_4R

In the aim of establishing a cellular model to study the role of mH_4R in the immune system, the expression of mH_4R in DC was investigated. In mouse model, DC and their subtypes exists in almost all tissues. In order to isolate a sufficient number, DC can be isolated from the spleen (lymphoid-tissues-resident DC) as well as from other tissues, or generated from bone marrow cells. BMDC were considered as a conventional DC generated *in vitro.*

Bone marrow cells from female C57BL/6 mice (10 weeks of age) were cultured in medium containing GM-CSF (see 3.1.2.3.) to be differentiated to DC as mentioned in Material and Methods. mRNA was isolated from bone marrow cells to inspect the expression of mH_4R by RT-PCR. On day 8 of culture, the cells were stained with PE-labeled anti-CD11c antibody and subjected to FACS assay to analyze the expression of CD11c, as a specific marker of mouse DC. The results show that 77.1% of the viable cells population were CD11c-positive DC (Fig. 3.1), indicating the successful differentiation. mRNA probe was also isolated to inspect the expression of mH_4R by RT-PCR.

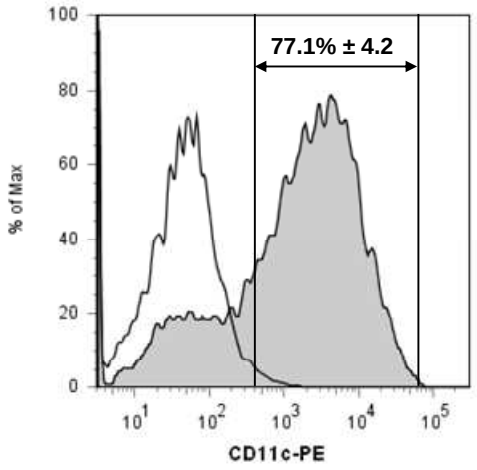

Fig. 3.1: The expression of CD11c on BMDC cells. BMDC express CD11c, the specific marker for mouse DC. FACS data show that 77.1 % of the living cells on day 8 were CD11c positive (gray) compared to the isotype staining (white). The experiment was performed in duplicate, the percentage represents mean of the values and SD.

BMDC generated during 8 days in the presence of GM-CSF are immature DC. The cells have not encountered any antigen to be processed and presented to T cells, which convert the immature DC to the mature status. Mature DC are characterized by co-expression of CD80, CD86 and MHC II in addition to CD11c.

In order to test for the expression of mH_4R mRNA in mature BMDC, immature BMDC were stimulated for 24 hours with 10 ng/ml of LPS. Thereafter, mRNA was isolated. The expression of mH_4R was analyzed by RT-PCR using cDNA from bone marrow, immature BMDC from day 8, and mature BMDC day 9 as templates, with the specific mH_4R primers and GAPDH as a positive control. RT-PCR results show a specific band with the mH_4R primers indicating the expression of mH_4R on the mRNA level in all these cell preparations (Fig. 3.2).

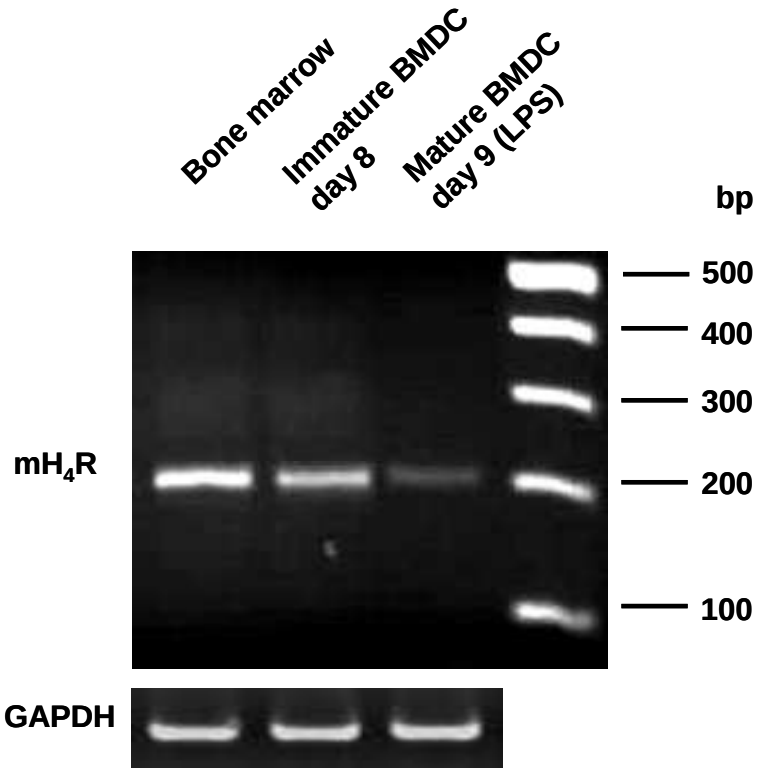

Fig. 3.2: the expression of mH_4R in immature and mature BMDC on the mRNA level. cDNA from bone marrow cells, immature and mature BMDC were analyzed by RT-PCR. The expected PCR product with the mH_4R primers indicated the expression of mH_4R in these cells.

3.1.2. Expression of known histamine receptors in immature BMDC

With the aim of characterizing the expression profile of other histamine receptors in BMDC, RT-PCR was performed with cDNA from immature BMDC and mH_1R, mH_2R, m H_3R, and mH_4R-specific primers and β-actin as a positive control. Fig 3.3 shows H_1R- H_2R- and H_4R-specific bands. However, no band was obtained with H_3R specific primers (Fig. 3.3).

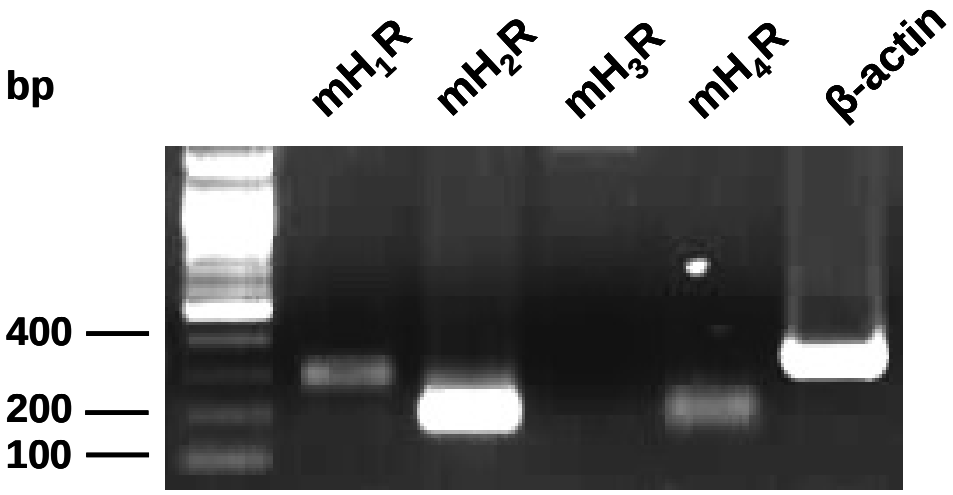

Fig. 3.3: Histamine receptor expression in immature BMDC. RT-PCR shows H_1, H_2 and H_4 receptors expression on the mRNA level in immature BMDC.

3.1.3. Regulation of mH_4R expression during bone marrow differentiation and maturation of BMDC

Since RT-PCR does not provide quantitative results, the same samples as in Fig. 3.2 were subjected to real-time PCR, to quantify the mRNA levels of mH_4R from bone marrow cells, immature and mature BMDC. The expression levels were normalized to the ribosomal RNA 18s as a house keeper (see 3.2.8.). Real-time PCR results show that the differentiation of bone marrow cells to BMDC was associated with down-regulation of mH_4R expression. The down-regulation was even stronger after BMDC maturation with LPS (Fig. 3.4).

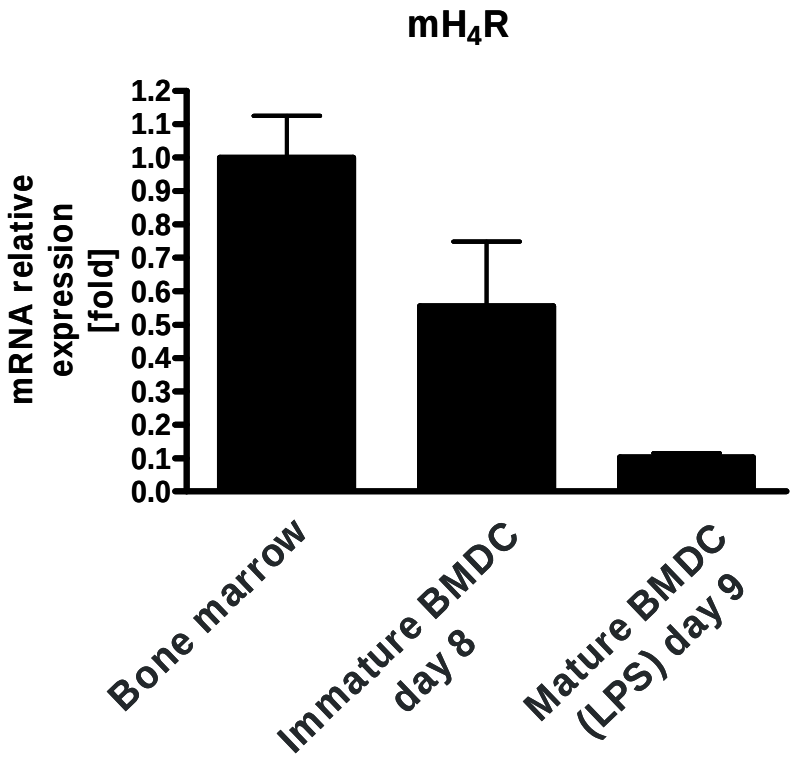

Fig. 3.4: Expression of mH_4R is down-regulated during bone marrow differentiation to BMDC and during BMDC maturation. Real-time PCR was performed in duplicates, and the expression of mH_4R was calculated relative to the house keeper 18s. The expression levels are put in relation to mH_4R expression in bone marrow cells. Data represent mean ± SD of the normalized values.

To validate the previous data with mH_4R expression in mature and immature BMDC, WT bone marrow cells were differentiated to BMDC, and subsequently stimulated for 24 h with 10 ng/ml LPS. The cells were stained for CD11c, CD86 and MHC II with flurochrome-labeled antibodies. The labeled cells were sorted by FACSAria® cell sorter. The sorting procedure was first to gate for the CD11c positive cells, and among this cell population sort the cells into immature BMDC (CD86-/MHC II-) and mature BMDC ($CD86^+$/MHC II^+). mRNA was isolated from the sorted cells (mature and immature BMDC), and then cDNA was subjected to real-time PCR with specific mH_4R primers and 18s as a house keeper. The data show that mature BMDC expressed less mRNA level of mH_4R than immature BMDC (Fig. 3.5), which confirms the previous data of mH_4R down-regulation during LPS-induced BMDC maturation.

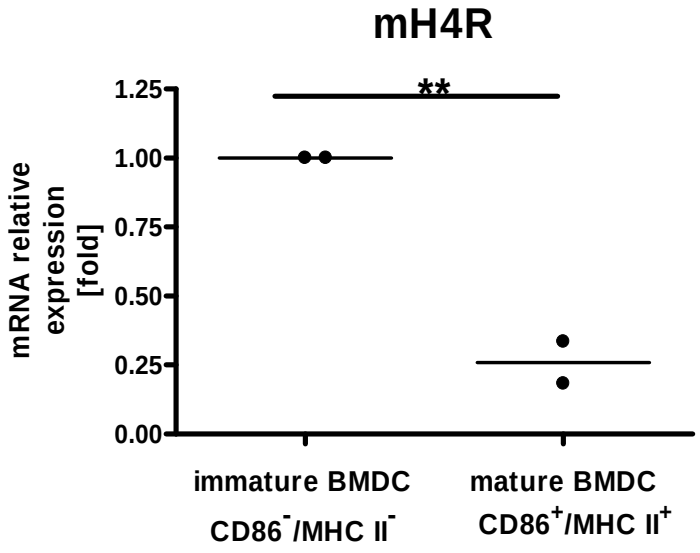

Fig. 3.5: Mature BMDC express less mH_4R mRNA than immature BMDC. Real-time PCR results of mH_4R expression in sorted immature BMDC (CD86-/MHCII-) and mature BMDC ($CD86^+$/$MHCII^+$). Each dot represents an independent experiment, performed in duplicate, and the expression was normalized relative to 18s and calculated as fold of immature BMDC values. ** $p < 0.005$ in two-way ANOVA test.

3.1.4. Role of histamine and 4-methylhistamine (4MEH) in the maturation of BMDC

Down-regulation of mH_4R during BMDC maturation raised the question whether mH_4R plays a role in the maturation of BMDC. In order to investigate this point, BMDC on day 8 were stimulated for 24 h with histamine and 4MEH in the presence or absence of LPS (50 ng/ml) (see 3.1.3.4.). After 24 h the cells were tested by FACS to determine the maturation status of BMDC population based on the expression of CD86 and MHC II among $CD11c^+$ cells (Fig. 3.6.a).

The results show a higher percentage of mature BMDC in the cell population stimulated with LPS in comparison to the non-stimulated cells. No effect on maturation was observed by histamine or 4MEH-stimulation. Also, no synergistic effect was obtained by combining stimulation of LPS with histamine or 4MEH (Fig. 3.6.b).

A)

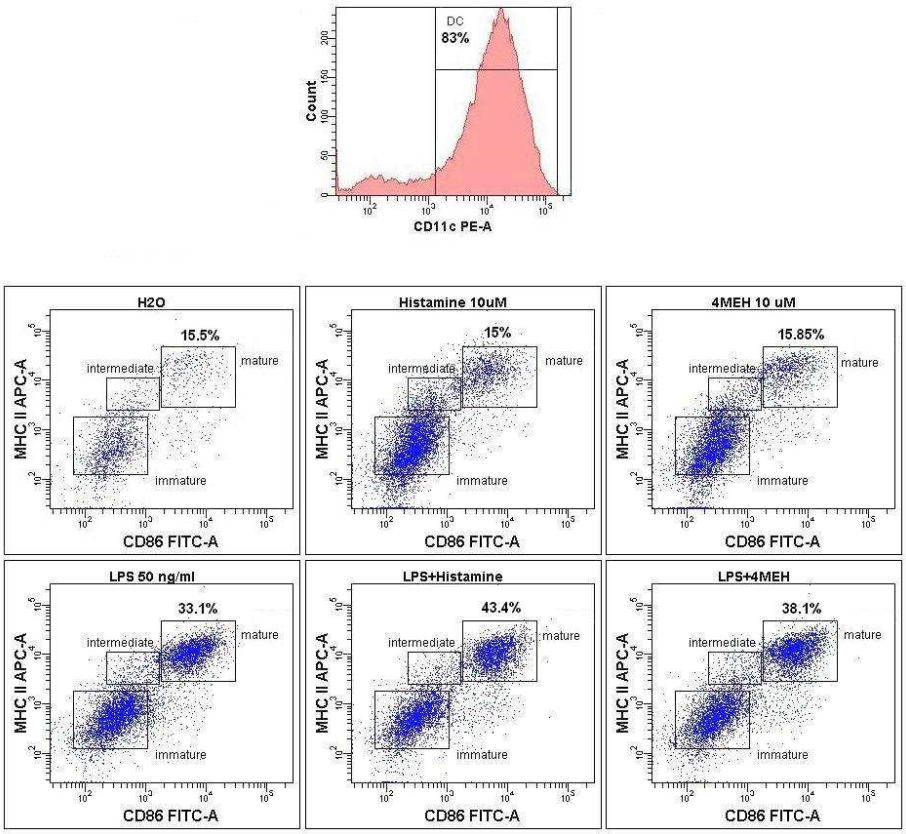

B)

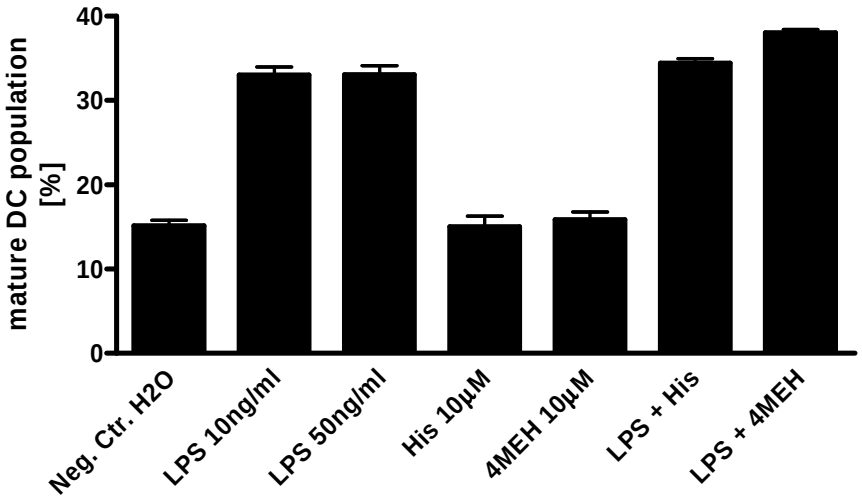

Fig. 3.6: BMDC mature and immature populations in response to LPS, histamine and 4MEH. A: The upper histogram shows that 83% of the cells were $CD11c^{+}$ cells (DC) in the gated population. From this population the expression of CD86 and MHCII was inspected, this resulted in three populations gated in three boxes. In the gate for mature cells double positive expression of CD86 and MHCII is found. In the gate for immature the cells double negative expression of CD86 and MHCII is found, cells with low expression of CD86 and MHCII were gated in the intermediate gate. The experiment was performed in duplicate. B: Percentages of mature BMDC obtained from the FACS data. The experiment was performed in duplicate and data show mean of the values ± SD.

3.2. The expression of mH_4R in immune organs and cells

3.2.1. Spleen and lymph nodes

The expression of mH_4R in immune organs was investigated in spleen and lymph nodes of female C57BL/6 mouse (10 weeks). The spleen, axillary and brachial lymph nodes were isolated, thereafter subjected to mRNA isolation and later to RT-PCR. The specific PCR product size was observed with mH_4R specific primers indicating that mH_4R is expressed on the mRNA level in these organs (Fig. 3.7)

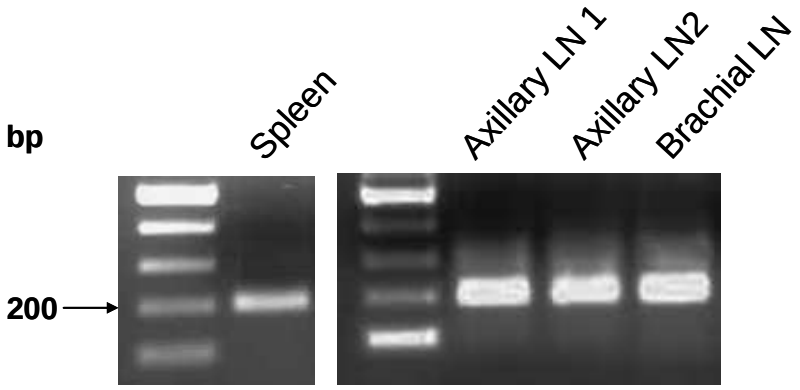

Fig. 3.7: The expression of mH_4R on mRNA level in spleen, axillary, and brachial lymph nodes of a 10 week old female C57BL/6 mouse.

3.2.2. $CD4^+$, $CD8^+$ -T cells and B cells

In order to investigate the expression of mH_4R in other immune cells, the next targets were $CD4^+$ T cells (T-helper cells), $CD8^+$ T cells (cytotoxic T cells) and B cells. The mouse spleen as a secondary lymphoid organ represents a suitable organ to isolate these lymphocytes. Therefore, the spleen from a C57BL/6 female mouse (11 weeks) was used to prepare a single cell suspension. Splenocytes were stained for CD3 and CD4, CD3 and CD8 or B220 separately with labelled-antibodies in order to be used in the cell sorting process. The cells were later sorted by FACS cell sorter which separates the cells according to their specific staining (Fig. 3.8).

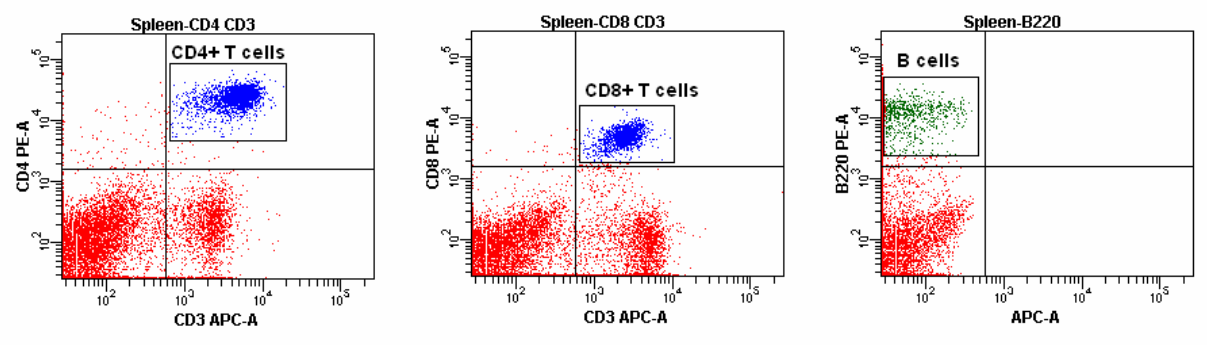

Fig. 3.8: CD4, CD8-T cells and B cells from the spleen according to the expression of the specific cell markers. In the left dot-blot, $CD3^+$ and $CD4^+$ cells (10.5% of splenocytes) were gated and sorted as $CD4^+$ T cells. In the middle dot-blot, $CD3^+$ and $CD8^+$ cells (6.5% of splenocytes) were gated and sorted as $CD8^+$ T cells. In the right dot-blot, $B220^+$ cells (26.5% of splenocytes) were gated and sorted as B-cells.

The sorted cells were subjected to RNA isolation and RT-PCR with mH_4R-specific primers. Specific PCR products were obtained from $CD4^+$ T cells and $CD8^+$ T cells, but not from B cells, indicating that mH_4R is expressed in $CD4^+$ and $CD8^+$ T cells but not in B cells on the mRNA level (Fig. 3.9)

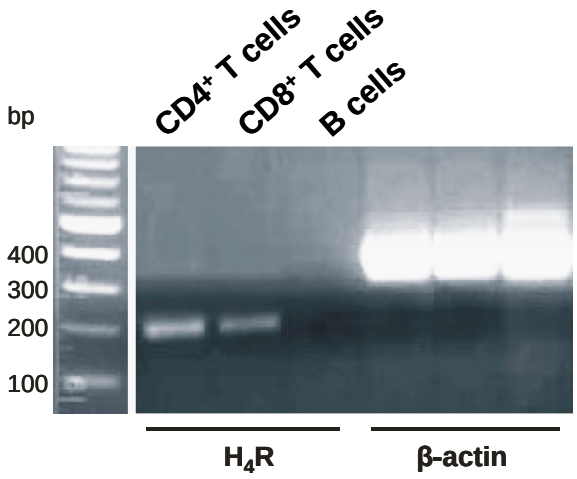

Fig. 3.9: The expression of mH_4R in $CD4^+$, $CD8^+$ T cells but not in B cells. RT-PCR was performed with cDNA from sorted $CD4^+$, $CD8^+$ T cells and B cells, β-actin was used as a positive control.

3.3. The role of mH_4R in macrophages

3.3.1. Screening several cell lines for the expression of mH_4R

The initial aim of the project was to identify a cellular model to examine expression, regulation as well as function of mH_4R. Therefore, primary and *ex vivo*-generated immune cells as well as several cell lines were screened to determine the expression of mH_4R. Cell lines were selected from cell types or tissues where the positive expression was expected, such as macrophage cell lines (RAW 264.7, J774.1 and Pu5-1.8), mast cells (P815), fibroblasts (WEHI 164) and Lung epithelial cell line (LA-4). RT-PCR results (Fig. 3.35) show an expression of mH_4R on the mRNA level.

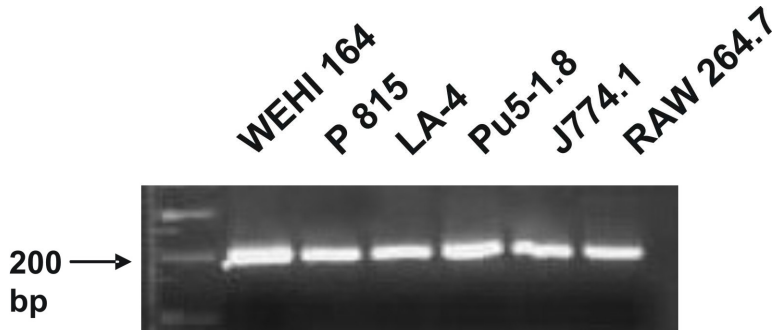

Fig. 3.10: RT-PCR shows the expression of mH_4R on mRNA level in several tested cell lines.

3.3.2. Isolation and characterization of macrophage populations

3.3.2.1 Bone marrow derived macrophages (BMDM)

The previous results showing the expression of mH_4R in macrophage cell lines (Fig. 3.10), in addition to the expression of human H_4R on monocytes mentioned the literature, raised the question about possible expression of mH_4R in *ex vivo* generated macrophages and primary macrophages [49].

BMDM were differentiated *in vitro* from bone marrow cells of a 12 week old female C57BL/6 mouse, in medium containing M-CSF (macrophage medium) for 7 days. FACS technique was used to monitor the macrophage population development during the 7 days. Macrophages were characterized as cells expressing F4/80

(specific macrophage marker), and CD11b (myeloid marker), the cells were analyzed on day 0 (bone marrow cells), day 5 and day 7. The results show a clear increase in the macrophage population starting from 2.9 % in bone marrow cells on day 0, to 95.1 % on day 5, and 98.4 % on day 7 (Fig. 3.11) indicating successful differentiation. RNA was isolated from BMDM on day 7 to perform RT-PCR (see 3.3.2).

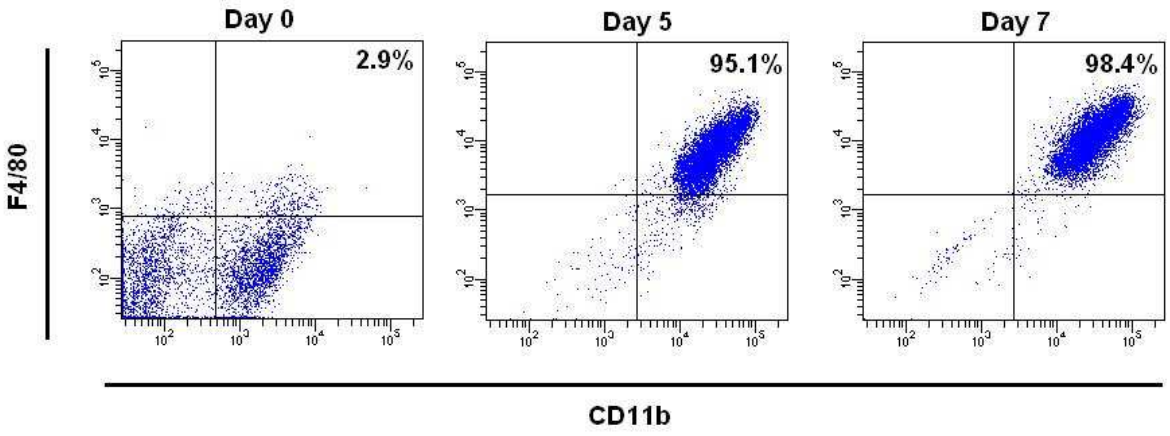

Fig. 3.11: Development of the macrophage population ($CD11b^+$ and $F4/80^+$) during bone marrow cells differentiation. FACS dot-plots show that bone marrow cells contained 2.9 % macrophages ($CD11b^+$ and $F4/80^+$ cells in the upper right square of the dot blot). The percentages increased to 95.1% on day 5 and 98.4% on day 7. The experiment was performed in duplicate and the percentages represent the means from one of four independent experiments.

3.3.2.2. Peritoneal macrophages

The expression of mH_4R in primary mouse macrophages was analyzed in peritoneal macrophages. These macrophages are the largest population among the PEC. Two female C57BL/6 mice at the age of 12 week old were used to isolate PEC (see 2.2.1.2.2.). The cells were pooled from both mice and incubated to adhere for two hours in RPMI medium. Part of the adherent cells were subjected to RNA isolation (see 3.3.2), and the rest were stained with labeled antibodies for the expression of CD11b and F4/80 in order to determine the percentage of macrophages by FACS. The results revealed that 82.7 % of the whole viable cell population consisted of macrophages ($F4/80^+/CD11b^+$) as shown in fig. 3.12.

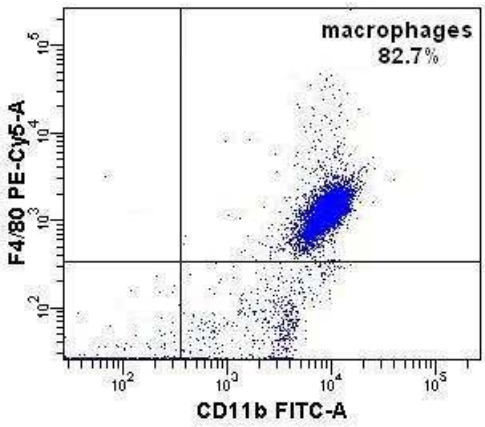

Fig. 3.12: Percentage of macrophages in PEC. Dot-plot FACS shows the macrophage population in the upper right square ($F4/80^+/CD11b^+$) consisting of 82.7% of the peritoneal exudate cells. The experiments were performed in duplicates. The figure represents one of two independent experiments.

3.3.2.3 Macrophage cell lines RAW 264.7, and J774.1

In order to examine other types of macrophages, macrophage cell lines RAW 264.7 and J774.1 were cultured in RPMI medium, and harvested after passage 7 for RAW 264.7 and passage 4 for J774.1 to isolate RNA and perform RT-PCR (see 3.3.2).

3.3.3. Expression of mH_4R in mouse macrophages

RNA samples from BMDM, peritoneal macrophages, RAW 264.7 and J774.1 were used in RT-PCR with specific primers for all mouse histamine receptors. Specific PCR-products were observed with H_1R, H_2R and H_4R-specific primers, indicating that these histamine receptors were expressed on the mRNA level in all types of the investigated macrophages. However, no expression of H_3R was observed in these cells (Fig. 3.13).

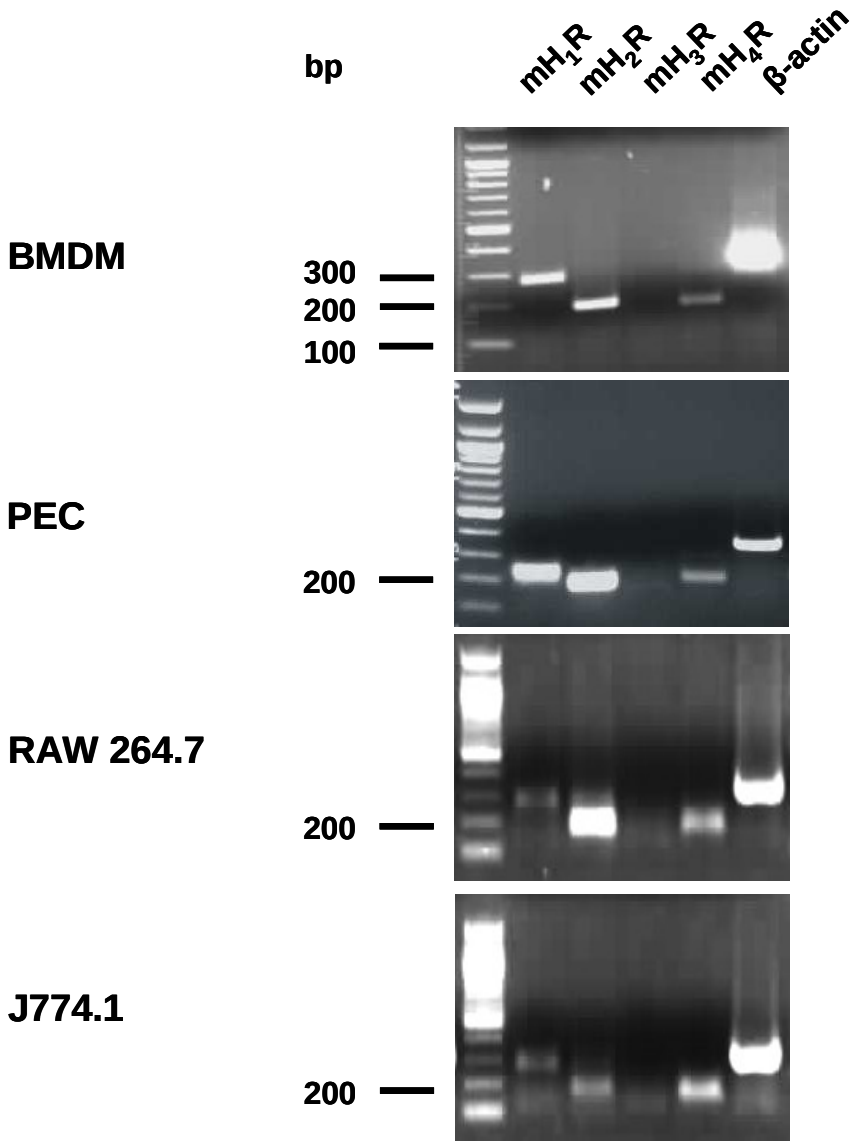

Fig. 3.13: The expression profile of histamine receptors in mouse macrophages. Several types of mouse macrophages were examined by RT-PCR for the histamine receptors expression. RT-PCR showed specific PCR products with H_1, H_2, H_4 and β-actin specific primers H_1, H_2 and H_4 receptors specific bands indicate the expression on the mRNA level, whereas H_3R was not detected.

3.3.4. Regulation of mH_4R expression in mouse macrophages

3.3.4.1. Regulation of mH_4R expression with pro-inflammatory cytokines in RAW 264.7 cells

In order to investigate the regulation of mH_4R expression in mouse macrophages, RAW 264.7 cells were stimulated with pro-inflammatory cytokines (IFN-α, IFN-γ, or TNF) for 3, 6, and 24 hours. The stimulated cells were subjected to RNA isolation at the indicated time points. Real-time PCR technique was used to

quantify the mRNA levels of mH_4R in the examined samples, which demonstrated that the expression of mH_4R is regulated in response to these stimuli in a transient way, while IFN-γ stimulation shows a stable up-regulation relative to the appropriate control (Fig. 3.14).

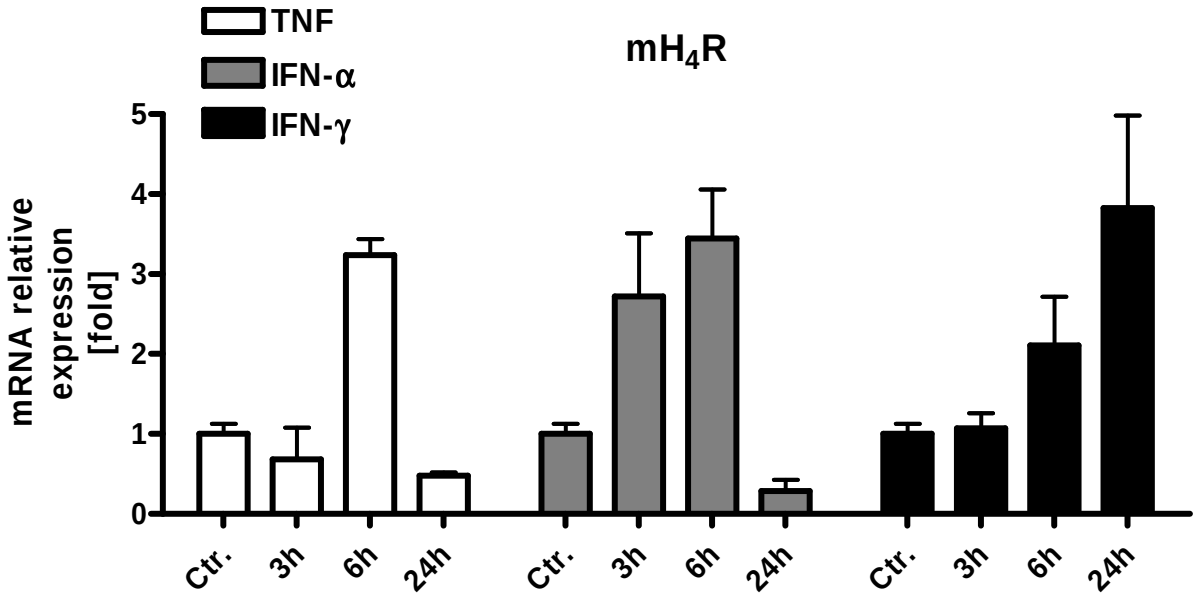

Fig. 3.14: TNF, IFN-α, and IFN-γ regulate the expression of mH_4R in different kinetic patterns. Expression of mH_4R was determined by real-time PCR after stimulating the cells with TNF, IFN-α, or IFN-γ for 3, 6 and 24 h. The real-time PCR experiment was performed in duplicate, and the expression was calculated relative to 18s. Results show the expression as fold of the value of the control cells. Data show the mean ± SD of the normalized values.

3.3.4.2. Effect of BMDM differentiation and activation on mH_4R expression

Based on previous data from BMDC, the question was whether the regulation of mH_4R expression in BMDM resembles that of BMDC, since both cell types differentiate from bone marrow, and they share several functions in the innate immunity such as chemotaxis, phagocytosis and antigen presentation.

Bone marrow cells from female C57BL/6 mice (14 weeks) were differentiated to BMDM. A part of the bone marrow cells was used to isolate RNA, and the rest were seeded in macrophage medium. On day 7, RNA was isolated from part of the cells and the other cultures were activated either with IFN-γ, or with LPS for 24 h. After this activation time the cells were harvested to isolate RNA. Real-time PCR results (Fig. 3.15) clearly showed a higher expression of mH_4R in bone marrow cells compared to BMDM. BMDM activation with IFN-γ for 24 h up-regulated the

expression of mH_4R around 4-fold relative to control cells. Conversely, LPS-activated macrophages for 24 h expressed very low level of mH_4R relative to the non-activated cells. The IL-4 activation did not show a significant effect on the mH_4R expression level after 24 hours.

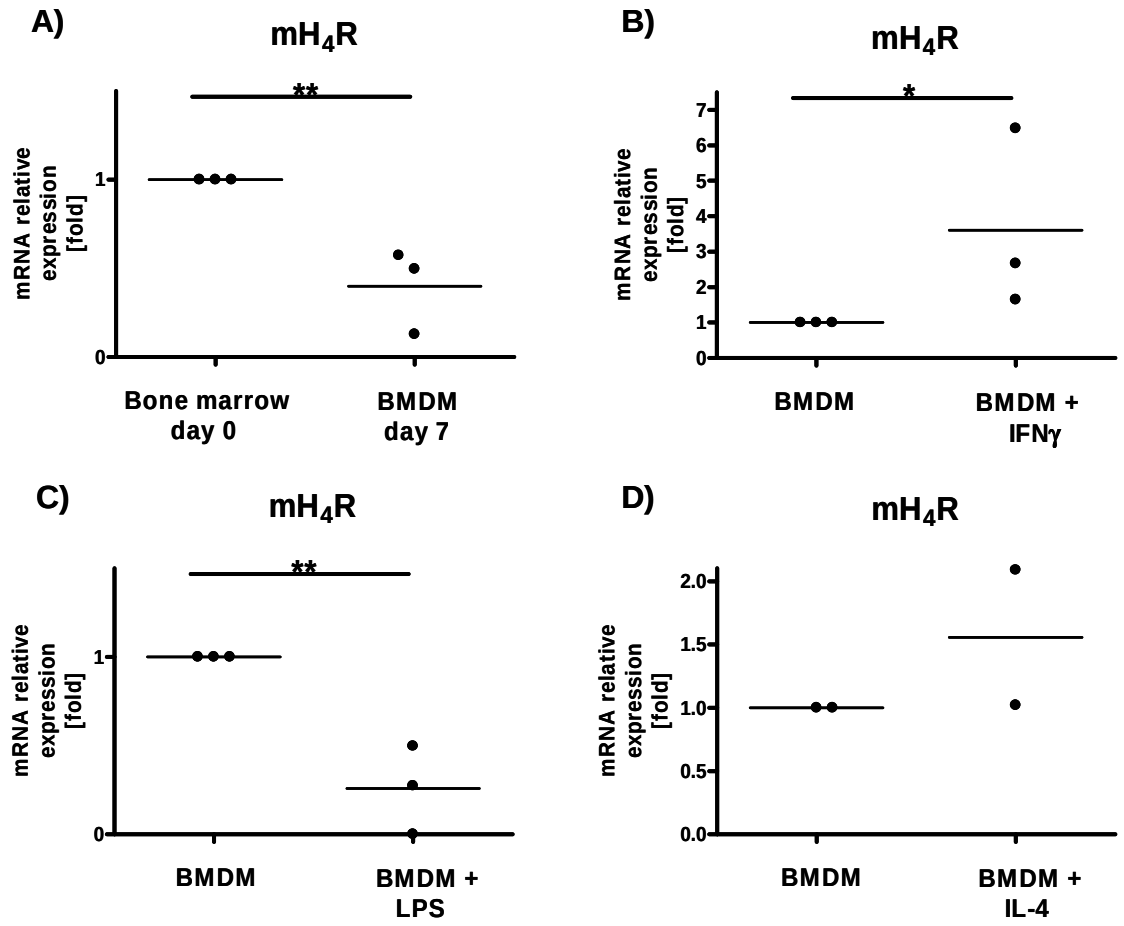

Fig. 3.15: Expression of mH_4R is regulated during bone marrow differentiation to macrophages and during macrophage activation. Using real-time PCR the expression of mH_4R was quantified to compare the expression between different cell states, A: bone marrow cells and BMDM on day 7. B: IFN-γ-activated BMDM for 24 h versus control cells. C: LPS-activated BMDM for 24 h versus control cells. D: IL-4-activated BMDM for 24 h versus control cells. Each dot represents an independent experiment, performed in duplicate, and expression was normalized relative to 18s and calculated as fold of control values. * $p<0.05$, ** $p<0.005$ in two-way ANOVA test.

3.3.5. Functional study of mH_4R on BMDM

3.3.5.1. Chemotaxis

Several publications have indicated that H_4R mediates a chemotactic effect on several immune cells like eosinophils, DC, and human monocytes [34]. Therefore, chemotaxis was one of the mH_4R functions investigated with mouse macrophages. In the assay setup, the specific H_4R agonist 4MEH was used to investigate whether it induces any chemotactic effect in BMDM or not. 4MEH was considered as a human H_2R agonist, but the discovery of H_4R revealed that it possesses 100-fold higher selectivity for human H_4R than human H_2R. Some other data show similar results for the mH_4R *in vitro* as well as *in vivo* [23;72].

3.3.5.1.1. mH_4R agonist induces chemotactic effect in BMDM

BMDM from day 7 culture were exposed to different concentrations of 4MEH in a chemotaxis chamber. After 1.45 hours, and after fixing and staining the cells on the filter, the migrated cells were counted under the microscope to assess cell migration (see 2.2.4.1.).

Chemotaxis assay data revealed a chemotactic effect of 4MEH on BMDM in a concentration dependent manner, with a peak around 100 nM of 4MEH. Unexpectedly, the cells showed also a significant migration in response to 100 µM of 4MEH, which is not typical for a chemotaxis bell-shape curve (Fig. 3.16) [49;115;116].

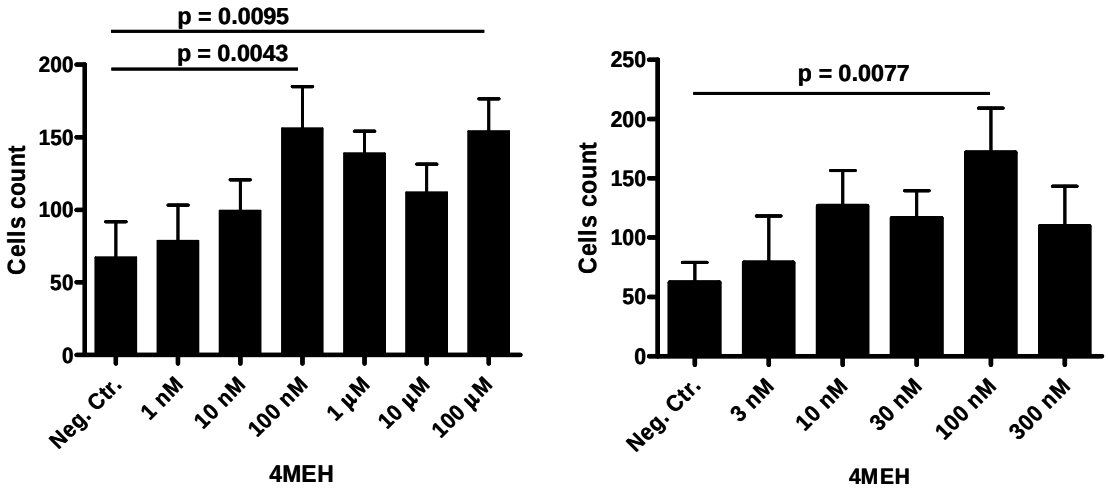

Fig. 3.16: 4MEH induced concentration dependent chemotaxis in BMDM. A chemotaxis assay was performed with BMDM day 7 in the presence of 4MEH. The cells migrated towards medium as negative control and towards 4MEH were counted. The experiments were performed in 6 wells for each concentration. Data show means ± SD, p values were calculated by two-way ANOVA test, representing one of at least 4 independent experiments.

3.3.5.1.2. mH_4R antagonist inhibited the chemotactic effect induced by 4MEH

Consequently, the next step was to answer the question whether 4MEH-induced chemotaxis is mediated by mH_4R or not. Therefore, BMDM day 7 were challenged with several concentrations of 4MEH in a chemotaxis assay after pre-incubating the cells with 1 µM of JNJ 7777120 as a selective mH_4R antagonist for 10 min before starting the assay. The results show that 1 µM of JNJ 7777120 was able to block the cells migration up to a concentration of 1 µM of 4 MEH (Fig. 3.17). At higher concentrations of 4MEH the cells resumed migration.

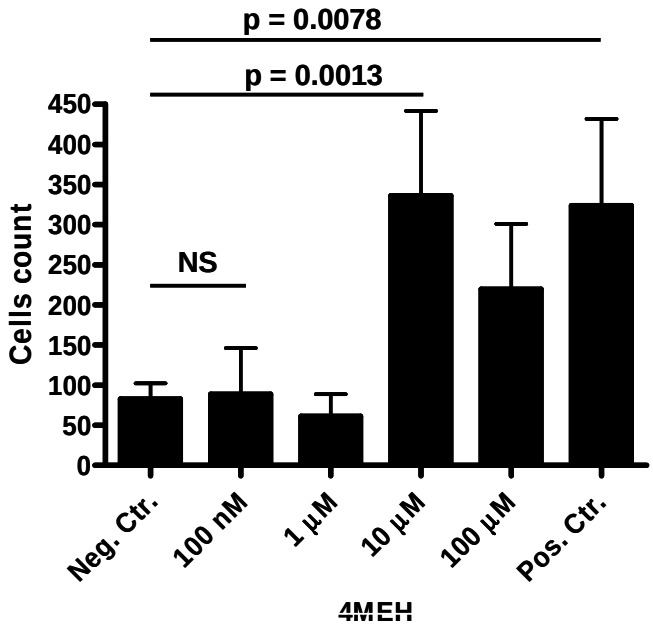

Fig. 3.17: JNJ 7777120 inhibited 4MEH-induced chemotaxis in BMDM. BMDM day 7 were incubated with 1 µM JNJ 7777120 for 10 min before performing a chemotaxis assay towards 100 nM, 1, 10, 100 µM of 4MEH. The experiments were performed in 6 wells for each concentration. Data show mean ± SD, p values were calculated by two-way ANOVA test, representing one of two independent experiments.

3.3.5.1.3. H_1 or H_2 receptors do not mediate 4MEH-induced chemotaxis in BMDM

The co-expression of H_1R and H_2R with H_4R in BMDM raised the question about the possible role of the other two histamine receptors in the chemotactic activity induced by 4MEH. Therefore, 100 nM of 4MEH was considered the suitable concentration to examine the chemotaxis in the presence of antagonists to H_1, H_2 and H_4 receptors.

BMDM day 7, were pre-incubated with 1 µM of mepyramine (H_1R antagonist), famotidine (H_2R antagonist), JNJ 7777120 (H_4R antagonist) and 0.01% DMSO as a control for the famotidine and JNJ 7777120 to exclude the solvent effect, 10 nM of fMLP was used as a positive control. The cell count of migrated cells (Fig. 3.18) revealed that neither H_1- or H_2- receptor antagonists could inhibit the migration towards 100 nM 4MEH, whereas cells pre-incubated with JNJ 7777120 had a significant inhibitory effect on the cell migration.

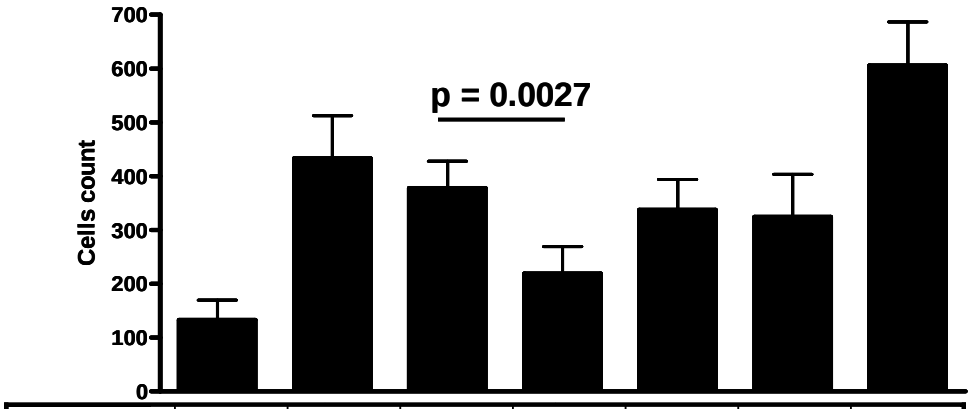

Pre-incubation	-	-	DMSO 0.01%	JN7777-120 1 µM	Mepyra-mine 1 µM	Famoti-dine 1 µM	-
Lower wells 4MEH	-	100 nM	100 nM	100 nM	100 nM	100 nM	fMLP 10 nM

Fig. 3.18: The role of H_1, H_2 and H_4R antagonists in 4MEH induced chemotaxis in BMDM. BMDM on day 7 were pre-incubated for 10 min with 1 µM of JNJ 7777120, mepyramine and famotidine separately before performing chemotaxis assay towards 100 nM of 4MEH. Cells pre-incubated with 0.01% DMSO were used in the assay as a control. The experiments were done in 6 wells for each concentration, data show means ± SD from one of two independent experiments, p value was calculated by two-way ANOVA test.

3.3.6. Comparing macrophages from C57BL/6 mice to those from $H_4R^{-/-}$ mice

$H_4R^{-/-}$ mice were used to generate BMDM, which represent a suitable model to investigate the functional differences between WT and $H_4R^{-/-}$ cells. Some of the main macrophage functions were used to dissect the differences between cells from mice these such as chemotaxis, phagocytosis, cytokine production as well as bone marrow differentiation to macrophages.

3.3.6.1. Genotyping $H_4R^{-/-}$ mice

In order to genotype the mice provided by Johnson & Johnson PCR was performed with genomic DNA isolated from the mice tails. The primer localisation in gene map of WT and $mH_4R^{-/-}$ mice is shown in 2.2.2.7. Both primer sets (5' JNJ11-31 and 3' JNJ11-32) and (5' Neo3b and 3' JNJ11-32) were tested with DNA from WT mice and $H_4R^{-/-}$ mice. PCR results showed the expected specific band size from both primers with both types of DNA. In order to control the breeding process of $mH_4R^{-/-}$ mice, the founding breeding pair provided from Johnson & Johnson were genotyped

and found to be homozygous for the knock-out. All the knock-out mice in the study were derived from that breeding pair (see 2.2.2.7.).

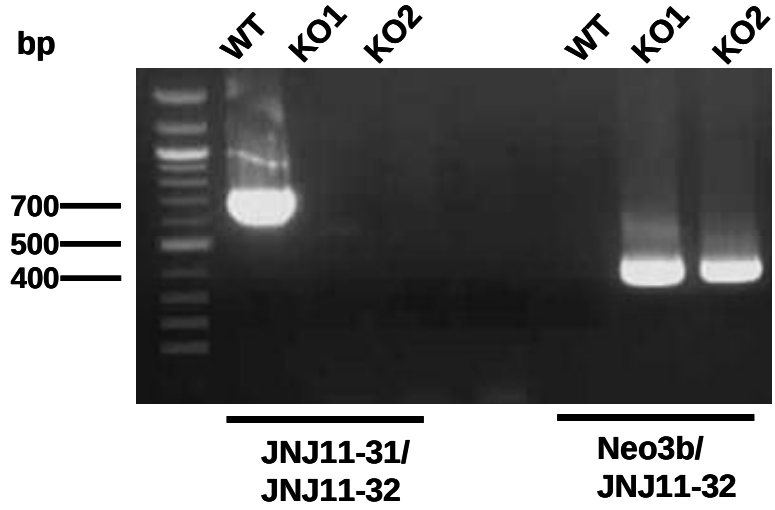

Fig. 3.19: Genotyping of $H_4R^{-/-}$ mice. PCR performed with genomic DNA from a C57BL/6 mouse (WT) and from the breeder mouse pair provided by Johnson & Johnson (KO1, KO2). The PCR products were at the expected size.

3.3.6.2. Chemotaxis

The role of 4MEH as a chemotatractant for WT-BMDM was compared to $H_4R^{-/-}$ BMDM in order to further validate the previous results. Therefore, WT-BMDM and $H_4R^{-/-}$ BMDM day 7 were used for chemotaxis assay in the presence of 100 nM and 100 µM of 4MEH.

Chemotaxis results revealed a significantly higher WT-BMDM migration towards 100 nM 4MEH compared to H_4R -/- BMDM. Moreover, both types of BMDM migrated towards 100 µM of 4MEH (Fig. 3.20).

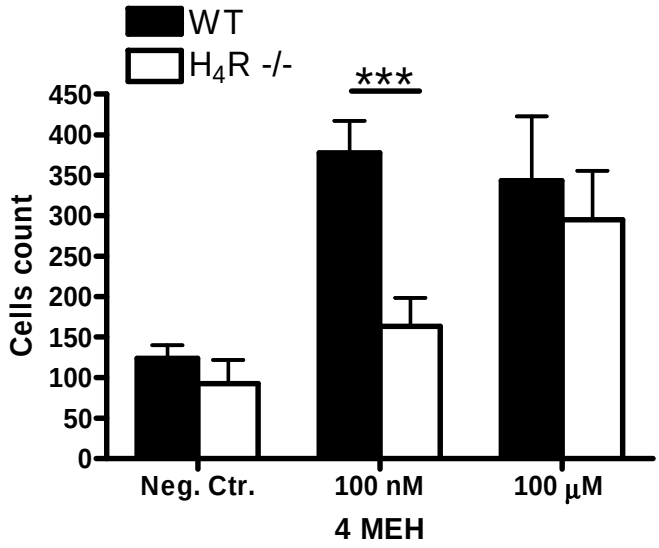

Fig. 3.20: Different chemotactic response to 4MEH between BMDM derived from WT and $H_4R^{-/-}$ mice. BMDM day 7 from WT and $H_4R^{-/-}$ were used in a chemotaxis assay with 100 nM and 100 µM of 4MEH. The experiments were performed in 6 wells for each concentration, data show means ± SD from one of two independent experiments. *** p = 0.0002 calculated by two-way ANOVA test.

3.3.6.3. Bone marrow differentiation to macrophages

In order to compare BMDM from WT and $H_4R^{-/-}$ mice, the first step was to compare bone marrow cell differentiation to macrophages of both strains. For that purpose, the percentage of macrophages ($CD11b^+$ and $F4/80^+$ cells) generated from bone marrow cells after 7 days was considered as a marker to compare the capability of bone marrow cells to differentiate to macrophages. Bone marrow cells from WT and $H_4R^{-/-}$ mice (similar age, sex and animal facility) were seeded in macrophage medium for 7 days. The number of the cells seeded per dish and the medium as well as the incubation conditions were strictly identical. On day 7, WT-BMDM and $H_4R^{-/-}$ BMDM were analyzed by FACS to determine the percentage of macrophages ($CD11b^+$ and $F4/80^+$) generated *in vitro*.

Interestingly, the cells from $H_4R^{-/-}$ mice contained a slightly higher number of macrophages in medium after 7 days than WT mice. The differences between WT and $H_4R^{-/-}$ was lower when macrophage percentage was high (over 90%), whereas the lower macrophage percentage in culture (around 80%) showed a clearer difference between the two mice types (Fig. 3.21).

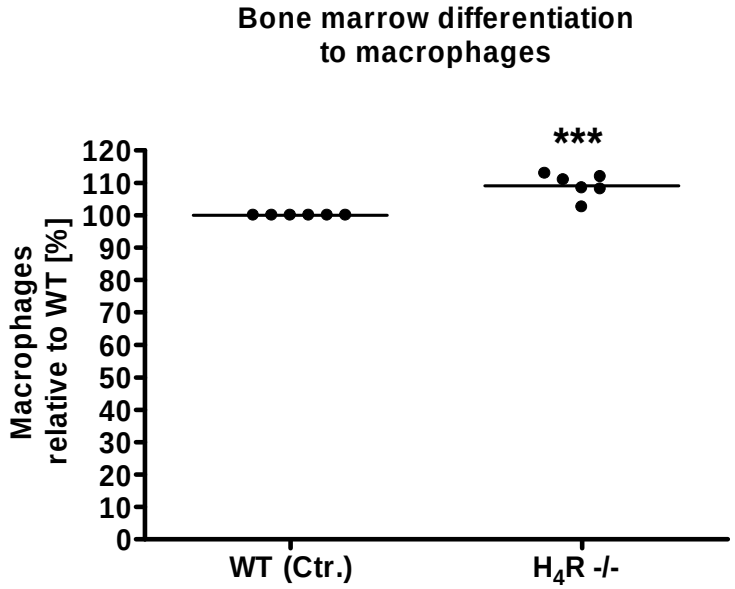

Fig. 3.21: Percentage of macrophages from $H_4R^{-/-}$ and WT mice after 7 days differentiation. FACS experiments show macrophage ($CD11b^+$ and $F4/80^+$ cells) percentages from $H_4R^{-/-}$ in culture after 7 days bone marrow differentiation to macrophages. Each dot represents an independent experiment (n = 11 per group), each individual experiment result was normalized to the WT values which were set as 100%, the age and sex were identical in each individual experiment. (*** p = 0.0005, paired t-test), the data were normalized to the control values as follow: (mean $H_4R^{-/-}$ /mean/mean WT) x 100. The age of the mice was between 11-16 weeks and the age and sex were matched in each individual experiment.

3.3.6.4. Spleen macrophages

The previous results obtained from *ex-vivo* generated macrophages have raised the question whether $H_4R^{-/-}$ mice have higher macrophages numbers residing in tissues.

Spleen macrophages were used to compare the actual percentage of macrophages existing *in vivo*. Therefore, the percentage of $CD11b^+$ and $F4/80^+$ in splenocytes was analyzed by FACS. The splenocytes were left to adhere to the cell culture Petri dishes to eliminate the non-adherent cells which are not macrophages.
No difference was observed between the mice strains, indicating that the number of macrophages residing in the spleen is identical in both mouse strains (Fig. 3.22).

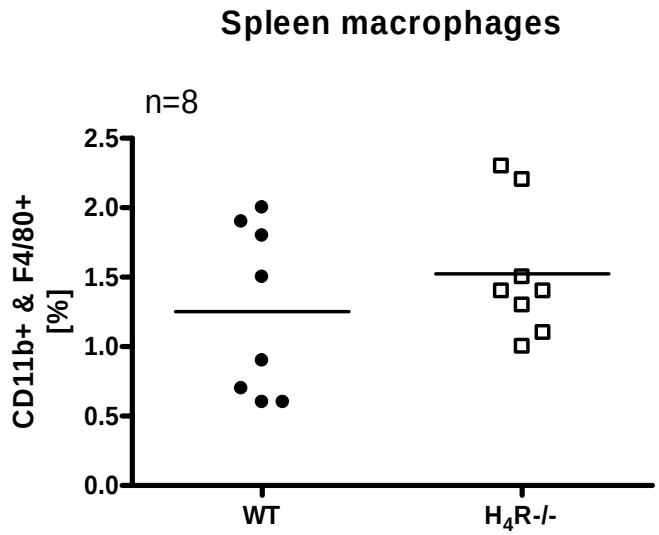

Fig. 3.22: The percentage of macrophage in adherent splenocytes of WT and $H_4R^{-/-}$ mice. The percentage of macrophages isolated from spleen of 15 week old male WT and $H_4R^{-/-}$ mice (n = 8) after a 2 h adherence step before analysing the cells by FACS. Data represents two independent experiments performed in duplicate.

3.3.6.5. Phagocytosis

3.3.6.5.1. Phagocytic activity in BMDM

Based on the previous results of a higher percentage of differentiated macrophages derived from $H_4R^{-/-}$ mice in culture, these macrophages were tested in functional assays. The phagocytosis assay was used to answer the question whether the higher percentage of macrophages from $H_4R^{-/-}$ mice was associated with a higher phagocytic activity than macrophages from WT mice. Therefore, BMDM day 7 from the previously mentioned experiments (see 3.3.5.2.) were subjected to phagocytosis using FITC-labeled microbeads. FACS techniques were used to perform the assay (see 2.2.4.1.), and the read out was the mean fluorescence intensity (MFI) to assess the amount of beads ingested in the cells.

Despite the higher percentage of $H_4R^{-/-}$ BMDM in culture, the WT-BMDM showed always significantly higher MFI values than $H_4R^{-/-}$ BMDM. Data from six independent experiments showed a difference of 15 -33% between the WT and the $H_4R^{-/-}$ values (Fig. 3.23), indicating that phagocytic activity in WT-BMDM is higher than in $H_4R^{-/-}$ BMDM.

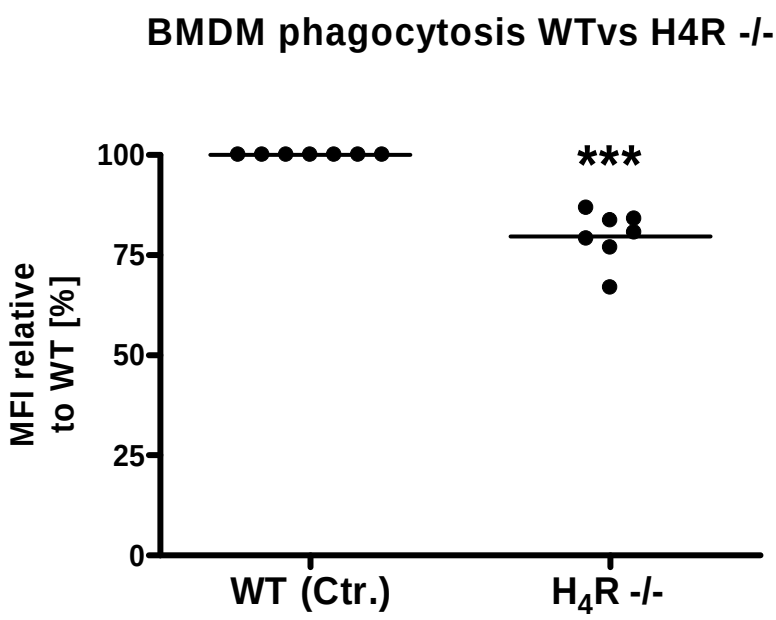

Fig. 3.23: Lower phagocytosis of BMDM from $H_4R^{-/-}$ relative to WT mice. BMDM day 7 from WT and $H_4R^{-/-}$ mice were incubated with FITC-labelled micro beads for 2 hours and then analyzed by FACS for the mean fluorescence intensity (MFI). Each dot represents an independent experiment (n = 14 mice per group). Mice were 11-16 week of age and were matched in age and sex in each individual experiment. The data were normalized to the control MFI values as follows: MFI $H_4R^{-/-}$ (mean) / MFI WT (mean) x 100. (*** $p<0.0001$, paired t-test).

The percentages of FITC positive cells (cells which ingested one bead at least) of both types did not significantly differ in both BMDM types which does not explain the MFI differences. Therefore, alignment of both flurescence histograms was performed to analyse the difference. The results showed that both types of macrophages can phagocyte low numbers of beads (up to three beads), but only WT-BMDM exhibited the capability of phagocytosing higher numbers of beads, this is demonstrated by a higher cell number with more than three beads ingested in comparison to $H_4R^{-/-}$ BMDM (Fig. 3.24).

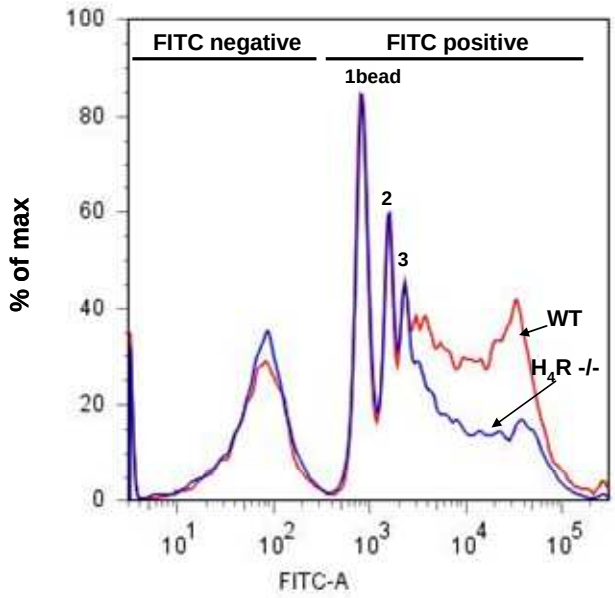

Fig. 3.24: Fewer ingested beads in $H_4R^{-/-}$ BMDM compared to WT-BMDM. The alignment of FACS fluorescence histogram from WT-BMDM and H4R $^{-/-}$ BMDM showed the difference between both types according to their beads content. $H_4R^{-/-}$ BMDM ingested fewer number of beads compared to WT BMDM. The data represent an example of phagocytosis histograms.

3.3.6.5.2. Phagocytic activity in PEC

The lower phagocytic activity in $H_4R^{-/-}$ BMDM raised the question whether other macrophage types have also similar phagocytic activity. To determine the phagocytic activity in another type of macrophages, peritoneal macrophages obtained from PEC were isolated and used in a phagocytosis assay. In order to focus on macrophage phagocytosis and exclude other cells like granulocytes in the PEC population which may contribute to phagocytosis, the cells were stained for F4/80 expression after the assay. The FITC-beads fluorescence signal was determined In $F4/80^+$ cells by FACS system (Fig. 3.25.A). Significant lower MFI values were obtained from $H_4R^{-/-}$ compared to WT macrophages. The difference was between 20-37% when WT values were set as 100 % activity (Fig. 3.25.B), indicating that peritoneal macrophages from $H_4R^{-/-}$ show also a lower phagocytic activity than peritoneal macrophages from WT mice.

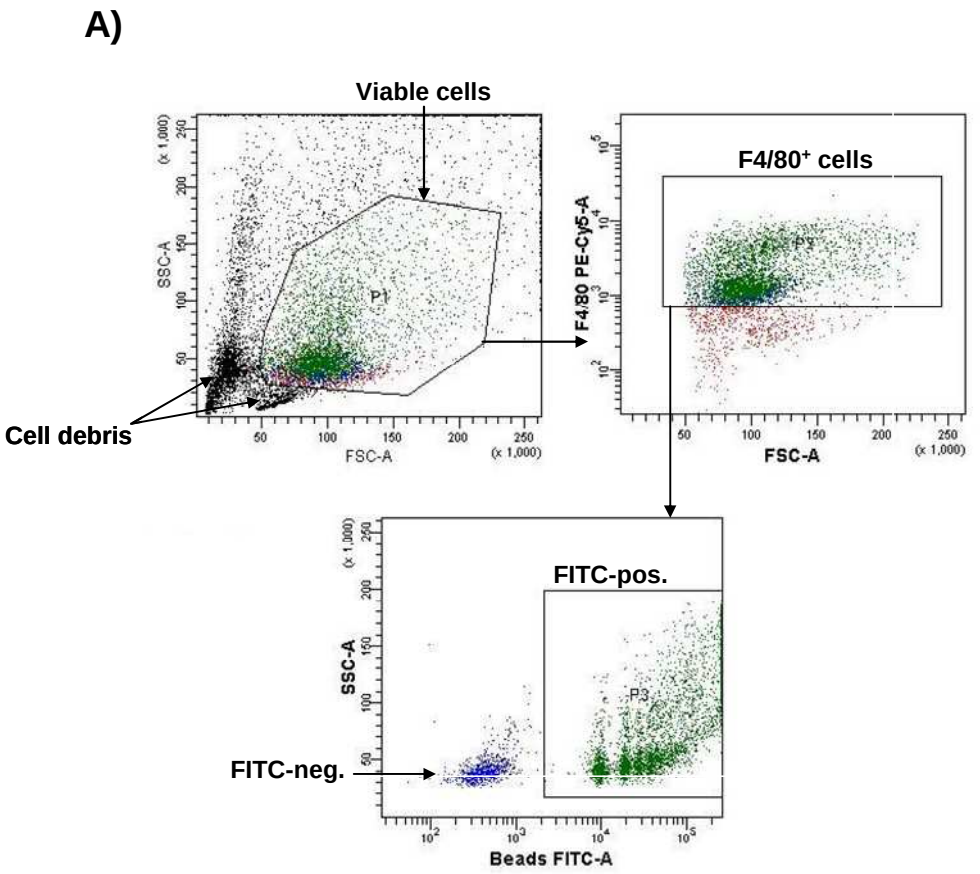

Fig. 3.25: F4/80^{+} cells of PEC from $H_4R^{-/-}$ show decreased phagocytosis compared to WT mice. Peritoneal macrophages were isolated from WT and $H_4R^{-/-}$ mice and incubated with FITC-micro beads for 2 hours, F4/80^{+} cells were stained before analysing the cells in FACS. (A) An example of the population in PEC phagocytosis. F4/80^{+} cells were gated and analyzed for FITC fluorescence. (B) MFI from WT macrophages were set as 100% activity and compared to $H_4R^{-/-}$ macrophages. Each dot represents a single experiment performed in duplicate (n = 4 of 12 weeks old female mice per group). ** p = 0.0039, two-way ANOVA test.

3.3.6.5.3. Phagocytosis of *Leishmania major* promastigotes labelled with CFSE

In order to validate the previous findings with another phagocytosis system which is closer to reality, BMDM from WT and $H_4R^{-/-}$ were challenged with labelled-*L. major* in phagocytosis assay. As previously mentioned in the Introduction, the clearance of this parasite is known to be a macrophage-dependent mechanism, and the ingested amastigotes remain in the phagosomes before being killed by the macrophages [127;128].

Therefore, *L. major* promastigotes were labelled with CFSE (see 2.2.4.2.3.) and incubated with WT and $H_4R^{-/-}$ BMDM day 7 for 6 hours. After washing away the non-phagocytosed parasites and fixing the cells, the cells were analyzed in FACS to determine the percentage of CFSE (FITC) positive cells. In agreement to the previous data, $H_4R^{-/-}$ BMDM showed a lower percentage of CFSE-positive cells than WT-BMDM. The difference was between 15-26 % when WT values were set as 100 %, indicating lower phagocytic activity (Fig. 3.26).

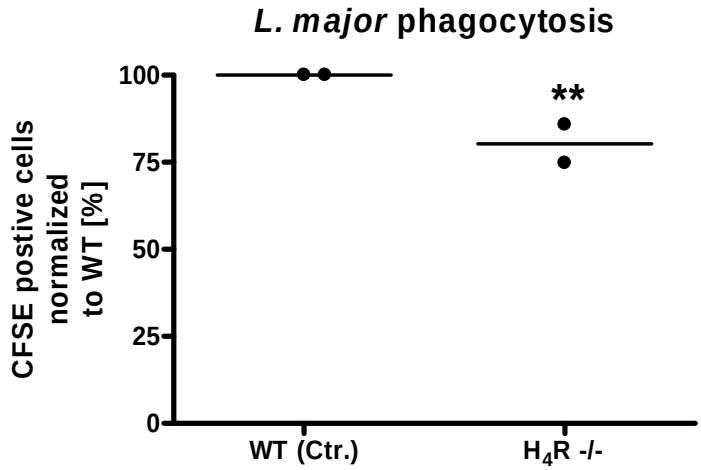

Fig. 3.26: *L. major* phagocytosis is impaired in $H_4R^{-/-}$ BMDM compared to WT-BMDM. BMDM day 7 generated from WT and $H_4R^{-/-}$ mice were incubated with living *L. major* promastigotes labelled with CFSE (around 6 parasites per cells). After 6 hours the percentage of CFSE-positive cells were determined by FACS, and calculated relative to WT values set as 100 %. Each dot represents an independent experiment performed in triplicate (n = 4 per group) (** p = 0.0015, two-way ANOVA test).

3.3.6.5.4. The role of histamine in WT-BMDM phagocytosis

The next aim was to identify the role of histamine in BMDM phagocytic activity. The aim was to examine whether stimulating BMDM by which histamine can modulate BMDM phagocytosis. Therefore, BMDM day 7 generated from two WT mice were used in a phagocytosis assay in the presence of serial concentrations of histamine. After 2 hours the cells were analyzed by FACS to determine the MFI levels. The results did not show any differences in the MFI levels between histamine-stimulated and non-stimulated cells (Fig. 3.27). Similar to MFI the percentage of FITC-positive cells did not differ (data not shown). These findings confirmed three previous experiments where 1 µM of histamine did not modulate phagocytic activity in BMDM day 7 of wild-type mice (data not shown).

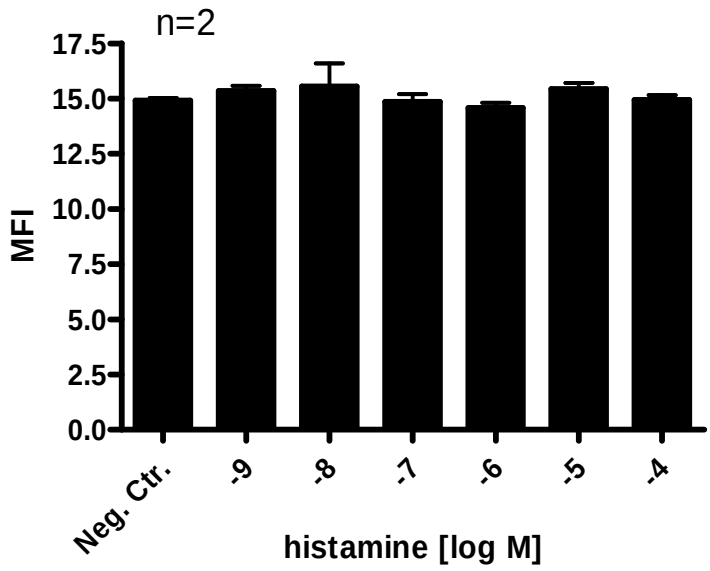

Fig. 3.27: Exogeneous histamine does not affect the phagocytosis of BMDM. BMDM day 7 from two male wild-type mice (11 weeks) were incubated with FITC-micro beads for 2 hours in the presence of the indicated histamine concentrations. MFI of the cells obtained by FACS showed no effect of histamine on phagocytosis in BMDM. The experiment was performed in duplicate, data show means ± SD performed in triplicate.

3.3.6.5.5. The effect of JNJ 7777120 in BMDM phagocytosis

The previous results showed that exogenous histamine did not modulate the phagocytosis activity in BMDM. But the expression of HDC in macrophages raised the question whether BMDM produce their own histamine. This histamine could act

like an autocrine stimulator acting through one of the histamine receptors expressed on macrophages. In order to assess this hypothesis, the next step was to block H_4R during the phagocytosis assay and examine the influence on phagocytosis.

BMDM day 7 generated from two WT mice were used in a phagocytosis assay in the presence of serial concentrations of JNJ 7777120. FACS results show that MFI levels did not reveal any significant effect of JNJ 7777120 in the phagocytic activity (Fig. 3.28). In three earlier experiments, 1 µM of JNJ 7777120 had no influence on phagocytosis activity (data not shown).

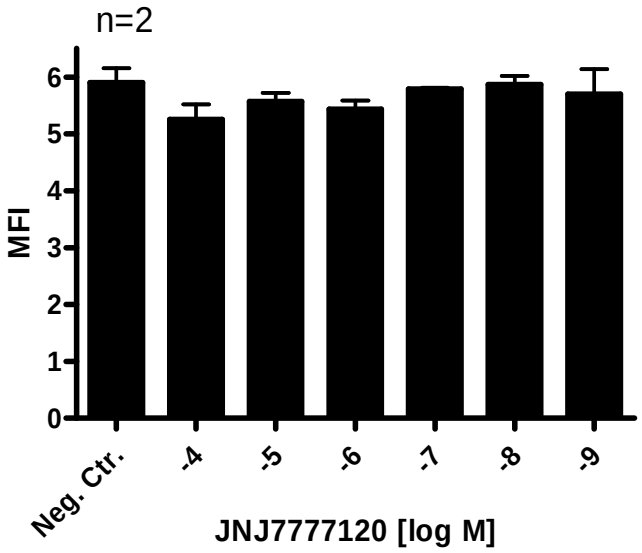

Fig. 3.28: JNJ 7777120 does not affect the phagocytosis of BMDM. BMDM day 7 from two male wild-type mice (12 weeks) were incubated with FITC-micro beads for 2 hours in the presence of the indicated JNJ 7777120 concentrations. The MFI of the cells analyzed per FACS showed no effect of JNJ 7777120 on phagocytosis of BMDM. The experiment was performed in duplicate, data show means ± SD performed in triplicate.

3.3.6.5.6. BMDM generation in the presence of JNJ 7777120

The previous data could partially reject the hypothesis of autocrine histamine action. The next hypothesis was that histamine could be produced in medium during the 7 days cell culture, and this might lead to improved differentiation via H_4R to fully active macrophages and less active cells when H_4R is absent.

In order to assess this hypothesis, bone marrow cells from two wild-type mice were cultured either in normal BMDM medium (WT), or in the same medium with 10 µM JNJ 7777120 (WT+JNJ). In parallel, bone marrow cells from two H4R $^{-/-}$ mice

were cultured in the same normal BMDM medium.On day 7, the cells were subjected to staining with anti-CD11b and anti-F4/80 in order to be analyzed by FACS. The number of macrophages showed that WT cells generated significantly higher numbers of macrophages than WT+JNJ cells, and both numbers were lower than macrophages from $H_4R^{-/-}$ mice. These results showed that the presence of H_4R antagonist did not have the same effect on macrophage differentiation than H_4R-deficiency (Fig. 3.29.A).

Cells were then subjected to a phagocytosis assay with FITC-microbeads. FACS results revealed that MFI values from BMDM of WT+JNJ and $H_4R^{-/-}$ BMDM were significantly lower compared to WT BMDM. (Fig. 3.29.B).

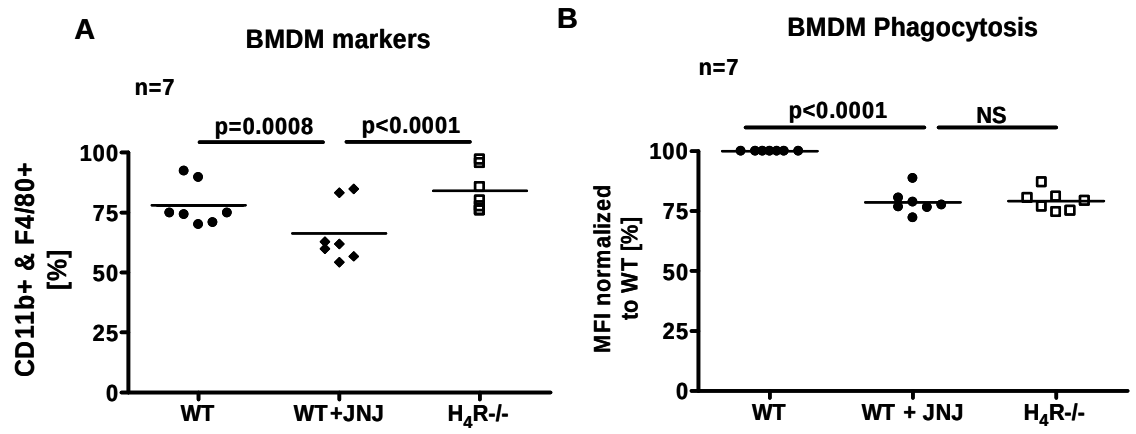

Fig. 3.29: Comparing macrophages numbers and phagocytosis in cells differentiated in the presence of JNJ 7777120. Bone marrow cells from wild-type mice (n = 7 of 15 weeks old) were cultured in normal BMDM medium (WT), and in BMDM medium containing 10 µM of JNJ 7777120 (WT+JNJ). Bone marrow cells from $H_4R^{-/-}$ mice (n = 7 age and sex matched) were cultured in normal BMDM medium ($H_4R^{-/-}$). After 7 days, the cells were used for analyzed by FACS for CD11b and F4/80 expression and for phagocytosis of FITC micro beads. (A) Percentage of $CD11b^+$ and $F4/80^+$ cells. (B) MFI values after phagocytosis assay normalized to WT as 100 % activity. Data represents two independent experiments performed in duplicate. P values were calculated by two-way ANOVA test.

3.3.6.6. Production of pro-inflammatory cytokines and NO

3.3.6.6.1. TNF and IL-6 production

TNF and IL-6 are pro-inflammatory cytokines produced by macrophages, and they are considered as markers for the classical activation of macrophages mediated by LPS. In order to examine the role of H_4R in the production of TNF and IL-6 from BMDM, WT and $H_4R^{-/-}$ BMDM day 7 generated in a 6 well plate were activated with

100 ng/ml of LPS for 24 hours. IL-6 and TNF concentrations were determined by ELISA in the supernatant.

After 10 hours, a clear morphological difference was observed between WT and $H_4R^{-/-}$ BMDM. WT-BMDM had the distinct podosome with dendritic shape typical for LPS activated macrophages, unlike $H_4R^{-/-}$ BMDM, which were more round (Fig. 3.30).

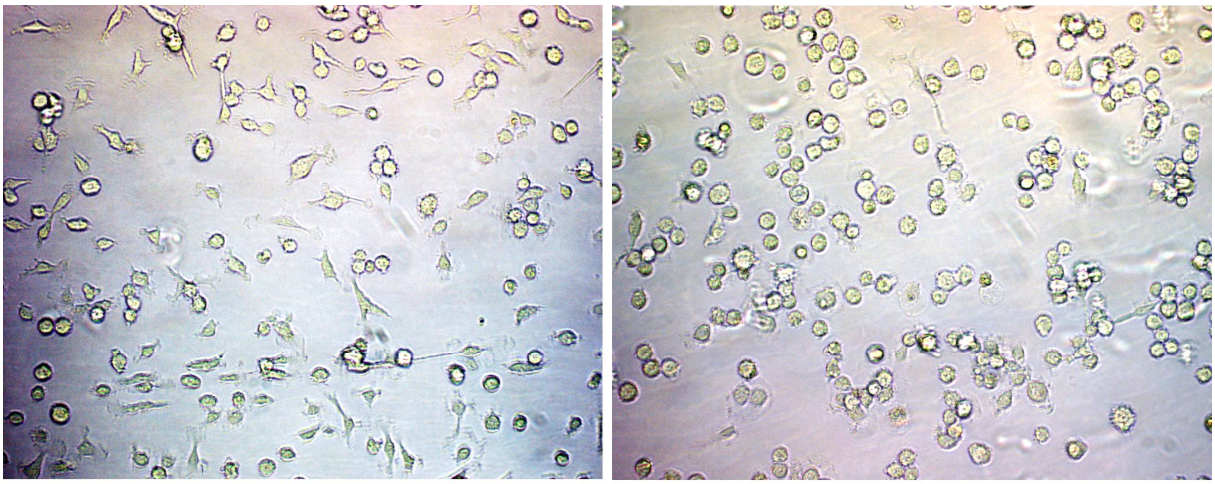

WT **H_4R-/-**

Fig. 3.30: LPS-activated BMDM from WT and $H_4R^{-/-}$ mice. The microscopic picture shows the different shape between WT-BMDM and $H_4R^{-/-}$ BMDM after activation with 100 ng/ml LPS for 10 hours.

The morphological difference was associated with lower TNF and IL-6 production in response to LPS. The values of TNF and IL-6 varied between different experiments, however the difference between BMDM from WT and $H_4R^{-/-}$ was always detectable (Fig. 3.31).

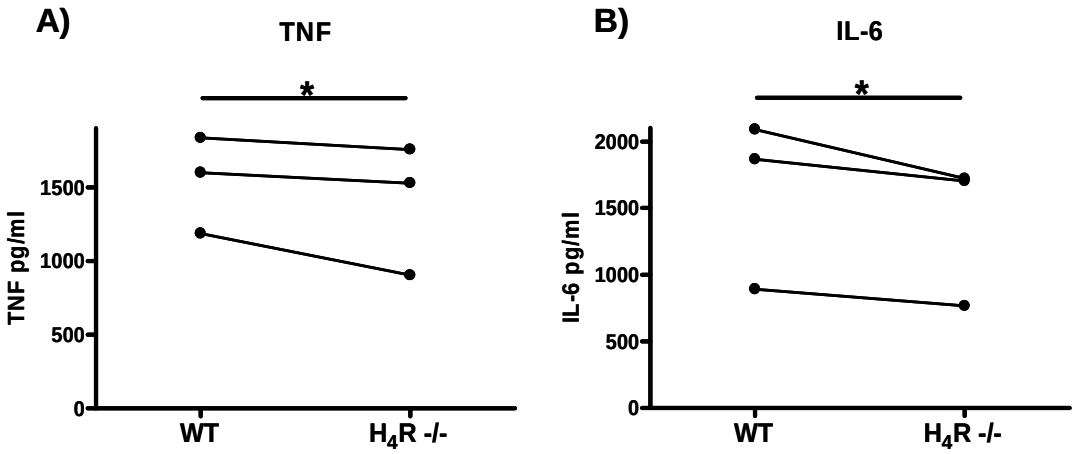

Fig. 3.31: BMDM day 7 generated from WT and $H_4R^{-/-}$ mice were incubated with 100 ng/ml LPS for 24 hours. TNF (A) and IL-6 (B) concentration were determined in the supernatant by ELISA. The connected dots represent an independent experiment (n = 4) Determinations were performed in triplicates, * $p < 0.05$ in two-way ANOVA test.

3.3.6.6.1.1. The role of histamine in TNF and IL-6 production

Similar to the phagocytosis aspect, the previous data raised the question about a possible role of histamine in TNF and IL-6 production. Therefore, BMDM day 7 were stimulated with serial concentrations of histamine for 24 h. Thereafter, TNF and IL-6 concentrations were determined by ELISA. TNF and IL-6 did not show any response to histamine stimulation after 24 h (Fig. 3.32). Moreover, TNF and IL-6 levels were close to the detection level of the ELISA assay, indicating that BMDM were not activated and the additional histamine did not change this state. In three other earlier experiments, BMDM day 7 cells were stimulated with 1 µM of histamine for 24 h. TNF and IL-6 determination did not show any effect of histamine on the production of the two cytokines (data not shown).

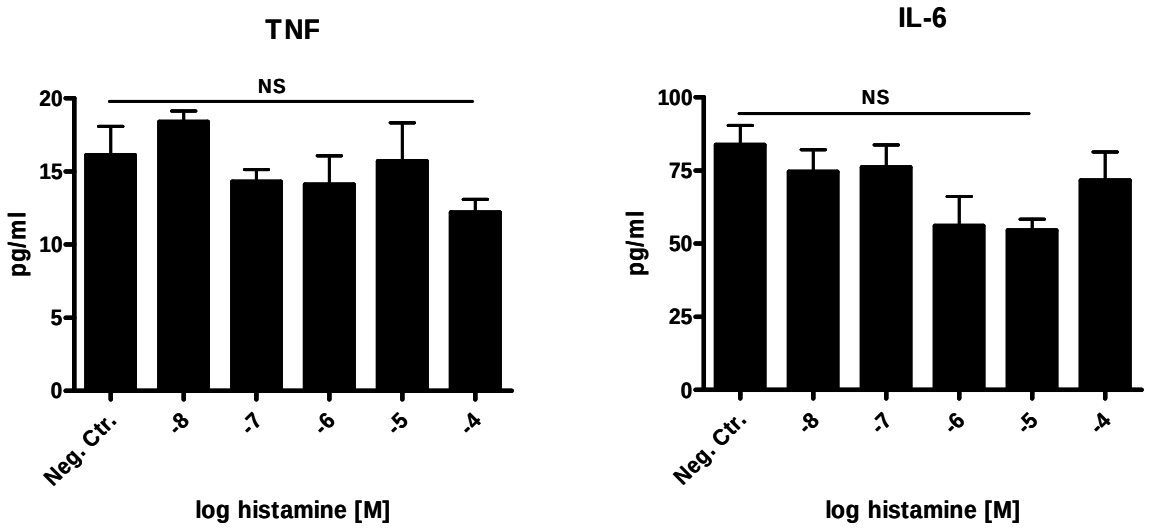

Fig. 3.32: No effect of exogenous histamine on TNF and IL-6 production in BMDM. BMDM on day 7 were incubated for 24 hours with different concentrations of histamine. The TNF and IL-6 concentrations were determined in the supernatant by ELISA. Histamine does not change the basal levels of TNF and IL-6 produced by the non-stimulated cells. The experiment was performed in duplicate and data show means ± SD. P values were calculated by two-way ANOVA test.

3.3.6.6.2. Nitric oxide (NO)

The impaired response to LPS observed in $H_4R^{-/-}$ BMDM brought to the attention other LPS-related macrophage activities such as NO production. NO is one of the anti-microbial compounds secreted by macrophages and other leukocytes in response to several bacterial compounds such as LPS. In addition, IFN-γ secreted from T-cells is also essential to activate macrophages and increase the secretion of NO. NO levels in supernatants were determined by Griess reagent (see 2.2.4.3). In the experiment setup the cells were activated with LPS and IFN-γ for 48 h. The longer incubation time is necessary to accumulate NO in the supernatant to reach detectable levels in the assay.

In order to compare NO production between WT and $H_4R^{-/-}$ BMDM, BMDM from two mice per group were generated as previously mentioned. Subsequently, on day 7 the cells were stimulated with IFN-γ (20 ng/ml) and 100 ng/ml LPS for 48 hours. NO levels in the supernatant medium of WT-BMDM were clearly higher than $H_4R^{-/-}$ BMDM. The NO values varied between different experiment, however the difference between BMDM from WT and $H_4R^{-/-}$ was always detectable (Fig. 3.33).

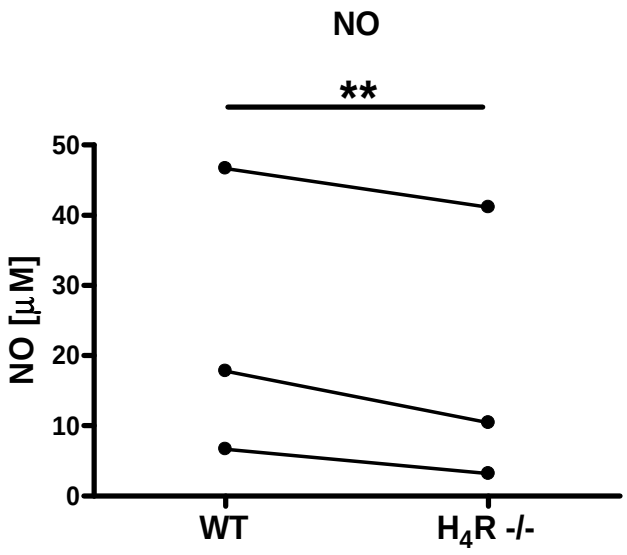

Fig. 3.33: $H_4R^{-/-}$ BMDM produce less NO than WT-BMDM. BMDM generated from WT and $H_4R^{-/-}$ mice were incubated with LPS (100 ng/ml) and IFN-γ (20 ng/ml) for 48 hours. NO concentrations were determined in the supernatant. WT-BMDM showed a higher accumulative NO production than $H_4R^{-/-}$ BMDM. The connected dots represents an independent experiment performed in duplicate (n = 5 per group). ** $p<0.005$ in two-way ANOVA test.

3.3.6.6.2.1. The role of histamine in NO production in BMDM

Similar to what was observed for the cytokines production, the direct effect of histamine on NO production had to be investigated. In this line, BMDM generated from WT mice were stimulated on day 7 with 1 µM histamine, 0.1% (V/V) DMSO and 1 µM JNJ 7777120 in the presence or without LPS 100 ng/ml for 48 h.

As expected, the cells without LPS did not produce NO, also not after histamine stimulation, whereas LPS treated cells show a clear detectable NO level. Histamine had a slight inhibitory effect on the NO production in LPS treated cells. However, this inhibition was not reversed when the cells were cultured in the presence of JNJ7777120 (Fig. 3.34).

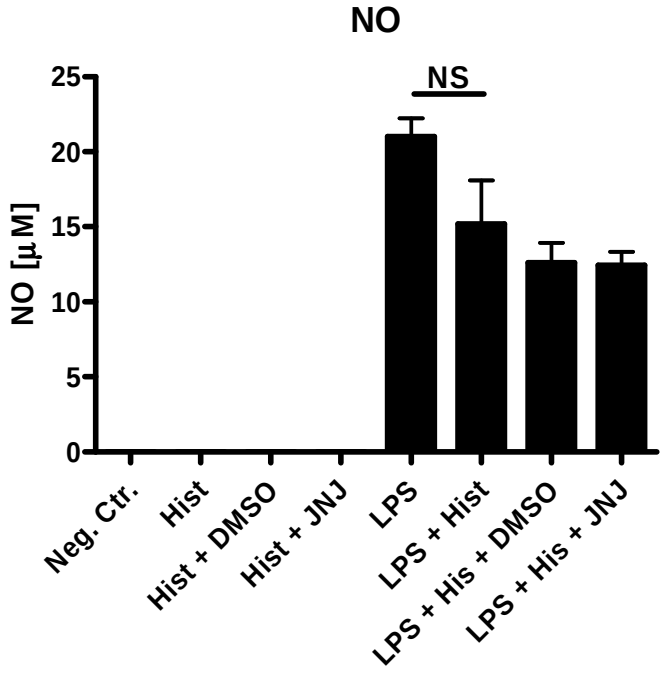

Fig. 3.34: No effect of histamine on NO production in BMDM. BMDM day 7 generated from WT mice were incubated for 48 hours in the presence of histamine 1 µM and 0.1% (V/V) DMSO and JNJ 7777120 1 µM with or without LPS 100 ng/ml. NO concentrations were measured in the supernatant. The experiments were performed in duplicate and data show means ± SD from one of two independent experiments. P value was calculated with two-way ANOVA test.

3.3.7. Comparison of WT mice and $H_4R^{-/-}$ mice in an experimental model of *Leishmaniasis*

In order to assess the physiological relevance of the previous data, Leishmaniasis was considered as a suitable model to challenge the $H_4R^{-/-}$ mice. As previously mentioned, T_H1 immune response is the key factor in the mouse immunity against *L. major.* This includes macrophage phagocytosis, production of pro-inflammatory cytokines as well as NO production. However, as it is already mentioned in the Introduction, C57BL/6 mice are resistant against *Leishmania* infection. In these mice the infection develops relatively slowly, and the mice recover from the infection after 8-9 weeks. Conversely, Leishmaniasis in BALB/c mice is a lethal infection because of the impaired T_H1 response in this strain [129;130].

Therefore, a high dose *Leishmania* infection in WT and $H_4R^{-/-}$ mice (n = 3 per group) was generated by injecting subcutaneously $3x10^6$ *L. major* promastigotes in the right foot. Thickness of both feet was measured every week after infection, and calculated relative to the non-infected foot.

$H_4R^{-/-}$ mice show a similar swelling pattern to the control mice with a general higher swelling level especially 2-3 weeks after the infection (Fig. 3.35), indicating that the absence of mH_4R from the immune cells has a moderate effect on the immunity against *L. major.*

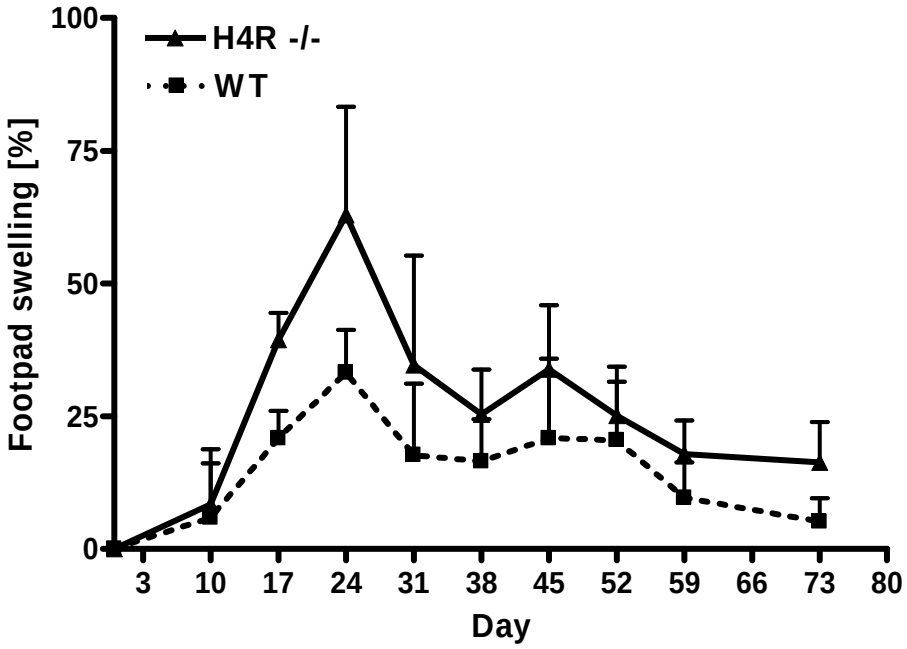

Fig. 3.35: Footpad swelling after *L. major* infection. $H_4R^{-/-}$ show a higher footpad swelling curve during Leishmaniasis than WT in high dose infection. Data show means ± SD.

3.4. Mouse anti-mH$_4$R antibody generation

3.4.1. Testing the commercially available antibodies in Western-blot

In order to validate the previously shown data of mH$_4$R expression on the mRNA level, and show the expression of mH$_4$R on the protein level, commercial antibody was used to perform western-blot with cells which express H$_4$R on the mRNA level by RT-PCR.

Western-blot was performed with the protein lysate of the different cells (see 3.3.1) in addition to BMDC day 8 (immature BMDC) and HEK-293 cells. The western blot results show that the commercial antibody had recognized non-specific antigens with molecular weights lower and higher than the expected mH$_4$R band (Fig. 3.36). Based on unpublished data, the molecular weight of mH$_4$R was detected at around 45 kD when tagged with V5 antigen. Due to the non-specificity of these antibodies no further experiments were performed with them.

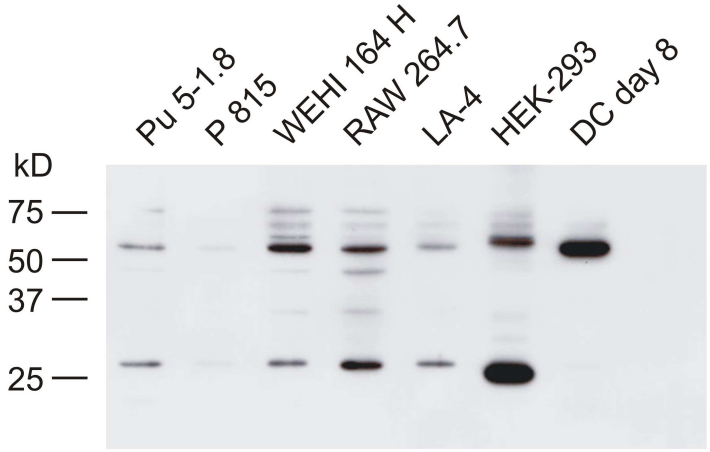

Fig. 3.36: Unspecific bands appeared in Western-blot with the commercial antibodies. Protein lysate from cell lines were examined by western-blot using commercial antibody from Santa-Cruz ®.

3.4.2. Immunizing H$_4$R $^{-/-}$ mice against two peptides from mH$_4$R

Based on the previous finding, the next aim was to generate mouse anti-mH$_4$R antibodies using the H$_4$R $^{-/-}$ mice. These mice can be immunized against the whole

mH_4R or part of the receptor because they lack the protein and can develop antibodies without affecting any self-antigen.

Therefore, two synthesized peptides (see 2.1.12) the first is the second extra-cellular domain (2^{nd}-ECD), and the second peptide is the third extra-cellular domain (3^{rd}-ECD) were used for immunization (see 2.2.5.1.). The approach behind using the extracellular peptides is to future use of the generated antibodies in immuno-assays such as FACS and fluorescent microscopy without the need to permeabilizing the cells and with the possibility of using the antibodies to test them for agonistic or antagonistic effects on the receptor.

3.4.3. Screening the antibody production in the serum of immunized mice

Antibody production was tested in mice sera before immunization and after each boost. The ELISA assay was used to determine the serum antibody titers against the respective peptide coupled to BSA instead of KLH to avoid the unspecificity (see 2.2.5.3.). Serum titer was determined as serum dilution with double O.D value than the negative control. ELISA results show that both mice produced antibodies against both peptides after the first boost (Fig. 3.37.A) with a better serum titer in the mouse immunized against 3^{rd}-ECD (12800) than the mouse immunized against 2^{nd}-ECD (3200). After the second boost (Fig. 3.37.B) both sera showed enhanced titers (25500) and (6400) respectively.

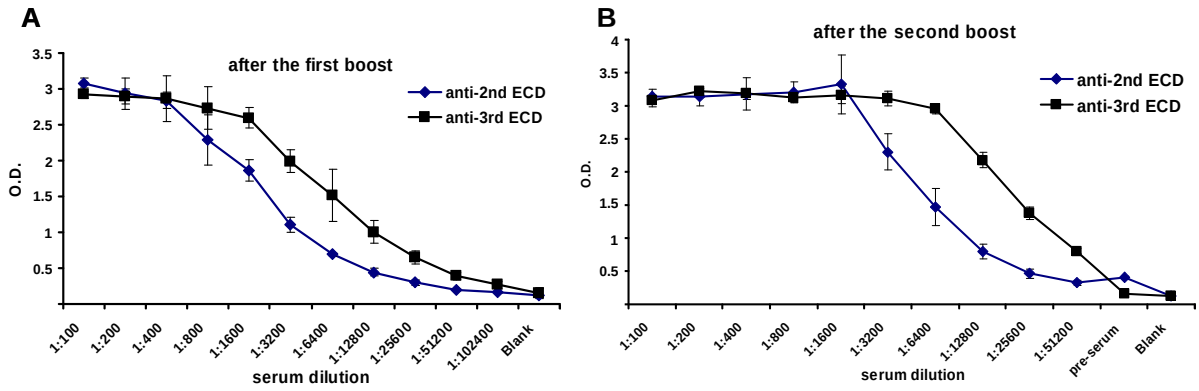

Fig. 3.37: Antibody production in mouse sera. ELISA test was used to determine the antibody production and titers after the first (A) and the second boost (B). ELISA test was performed with BSA-coupled peptides in 96 well plate as triplicate, the blank values were obtained from wells without serum. Values represent mean and standard deviations.

3.4.4. Western-blot using immunized mice serum

The two sera (after second boost) were used in a Western-blot experiment with protein lysates from cells expressing H_4R on the mRNA level (bone marrow and BMDM) as well as Sf9 cells infected with Baculovirus containing mH_4R in an expressing vector. As negative control, a protein lysate was used from bone marrow, BMDM from $H_4R^{-/-}$ mice, and Sf9 cells infected with Baculovirus containing an empty vector. Serum containing anti-2nd-ECD did not show any band, whereas serum containing anti-3rd-ECD (Fig. 3.39) showed some unspecific bands in both positive and negative cells, indicating that sera from these immunized mice could not be directly used to detect mH_4R expression on the protein level.

However, the successful immunization as detected by ELISA (Fig. 3.37.) gives the chance to generate monoclonal antibodies from plasma cells residing in the spleen. Therefore, both spleens were isolated and frozen three days after the second boost in liquid nitrogen for further experiments.

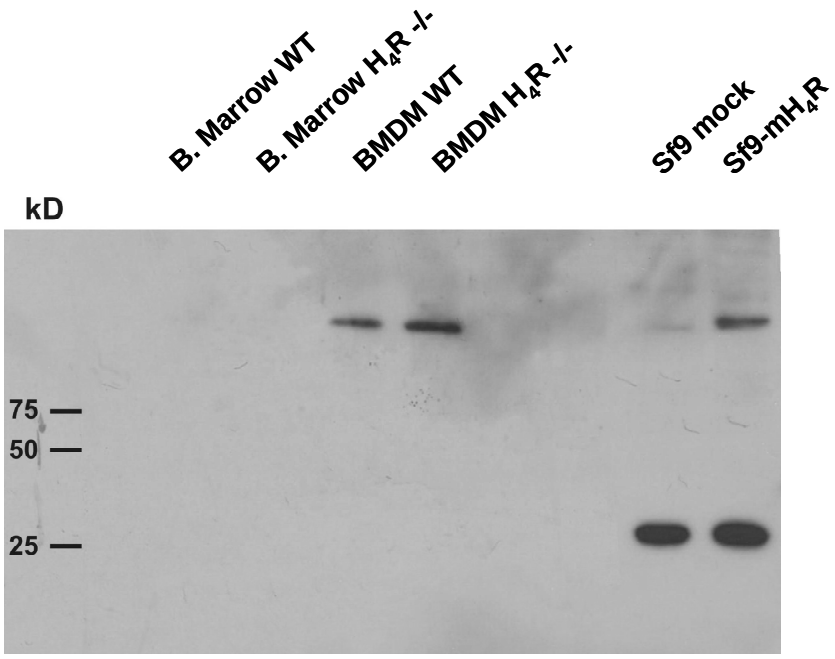

Fig. 3.38: Testing the anti-serum in western-blot. The anti serum from the mouse after the second boost (anti-3rd ECD) was used in western-blot. Non-specific binding was observed indicating that the serum is not suitable for the determination of mH_4R in this assay.

4. Discussion

In order to elucidate the biological role of H_4R in a mouse model, it was essential to focus on one cellular model. Therefore, the main part of the work was analysing the expression H_4R in several immune cells, and determination of a suitable cellular model. The regulation of H_4R was a crucial point on the way to understand the mechanism by which H_4R modulates immune mechanisms. Therefore, mouse macrophages as a cellular model to study the functions of H_4R, were analyzed in functional assays upon H_4R stimulation or inhibition. Moreover, $H_4R^{-/-}$ mice represented a valuable tool in order to compare macrophages in the presence or absence of H_4R, and the effect of H_4R on their immune functions.

Furthermore, the absence of suitable commercial antibodies against mH_4R has imposed the generation of antibodies against H_4R, as an additional goal of this work. Such antibodies could be used in the determination and quantification of H_4R on the protein level.

4.1 H_4R and DC

H_4R is predominantly expressed in haematopoietic immune cells. Further reports revealed that other cells and tissues show also a detectable expression level of the receptor [34]. Among the haematopoietic immune cells, DC as key cells relating the innate and adaptive immunity were shown to express H_4R as well as other histamine receptors in human and mouse [49;63-65].

In the early stages of this work, no clear H_4R expression had been shown in mouse DC. Therefore, BMDC were used to examine theses cells. BMDC generation represents a suitable tool to generate sufficient number of immature DC *in vitro*. These cells are functional DC with the ability of presenting antigen to T cells and activate them. The supernatant of X6310 cells is an appropriate source of GM-CSF,

the essential growth factor for bone marrow cell differentiation to DC. This was confirmed by the expression of CD11c on the cells, and the expression of CD86 and MHC II upon LPS stimulation, which confirmed that the generated DC have the main DC markers [133].

The expression of H_4 as well as H_1 and H_2 receptors was detected on the mRNA level, in both mature and immature BMDC, as well as in bone marrow cells. These data were confirmed later by several publications in which a functional expression of H_4R in human and mouse DC was observed, claiming a role of H_4R in DC chemotactic activity. Another report has observed the expression of H_3R in addition to H_1, H_2 and H_4R in DC [65]. Furthermore, the regulation of mH_4R during bone marrow differentiation to DC and DC maturation with LPS was investigated by real-time PCR. The continuous down-regulation of mH_4R during differentiation and maturation may hint at the role of H_4R role in both processes.

The BMDC maturation state represented by the expression of CD86 and MHC II on $CD11c^+$ cells did not show any change upon histamine or 4MEH stimulation, indicating that H_4R did not play any direct role in the maturation process. Similarly, a report from Pavlinkova *et al*. in 2003, H_1R and H_2R were down-regulated after LPS or TNF stimulation of immature BMDC from BALB/c mice. Furthermore, histamine did not modulate the expression of CD86 on stimulated BMDC. From the same report, histamine slightly up-regulates IL-12p40 production from immature BMDC, in a dose response manner, claiming a role in BMDC maturation [138]. Different results were reported by Guzmer at al. in 2005 showing that H_4R stimulation dowregulates IL-12p70 from human DC [64]. In 2001, Caron *et al*. showed that histamine induces CD86 expression and IL-8 production from human monocyte-derived DC. The effect was inhibited by preincubation with H_1 or H_2 receptor antagonists, but not in thioperamide-treated cells, but the authors mentioned that histamine-stimulated DC did not have the phenotype of fully mature DC [67]. The previous contradictory data are possibly due to the differences between human and mouse cells, and the different protocols used to generate human DC. Another factor that could interfere in the results is the FCS used as a supplementary medium in cell culture. In general, FCS contains a variable amount of LPS traces depending on the provider and sometimes even on the batches from the same provider. These LPS contamination varies between very low amounts and higher levels which could be sufficient to stimulate the cells, especially APC such as DC and macrophages.

Therefore, and based on the down-regulation of mH_4R upon LPS stimulation as mentioned in Fig 3.4 - 3.5, LPS levels in the medium have to be controlled.

Histamine production and its autocrine effect on mouse DC was reported previously in both, human and mouse cells [65;69]. Therefore, the role of histamine in DC maturation had to be studied considering that histamine is secreted in the medium from the cells. This amount of histamine produced from immune cells is lower than mast cell-derived histamine, and these cells might not respond to the additional amounts of histamine. Therefore, the low expression level of H_4R in mature BMDC might be a physiological response to the histamine produced in medium, in order to minimize the autocrine effect. This, in addition to the relatively high affinity of H_4R for histamine are reasons to speculate about a role of H_4R in the autocrine effect of histamine in DC [61;62;139-141].

4.2. H_4R and T lymphocytes

The expression of H_4R on the mRNA level in human spleen and lymph node cells was reported in earlier publications simultaneously with the discovery of H_4R [142;143]. In the mouse model, Hofstra *et al.* from the Johnson and Johnson research group has mentioned in 2002 that H_4R is exclusively expressed in mast cells and eosinophils. In addition, no detectable expression was found in spleen, lymph nodes, $CD4^+$, $CD8^+$ T cells, B cells or macrophages [73]. From the same research group and three years later, Dunford *et al.* reported that H_4R on $CD4^+$ T cells modulate the immune response during asthma development [69]. Additional reports claimed a functional expression of mH_4R in T cells, without showing the expression neither on mRNA nor protein levels. Therefore, the expression of H_4R in the previously mentioned immune organs and cells was important to investigate the role of H_4R. The expression of mH_4R in spleen and axillary lymph nodes found in this work was similar to the human data mentioned before. Notably, the total amount of RNA in spleen and lymph nodes as secondary lymphatic organs mainly consisted of RNA from T and B cells in addition to antigen presenting cells (DC, macrophages). The expression of H_4R in $CD4^+$, $CD8^+$ T cells sorted from spleen, as well as DC and macrophages can explain the previous data of positive H_4R in spleen and lymph nodes. The negative expression of H_4R in B cells confirms the literature data where no expression or role of H_4R in B cells has been reported.

HDC activity in T cells and histamine production was also reported by several reports. Therefore, histamine must be considered as an important factor in any research regarding H_4R effect on T cells [4;5;144].

As a conclusion, the expression of H_4R in all the previously mentioned organs and cells adds evidence to the role of H_4R as an immune modulator, since all the immune cells in their general definition except B cells express H_4R.

4.3. H_4R and macrophages

4.3.1. Expression and regulation

The successful differentiation of bone marrow cells to macrophages using L929 supernatant medium as a source of M-CSF indicates that this method is appropriate with low costs to generate inactivated macrophages *in vitro*. In order to control the concentration of M-CSF in medium recombinant M-CSF can also be used for differentiation. The generated macrophages express the main surface markers for mouse macrophages, without expression of IL-6 or TNF indicating that the generated cells are not activated. Macrophage activation can be encountered due to several factors such as contamination, cell culture medium or type of dishes. Moreover, these cells are similar to fully functional macrophages with respect to their capability of chemotaxis, phagocytosis, pro-inflammatory cytokines production, and IL-10 production as an anti-inflammatory cytokine (data not shown). The cell culture techniques and materials used especially the square dishes used for the BMDM generation are very essential factors in order to obtain functionally intact cells. Previous protocols used cell adherence as an essential step to generate BMDM, but detaching the cells without damaging them remains an important factor. In this term, the cells were sometimes generated in Teflon-coated cell culture dishes or even in Falcon® tubes and the very marginally attached cells were harvested by gently aspiring the medium [136;145]. In the method used in this work, the macrophages generated in Sterilin square Petri dishes were slightly attached to the bottom, and the gentle scraping of the cells did not cause any remarkable damage or activation effect like IL-6 production (data not shown). Unfortunately, no clear information was available about coating materials used in those dishes from the provider.

Peritoneal macrophages are the most commonly used primary mouse macrophages. In order to isolate a fair number of cells, sub-inflammation state has to

be induced prior to the cell harvest. This manipulation leads to more macrophages migrating to the inflamed site and increasing the yield of the elicited cells. Several methods were used in this respect, such as injecting PBS, thioglycolate or protease peptone into the mouse peritoneum for different lengths of time. The activation state of elicited-macrophages varies depending on the injected substances and the time. Sterile PBS injection for 14 h is considered as the least activating material, although it is known that the harvested cells are slightly activated [146]. The percentage of macrophages in the harvested cells can also differ according to the method, but in all methods the majority of the adherent cells are mouse macrophages as shown in Fig. 3.11.

Other macrophage types used in this work are macrophage cell lines RAW 264.7 and J774.1. These cells were used at the early stages of this work to screen the expression of H_4R in several cell lines. High passage numbers were avoided in RAW 264.7 cells because the cells showed some morphological abnormalities associated with low expression level of H_1 and H_4 receptors in RT-PCR (data not shown). Therefore, those cells were replaced every 8-10 weeks with a new aliquot from liquid nitrogen frozen cells.

The similar HR expression pattern in all the previous macrophage types indicates and validates the fact that mH_4R is expressed in mouse macrophages on the mRNA level. Until now no data have been reported on positive expression of H_4R in mouse macrophages, while one report in 2002 mentioned that only mouse mast cells and eosinophils express H_4R but no other immune cells [73]. This novel finding in the mouse system was confirmed by two reports about human monocytes which are the closest cells to macrophages on the differentiation level [48;49].

The regulation of mH_4R in response to different stimuli in RAW 264.7 and BMDM cells showed a similar response to IFN-γ, demonstrated by significantly up-regulation of mH_4R expression. Moreover, RAW 264.7 cells up-regulated mH_4R in response to IFN-α and TNF within 6 hours upon stimulation, whereas longer exposure to these stimuli down-regulated mH_4R. Similar results reported by Dijkstra *et al*. in 2007 revealed that human monocytes up-regulate the expression of H_4R upon IFN-γ stimulation as well as in combination with TNF [48]. *In-silico* inspection of potential transcription factors in the promoters of human and mouse H_4R gives a possible explanation of mH_4R up-regulation upon interferon stimulation. Notably, several potential binding sites of *Interferon-stimulated response element* (ISRE also

known as *Interferon regulatory factors* IRF-7) exist in both promoters. According to the same report, NFκB potential binding sites exist also in the promoter region, this can also explain the mechanism by which LPS and TNF influence the gene expression. The sequence alignment between mouse and human H_4R promoters shows in addition to the previous transcription factors, that binding sites for GATA-1, 3 and STAT-5 potentially exist in the both promoters. These transcription factors are essential in the development of haematopoietic cells (data not shown) [143].

BMDM showed in a similar manner as BMDC lower mH_4R expression than bone marrow cells. This can also indicate the similarities between both cell types since both are APC and share a long list of common functions (*e.g.* cytokine production and tissue distribution). Similar to the findings in BMDC, mH_4R expression was down-regulated upon LPS activation, indicating that LPS-activated BMDM express a very low levels of mH_4R after 24 h. Interestingly, in a report about human macrophages, Laszlo *et al.* in 2001 reported a higher HDC activity in LPS-activated macrophages, suggesting that these cells produce histamine [59]. Therefore, and similar to the BMDC speculation the down-regulation of mH_4R in response to LPS can be a physiological response to reduce the effect of the self-produced histamine on the cells.

4.3.2. Chemotaxis response

In this respect the first question to answer was to find a possible role of mH_4R in mouse macrophages. At the time being, most of the known functions of H_4R in general were induction of chemotaxis in eosinophils, mast cells and DC. Thus, chemotactic activity of BMDM in response to mH_4R stimulation was investigated. Therefore, and in order to minimize the effect of histamine on H_1 and H_2 receptors, 4MEH was used instead of histamine to activate mH_4R. As previously mentioned, 4MEH, the selective H_4R agonist, shows an agonistic activity on H_2R but with more than 100-fold higher EC_{50} value than H_4R. 4MEH shows also some activity when binding to H_1R but only in higher concentrations than H_2R [19].

BMDM migrated towards 4MEH in a dose-response manner. The curve number of migrated cells revealed a bell shape in between 1 nM and 10 µM on a logarithmic scale, with the highest peak at 100 nM. However, the curve also revealed a non-typical shape by a significant migration towards 100 µM. The fact that 4MEH is

also an H_2R agonist can explain the second peak, although in a previous report from 1975 high histamine concentrations inhibited histamine-induced chemotaxis via H_2R activation in human eosinophils [147].

Histamine-induced chemotaxis was reported in human monocytes (THP-1 clone 15 cell line) by Damaj *et al*. in 2007. The cells responded in a dose response manner to the histamine concentrations with the highest peak at 10-100 nM, without showing the second peak [49]. The inhibition of 4MEH-induced (up 1 µM) chemotaxis by pre-incubating the cells with 1 µM of JNJ 7777120, and the migration of cells towards 10 and 100 µM indicate that the second peak is mediated by another receptor than H_4R. Furthermore, blocking H_1 and H_2 receptors separately did not influence the migration towards 100 nM of 4MEH, whereas only JNJ 7777120 inhibited migration. This migration in the presence of JNJ 7777120 towards fMLP or the high concentrations of 4MEH indicated that the chemotaxis machinery was not inhibited due to cytotoxicity of this compound. Based on the previous finding, it can be concluded that mH_4R mediates a chemotactic effect in response to 4MEH. As an additional confirmation of the previous results, $H_4R^{-/-}$ BMDM did not migrate towards 100 nM of 4MEH, whereas the cells migrated in the presence of 100 µM of 4MEH. The receptor mediating the 100 µM migration remains unknown. This novel role of mH_4R in mouse macrophages revealed that H_4R is a chemotactic mediator in a variety of immune cells in both human and mouse.

4.3.3. Comparing BMDM from WT and $H_4R^{-/-}$ mice

4.3.3.1. BMDM differentiation

The first step in the comparison concerned the expression of the macrophage markers. This step was essential to examine the capability of bone marrow cells to differentiate to macrophages in the absence of mH_4R. Unexpectedly, higher numbers of $CD11b^+$ and $F4/80^+$ cells were observed in $H_4R^{-/-}$ cells indicating that these cells generated more macrophages than WT cells. The exact mechanism could not be elucidated. Notably, the percentages of macrophages slightly differed between several experiments, possibly because of the variation in M-CSF concentrations in medium. However, the fact that WT and $H_4R^{-/-}$ cells were differentiated in the same medium in each experiment revealed that the differentiation mechanism is affected by the absence of mH_4R. The difference between WT and $H_4R^{-/-}$ was lower when the

macrophage percentage was high (over 90%), whereas lower macrophage percentages in culture (around 80%) showed a clearer difference between the two mouse types. No morphological differences were observed between both types under the microscope, nor in FACS analyze when comparing cell size (forward scatter FSC) and granulation (sideward scatter SSC) (data not shown). The fact that precursor macrophages express higher HDC in response to M-CSF suggests that histamine is present during the differentiation from bone marrow cells to macrophages. These findings support the previous hypothesis about an autocrine effect of histamine through H_4R on the immune cells [59].

4.3.3.2. Phagocytosis

The previous surprising finding urged another question about the functionality of these macrophages. Surprisingly, phagocytosis as one of the main macrophage functions appeared to be affected in $H_4R^{-/-}$ BMDM. This was shown by a significantly lower capability of ingesting FITC-microbeads. This was not due to any morphological variations between the cells, since both macrophage types were similar in size and granulation levels.

In order to validate the BMDM findings, the phagocytosis had to be inspected in peritoneal macrophages from $H_4R^{-/-}$ mice. The isolation of peritoneal macrophages is always associated with non-macrophage immune cells such as neutrophils and other granulocytes up to certain levels depending on the method as mentioned before. These cells have the capability to also phagocytose the FITC-microbeads. Therefore, the role of these cells had to be excluded by staining the macrophages with anti-F4/80-labelled antibodies, and analyze the phagocytosis in the $F4/80^+$ cells only. Similar to BMDM data, the cells from $H_4R^{-/-}$ showed lower phagocytic activity, which revealed that not only the cells generated *in vitro* but also primary cells were affected by the absence of mH_4R.

The fact that *L. major* lives in macrophages, as a part of the pathophysiology of Leishmaniasis, raised the question about the phagocytic activity in this model. Therefore, BMDM from both mouse types were challenged with CFSE-labelled *L. major* promastigotes in phagocytosis. The difference was similar to the results obtained from the previous two phagocytosis models.

It was recently reported that stimulation of H_4R in human T_H2 cells and DC leads to induction of activator protein-1 (AP-1) signal transduction. This transcription factor is modulating a wide range of genes including several cytokines in the immune system such as IL-4, IL-5 and IL-13 [148-150]. As previously mentioned, H_4R stimulation leads to MAPK activation. These MAPKs induce the expression of AP-1 family transcription factors such as Fos and Jun and activate the transcriptional activity of AP-1 proteins by phosphorylation of their transcription activation domains. Moreover, AP-1 was also reported as an important transcription factor in immune cells and bone formation [151;152]. The previous point could give a hint at the mechanism in which H_4R modulates the immune response.

Surprisingly, histamine as a biological ligand of H_4R did not show any induction of phagocytic activity in BMDM, this gave rise to the hypothesis about potential self-produced histamine and its autocrine effect on the whole mechanism, which means that the cells produce the necessary amount of histamine and the additional histamine is not capable to induce phagocytosis to a higher level. To proof this point a phagocytosis assay was performed in the presence of several concentrations of JNJ 7777120. However, the results revealed that blocking mH_4R during the phagocytosis assay did not influence the BMDM phagocytic activity. This speaks against the hypothesis about any role of self-produced histamine in phagocytosis, but does not answer the question about a possible role of histamine during BMDM differentiation.

To answer this question, BMDM generated in the presence of JNJ 7777120 were compared to WT-BMDM and $H_4R^{-/-}$ BMDM. In this model the cells generated in the presence of JNJ 7777120 showed a lower phagocytic activity compared to WT-BMDM and similar to $H_4R^{-/-}$ BMDM, but the percentage of macrophages were also lower than WT-BMDM unlike $H_4R^{-/-}$ BMDM. The interpretation of these results could be that JNJ 7777120 partially inhibited bone marrow differentiation to macrophages. The exact effect of JNJ 7777120 on bone marrow differentiation has to be further investigated.

4.3.3.3. TNF, IL-6 and NO production

In order to examine other macrophage functions of $H_4R^{-/-}$ BMDM, the capability of pro-inflammatory cytokine production was examined in comparison to WT-BMDM. Therefore, IL-6 and TNF production was determined in the supernatant of LPS activated cells, and NO was measured upon LPS and IFN-γ activation. Similar to the phagocytosis results, IL-6, TNF and NO production was partially inhibited in the $H_4R^{-/-}$ BMDM. Based on these results, the effect of histamine on the production of previous parameters was examined. Similar results were observed with no direct effect of histamine on the production of IL-6, TNF and NO in BMDM. Histamine as an inducer of IL-6 production from human lung macrophages was mentioned in a single report, with no other evidence of a histamine role in macrophage activation [55].

4.3.3.5. Hypothesis to explain the H_4R effect

The mechanism by which the absence of H_4R influences macrophage functions whereas histamine did not show any effect, induced a speculation of three possible mechanisms (Fig. 4.1).

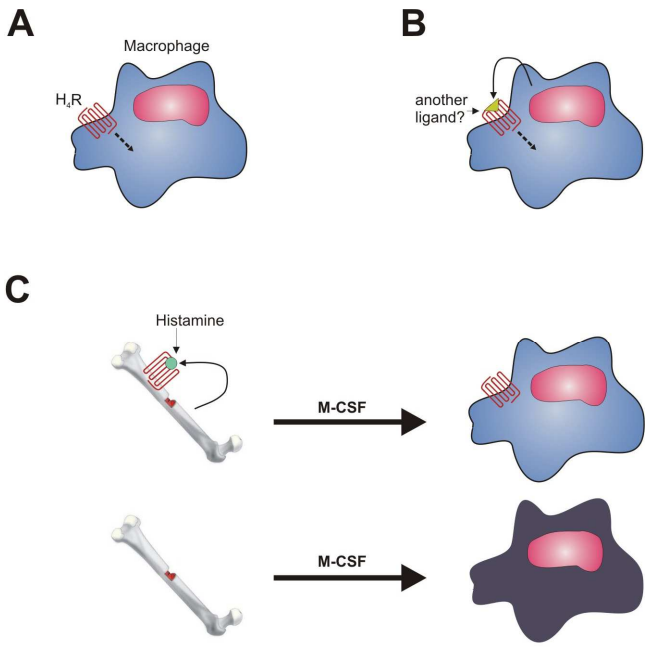

Fig. 4.1: Possible mechanisms of H_4R effect in macrophages. A: mH_4R has a constitutive activity in which histamine is not necessary to keep the basal activity. B: Another ligand than histamine is produced by macrophages and plays a role in an autocrine manner via mH_4R. C: Histamine is produced from bone marrow cells and can act as an autocrine stimulator, which is important to generate fully active macrophages.

In the first potential mechanism, the H_4R is constitutively active in the absence of histamine. Such a constitutive activity of HR has been reported in all human receptors but no clear proof of any constitutive activity in the mouse model has been obtained so far. However, based on unpublished data from a colleague (David Schnell, PhD thesis), no constitutive activity of the mH_4R was observed when the receptor activity was measured in the GTPase assay. In the second hypothesis, macrophages can produce another ligand to mH_4R *e.g.* a chemokine that can bind to the receptor and induce the functions. In this respect, the ability of CCL16 to bind to human H_4R and induce chemotaxis was reported in one publication without any further reports supporting or denying it [34;153]. However, no analogue of the human CCL16 has been documented in the mouse system up till now. The third hypothesis speculates that histamine plays a role in bone marrow differentiation to macrophages in an autocrine manner through mH_4R. This suggests that the expression of mH_4R on bone marrow cells is necessary to differentiate the cells to the normal macrophages. This hypothesis is supported by the higher expression level of mH_4R found in bone marrow cells than in macrophages. Moreover, it was reported that precursor macrophages express high level of HDC when stimulated with M-CSF, suggesting that these cells produce histamine in the presence of M-CSF [59;154;155].

4.3.4. The role of mH_4R in Leishmaniasis

In order to examine the effect of mH_4R on the immune system and validate the previous findings in macrophages, Leishmaniasis was analyzed in WT and $H_4R^{-/-}$ mice. The footpad swelling in both mouse strains showed the typical swelling pattern of C57BL/6 mice, where the highest swelling point was observed within three weeks followed by diminution of the swelling, later on the curve showed another lower peak before the footpad regained the normal size. In general, higher footpad swelling levels in $H_4R^{-/-}$ mice were observed in comparison to WT, especially within the first three weeks. This higher swelling level did not affect the development of the disease, indicating that the effect of mH_4R did not play an important role in the immunity against Leishmaniasis.

4.4. The generation of antibodies against mH_4R

With the aim of detecting the expression of mH_4R on the protein level, commercially available polyclonal antibodies were tested in western-blot analysis. The cell protein lysates used in the assay were validated by RT-PCR, and showed a positive expression of mH_4R. Surprisingly, these antibodies did not recognize any protein of the expected molecular weight of mH_4R, however some other unspecific bands were observed, indicating that no further experiments could be performed with these antibodies.

The first attempt to generate antibodies against mH_4R was performed in rabbits to generate polyclonal antibodies (data not shown). The rabbits sera as well as the purified IgG antibodies from the rabbits sera showed non-specific binding in western-blot. In another attempt, $H_4R^{-/-}$ mice were used to generate mouse anti-mH_4R. As previously mentioned, the mouse system is mainly used to generate monoclonal antibodies, because of the limited volume of serum that can be obtained from mice. The ELISA screening results revealed that the immunization was successful and both mice generated antibodies in their serum against the injected peptides. As expected, the boost increased titers in the immunized mice. Unfortunately, the mouse sera did not appear to be a good source of antibodies when tested in western-blot, because only non-specific bands were obtained when cells from WT and $H_4R^{-/-}$ mice were used. The antibodies seemed to recognize only the peptides but not the native receptor on the cells. One of the possible reasons of

the negative results is the glycosylation of the second and third extracellular domains in the native receptor, which might inhibit the antibody recognition. Another possible reason is the protein 3D structure, where the antibodies could not recognize their epitopes due to the inaccessibility. The protein lysates were treated under reductive conditions with β-meracptoethanol and dithiothreitol (DTT) separately at high temperature, which cleaves the disulphide bridges in proteins and unfolds the protein structure. The non-specificity of produced antibodies against other GPCRs is a commonly encountered problem as discussed by Michel *et al.* and Gupta *et al* [156;157]. However, generation of monoclonal antibodies using the spleens of the immunized mice could be a promising to generate a specific tool for mouse H_4R research.

Summary

Several reports have identified the H_4R as an important receptor in inflammatory mechanisms and thus, as a therapeutic target for several diseases. The focus of this work was to identify and further characterize the role of mH_4R on mouse myeloid immune cells.

A novel finding of this thesis is the expression of mH_4R in DC macrophages, and T cells ($CD4^+$, $CD8^+$) which was determined on the mRNA level. The expression was down-regulated during bone marrow differentiation to BMDC as well as to BMDM, and both cell types expressed lower mH_4R levels when stimulated by LPS, but IFN-γ seemed to be an inducer of mH_4R expression.

A novel function of mH_4R is the chemotactic effect on BMDM in response to 4MEH. This finding supported other findings from human and mouse cells. In the functional analysis, histamine was found not to have any direct effect on BMDM functions such as phagocytosis, TNF, IL-6 and NO production. Conversely, the absence of the mH_4R on macrophages revealed a partial functional defect in phagocytosis and the production of cytokine. These findings indicate a possible role of mH_4R in bone marrow differentiation to macrophages.

Based on the findings in this thesis several topics should be further investigated, and the exact role of mH_4R on myeloid cells should be analyzed on the molecular level with the advantage of the $H_4R^{-/-}$ mice.

Reference List

1. Akdis CA and Simons FE, Histamine receptors are hot in immunopharmacology. Eur.J.Pharmacol. 533: 69-76, 2006.

2. Maintz L and Novak N, Histamine and histamine intolerance. Am.J.Clin.Nutr. 85: 1185-1196, 2007.

3. Parsons ME and Ganellin CR, Histamine and its receptors. Br.J.Pharmacol. 147 Suppl 1: S127-S135, 2006.

4. Kubo Y and Nakano K, Regulation of histamine synthesis in mouse CD4+ and CD8+ T lymphocytes. Inflamm.Res. 48: 149-153, 1999.

5. Jutel M, Blaser K, and Akdis CA, The role of histamine in regulation of immune responses. Chem.Immunol.Allergy 91: 174-187, 2006.

6. Kawaguchi-Nagata K, Okamura H, Tamura T, Yamatodani A, Watanabe T, Wada H, Taguchi T, Kitamura Y, and Shoji K, Induction of histidine decarboxylase activity in the spleen of mice treated with staphylococcal enterotoxin A and demonstration of its non-mast cell origin. Biochem.Biophys.Res.Commun. 129: 187-192, 1985.

7. Schwelberger HG and Bodner E, Purification and characterization of diamine oxidase from porcine kidney and intestine. Biochim.Biophys.Acta 1340: 152-164, 1997.

8. Schwelberger HG, Hittmair A, and Kohlwein SD, Analysis of tissue and subcellular localization of mammalian diamine oxidase by confocal laser scanning fluorescence microscopy. Inflamm.Res. 47 Suppl 1: S60-S61, 1998.

9. Klocker J, Matzler SA, Huetz GN, Drasche A, Kolbitsch C, and Schwelberger HG, Expression of histamine degrading enzymes in porcine tissues. Inflamm.Res. 54 Suppl 1: S54-S57, 2005.

10. Yamauchi K, Sekizawa K, Suzuki H, Nakazawa H, Ohkawara Y, Katayose D, Ohtsu H, Tamura G, Shibahara S, Takemura M, and ., Structure and function of human histamine N-methyltransferase: critical enzyme in histamine metabolism in airway. Am.J.Physiol 267: L342-L349, 1994.

11. Kuefner MA, Schwelberger HG, Weidenhiller M, Hahn EG, and Raithel M, Both catabolic pathways of histamine via histamine-N-methyltransferase and diamine oxidase are diminished in the colonic mucosa of patients with food allergy. Inflamm.Res. 53 Suppl 1: S31-S32, 2004.

12. Raithel M, Kufner M, Ulrich P, and Hahn EG, The involvement of the histamine degradation pathway by diamine oxidase in manifest gastrointestinal allergies. Inflamm.Res. 48 Suppl 1: S75-S76, 1999.

13. Hough LB, Genomics meets histamine receptors: new subtypes, new receptors. Mol.Pharmacol. 59: 415-419, 2001.

14. Liu C, Wilson SJ, Kuei C, and Lovenberg TW, Comparison of human, mouse, rat, and guinea pig histamine H_4 receptors reveals substantial pharmacological species variation. J.Pharmacol.Exp.Ther. 299: 121-130, 2001.

15. Nakamura T, Itadani H, Hidaka Y, Ohta M, and Tanaka K, Molecular cloning and characterization of a new human histamine receptor, HH_4R. Biochem.Biophys.Res.Commun. 279: 615-620, 2000.

16. Oda T, Morikawa N, Saito Y, Masuho Y, and Matsumoto S, Molecular cloning and characterization of a novel type of histamine receptor preferentially expressed in leukocytes. J.Biol.Chem. 275: 36781-36786, 2000.

17. Jablonowski JA, Grice CA, Chai W, Dvorak CA, Venable JD, Kwok AK, Ly KS, Wei J, Baker SM, Desai PJ, Jiang W, Wilson SJ, Thurmond RL, Karlsson L, Edwards JP, Lovenberg TW, and Carruthers NI, The first potent and selective non-imidazole human histamine H_4 receptor antagonists. J.Med.Chem. 46: 3957-3960, 2003.

18. Thurmond RL, Desai PJ, Dunford PJ, Fung-Leung WP, Hofstra CL, Jiang W, Nguyen S, Riley JP, Sun S, Williams KN, Edwards JP, and Karlsson L, A potent and selective histamine H_4 receptor antagonist with anti-inflammatory properties. J.Pharmacol.Exp.Ther. 309: 404-413, 2004.

19. Lim HD, van Rijn RM, Ling P, Bakker RA, Thurmond RL, and Leurs R, Evaluation of histamine H_1-, H_2-, and H_3-receptor ligands at the human histamine H_4 receptor: identification of 4-methylhistamine as the first potent and selective H_4 receptor agonist. J.Pharmacol.Exp.Ther. 314: 1310-1321, 2005.

20. Ohki E, Suzuki M, Aoe T, Ikawa Y, Negishi E, and Ueno K, Expression of histamine H_4 receptor in synovial cells from rheumatoid arthritic patients. Biol.Pharm.Bull. 30: 2217-2220, 2007.

21. Schneider EH, Schnell D, Papa D, and Seifert R, High Constitutive Activity and a G-Protein-Independent High-Affinity State of the Human Histamine H(4)-Receptor (dagger). Biochemistry, 2009.

22. Varga C, Horvath K, Berko A, Thurmond RL, Dunford PJ, and Whittle BJ, Inhibitory effects of histamine H_4 receptor antagonists on experimental colitis in the rat. Eur.J.Pharmacol. 522: 130-138, 2005.

23. Gutzmer R, Mommert S, Gschwandtner M, Zwingmann K, Stark H, and Werfel T, The histamine H_4 receptor is functionally expressed on T(H)2 cells. J.Allergy Clin.Immunol. 123: 619-625, 2009.

24. Connelly WM, Shenton FC, Lethbridge N, Leurs R, Waldvogel HJ, Faull RL, Lees G, and Chazot PL, The histamine H_4 receptor is functionally expressed on neurons in the mammalian CNS. Br.J.Pharmacol. 157: 55-63, 2009.

25. Cowart MD, Altenbach RJ, Liu H, Hsieh GC, Drizin I, Milicic I, Miller TR, Witte DG, Wishart N, Fix-Stenzel SR, McPherson MJ, Adair RM, Wetter JM, Bettencourt BM, Marsh KC, Sullivan JP, Honore P, Esbenshade TA, and Brioni JD, Rotationally constrained 2,4-diamino-5,6-disubstituted pyrimidines: a new class of histamine H_4 receptor antagonists with improved

druglikeness and in vivo efficacy in pain and inflammation models. J.Med.Chem. 51: 6547-6557, 2008.

26. Leurs R, Chazot PL, Shenton FC, Lim HD, and de Esch IJ, Molecular and biochemical pharmacology of the histamine H_4 receptor. Br.J.Pharmacol. 157: 14-23, 2009.

27. Lim HD, Adami M, Guaita E, Werfel T, Smits RA, de Esch IJ, Bakker RA, Gutzmer R, Coruzzi G, and Leurs R, Pharmacological characterization of the new histamine H_4 receptor agonist VUF 8430. Br.J.Pharmacol. 157: 34-43, 2009.

28. Smit MJ, Leurs R, Alewijnse AE, Blauw J, Nieuw Amerongen GP, Van D, V, Roovers E, and Timmerman H, Inverse agonism of histamine H_2 antagonist accounts for upregulation of spontaneously active histamine H_2 receptors. Proc.Natl.Acad.Sci.U.S.A 93: 6802-6807, 1996.

29. Smits RA, de Esch IJ, Zuiderveld OP, Broeker J, Sansuk K, Guaita E, Coruzzi G, Adami M, Haaksma E, and Leurs R, Discovery of quinazolines as histamine H_4 receptor inverse agonists using a scaffold hopping approach. J.Med.Chem. 51: 7855-7865, 2008.

30. Smits RA, Leurs R, and de Esch IJ, Major advances in the discovery of histamine H(4) receptor ligands. Drug Discov.Today, 2009.

31. Strakhova MI, Cuff CA, Manelli AM, Carr TL, Witte DG, Baranowski JL, Vortherms TA, Miller TR, Rundell L, McPherson MJ, Adair RM, Brito AA, Bettencourt BM, Yao BB, Wetter JM, Marsh KC, Liu H, Cowart MD, Brioni JD, and Esbenshade TA, In vitro and in vivo characterization of A-940894: a potent histamine H_4 receptor antagonist with anti-inflammatory properties. Br.J.Pharmacol. 157: 44-54, 2009.

32. Zampeli E and Tiligada E, The role of histamine H_4 receptor in immune and inflammatory disorders. Br.J.Pharmacol. 157: 24-33, 2009.

33. Huang JF and Thurmond RL, The new biology of histamine receptors. Curr.Allergy Asthma Rep. 8: 21-27, 2008.

34. Thurmond RL, Gelfand EW, and Dunford PJ, The role of histamine H_1 and H_4 receptors in allergic inflammation: the search for new antihistamines. Nat.Rev.Drug Discov. 7: 41-53, 2008.

35. Seifert R and Wenzel-Seifert K, Constitutive activity of G-protein-coupled receptors: cause of disease and common property of wild-type receptors. Naunyn Schmiedebergs Arch.Pharmacol. 366: 381-416, 2002.

36. Milligan G, Bond RA, and Lee M, Inverse agonism: pharmacological curiosity or potential therapeutic strategy? Trends Pharmacol.Sci. 16: 10-13, 1995.

37. Bakker RA, Wieland K, Timmerman H, and Leurs R, Constitutive activity of the histamine H(1) receptor reveals inverse agonism of histamine H(1) receptor antagonists. Eur.J.Pharmacol. 387: R5-R7, 2000.

38. Leurs R, Church MK, and Taglialatela M, H_1-antihistamines: inverse agonism, anti-inflammatory actions and cardiac effects. Clin.Exp.Allergy 32: 489-498, 2002.

39. Morisset S, Rouleau A, Ligneau X, Gbahou F, Tardivel-Lacombe J, Stark H, Schunack W, Ganellin CR, Schwartz JC, and Arrang JM, High constitutive activity of native H_3 receptors regulates histamine neurons in brain. Nature 408: 860-864, 2000.

40. Leff P, The two-state model of receptor activation. Trends Pharmacol.Sci. 16: 89-97, 1995.

41. Roland Seifert and Thomas Wieland. G Protein-Coupled Receptors. WILEY-VCH Verlag GmbH & Co. KGaA, Weinheim. 3-527-30819-9. 2005.

42. Schneider EH and Seifert R, Histamine H(4) receptor-RGS fusion proteins expressed in Sf9 insect cells: A sensitive and reliable approach for the functional characterization of histamine H(4) receptor ligands. Biochem.Pharmacol., 2009.

43. Dy M and Schneider E, Histamine-cytokine connection in immunity and hematopoiesis. Cytokine Growth Factor Rev. 15: 393-410, 2004.

44. Zhang M, Thurmond RL, and Dunford PJ, The histamine H(4) receptor: a novel modulator of inflammatory and immune disorders. Pharmacol.Ther. 113: 594-606, 2007.

45. Zhang M, Venable JD, and Thurmond RL, The histamine H_4 receptor in autoimmune disease. Expert.Opin.Investig.Drugs 15: 1443-1452, 2006.

46. Shahid M, Walker GB, Zorn SH, and Wong EH, Asenapine: a novel psychopharmacologic agent with a unique human receptor signature. J.Psychopharmacol. 23: 65-73, 2009.

47. Triggiani M, Petraroli A, Loffredo S, Frattini A, Granata F, Morabito P, Staiano RI, Secondo A, Annunziato L, and Marone G, Differentiation of monocytes into macrophages induces the upregulation of histamine H_1 receptor. J.Allergy Clin.Immunol. 119: 472-481, 2007.

48. Dijkstra D, Leurs R, Chazot P, Shenton FC, Stark H, Werfel T, and Gutzmer R, Histamine downregulates monocyte CCL2 production through the histamine H_4 receptor. J.Allergy Clin.Immunol. 120: 300-307, 2007.

49. Damaj BB, Becerra CB, Esber HJ, Wen Y, and Maghazachi AA, Functional expression of H_4 histamine receptor in human natural killer cells, monocytes, and dendritic cells. J.Immunol. 179: 7907-7915, 2007.

50. Takahashi HK, Morichika T, Iwagaki H, Tamura R, Kubo S, Yoshino T, Mori S, Akagi T, Tanaka N, and Nishibori M, Histamine downregulates CD14 expression via H_2 receptors on human monocytes. Clin.Immunol. 108: 274-281, 2003.

51. Elenkov IJ, Webster E, Papanicolaou DA, Fleisher TA, Chrousos GP, and Wilder RL, Histamine potently suppresses human IL-12 and stimulates IL-10 production via H_2 receptors. J.Immunol. 161: 2586-2593, 1998.

52. van der Pouw Kraan TC, Snijders A, Boeije LC, de Groot ER, Alewijnse AE, Leurs R, and Aarden LA, Histamine inhibits the production of interleukin-12 through interaction with H_2 receptors. J.Clin.Invest 102: 1866-1873, 1998.

53. Dohlsten M, Kalland T, Sjogren HO, and Carlsson R, Histamine inhibits interleukin 1 production by lipopolysaccharide-stimulated human peripheral blood monocytes. Scand.J.Immunol. 27: 527-532, 1988.

54. Takahashi HK, Iwagaki H, Mori S, Yoshino T, Tanaka N, and Nishibori M, Histamine inhibits lipopolysaccharide-induced interleukin (IL)-18 production in human monocytes. Clin.Immunol. 112: 30-34, 2004.

55. Marone G, Gentile M, Petraroli A, De Rosa N, and Triggiani M, Histamine-induced activation of human lung macrophages. Int.Arch.Allergy Immunol. 124: 249-252, 2001.

56. Triggiani M, Gentile M, Secondo A, Granata F, Oriente A, Taglialatela M, Annunziato L, and Marone G, Histamine induces exocytosis and IL-6 production from human lung macrophages through interaction with H_1 receptors. J.Immunol. 166: 4083-4091, 2001.

57. Hotermans G, Bury T, and Radermecker MF, Effect of histamine on tumor necrosis factor production by human monocytes. Int.Arch.Allergy Appl.Immunol. 95: 278-281, 1991.

58. Azuma Y, Shinohara M, Wang PL, Hidaka A, and Ohura K, Histamine inhibits chemotaxis, phagocytosis, superoxide anion production, and the production of TNFalpha and IL-12 by macrophages via H_2-receptors. Int.Immunopharmacol. 1: 1867-1875, 2001.

59. Laszlo V, Rothe G, Hegyesi H, Szeberenyi JB, Orso E, Schmitz G, and Falus A, Increased histidine decarboxylase expression during in vitro monocyte maturation; a possible role of endogenously synthesised histamine in monocyte/macrophage differentiation. Inflamm.Res. 50: 428-434, 2001.

60. Handley SA, Dube PH, and Miller VL, Histamine signaling through the H(2) receptor in the Peyer's patch is important for controlling Yersinia enterocolitica infection. Proc.Natl.Acad.Sci.U.S.A 103: 9268-9273, 2006.

61. Higuchi S, Tanimoto A, Arima N, Xu H, Murata Y, Hamada T, Makishima K, and Sasaguri Y, Effects of histamine and interleukin-4 synthesized in arterial intima on phagocytosis by monocytes/macrophages in relation to atherosclerosis. FEBS Lett. 505: 217-222, 2001.

62. Sasaguri Y and Tanimoto A, Role of macrophage-derived histamine in atherosclerosis--chronic participation in the inflammatory response --. J.Atheroscler.Thromb. 11: 122-130, 2004.

63. Mazzoni A, Young HA, Spitzer JH, Visintin A, and Segal DM, Histamine regulates cytokine production in maturing dendritic cells, resulting in altered T cell polarization. J.Clin.Invest 108: 1865-1873, 2001.

64. Gutzmer R, Diestel C, Mommert S, Kother B, Stark H, Wittmann M, and Werfel T, Histamine H_4 receptor stimulation suppresses IL-12p70 production and mediates chemotaxis in human monocyte-derived dendritic cells. J.Immunol. 174: 5224-5232, 2005.

65. Amaral MM, Davio C, Ceballos A, Salamone G, Canones C, Geffner J, and Vermeulen M, Histamine improves antigen uptake and cross-presentation by dendritic cells. J.Immunol. 179: 3425-3433, 2007.

66. Baumer W, Wendorff S, Gutzmer R, Werfel T, Dijkstra D, Chazot P, Stark H, and Kietzmann M, Histamine H_4 receptors modulate dendritic cell migration through skin--immunomodulatory role of histamine. Allergy 63: 1387-1394, 2008.

67. Caron G, Delneste Y, Roelandts E, Duez C, Bonnefoy JY, Pestel J, and Jeannin P, Histamine polarizes human dendritic cells into Th2 cell-promoting effector dendritic cells. J.Immunol. 167: 3682-3686, 2001.

68. Krouwels FH, Hol BE, Lutter R, Bruinier B, Bast A, Jansen HM, and Out TA, Histamine affects interleukin-4, interleukin-5, and interferon-gamma production by human T cell clones from the airways and blood. Am.J.Respir.Cell Mol.Biol. 18: 721-730, 1998.

69. Dunford PJ, O'Donnell N, Riley JP, Williams KN, Karlsson L, and Thurmond RL, The histamine H_4 receptor mediates allergic airway inflammation by regulating the activation of CD4+ T cells. J.Immunol. 176: 7062-7070, 2006.

70. Gantner F, Sakai K, Tusche MW, Cruikshank WW, Center DM, and Bacon KB, Histamine h(4) and h(2) receptors control histamine-induced interleukin-16 release from human CD8(+) T cells. J.Pharmacol.Exp.Ther. 303: 300-307, 2002.

71. Bryce PJ, Mathias CB, Harrison KL, Watanabe T, Geha RS, and Oettgen HC, The H_1 histamine receptor regulates allergic lung responses. J.Clin.Invest 116: 1624-1632, 2006.

72. Morgan RK, McAllister B, Cross L, Green DS, Kornfeld H, Center DM, and Cruikshank WW, Histamine 4 receptor activation induces recruitment of FoxP3+ T cells and inhibits allergic asthma in a murine model. J.Immunol. 178: 8081-8089, 2007.

73. Hofstra CL, Desai PJ, Thurmond RL, and Fung-Leung WP, Histamine H_4 receptor mediates chemotaxis and calcium mobilization of mast cells. J.Pharmacol.Exp.Ther. 305: 1212-1221, 2003.

74. Ling P, Ngo K, Nguyen S, Thurmond RL, Edwards JP, Karlsson L, and Fung-Leung WP, Histamine H_4 receptor mediates eosinophil chemotaxis with cell shape change and adhesion molecule upregulation. Br.J.Pharmacol. 142: 161-171, 2004.

75. Buckland KF, Williams TJ, and Conroy DM, Histamine induces cytoskeletal changes in human eosinophils via the H(4) receptor. Br.J.Pharmacol. 140: 1117-1127, 2003.

76. Barnard R, Barnard A, Salmon G, Liu W, and Sreckovic S, Histamine-induced actin polymerization in human eosinophils: an imaging approach for histamine H_4 receptor. Cytometry A 73: 299-304, 2008.

77. Wadee AA, Anderson R, and Sher R, In vitro effects of histamine on eosinophil migration. Int.Arch.Allergy Appl.Immunol. 63: 322-329, 1980.

78. Clark RA, Sandler JA, Gallin JI, and Kaplan AP, Histamine modulation of eosinophil migration. J.Immunol. 118: 137-145, 1977.

79. Masini E, Ragazzo E, Vinci MC, Nistri S, Cinci L, Mastroianni R, Thurmond RL, and Salvemini D, A selective H_4R antagonist prevents antigen-induced asthma-like reaction and airway inflammation in guinea pigs. Inflamm.Res. 58 Suppl 1: 9-10, 2009.

80. Dunford PJ, Williams KN, Desai PJ, Karlsson L, McQueen D, and Thurmond RL, Histamine H_4 receptor antagonists are superior to traditional antihistamines in the attenuation of experimental pruritus. J.Allergy Clin.Immunol. 119: 176-183, 2007.

81. Rossbach K, Wendorff S, Sander K, Stark H, Gutzmer R, Werfel T, Kietzmann M, and Baumer W, Histamine H_4 receptor antagonism reduces hapten-induced scratching behaviour but not inflammation. Exp.Dermatol. 18: 57-63, 2009.

82. Coruzzi G, Adami M, Guaita E, de Esch IJ, and Leurs R, Antiinflammatory and antinociceptive effects of the selective histamine H_4-receptor antagonists JNJ7777120 and VUF6002 in a rat model of carrageenan-induced acute inflammation. Eur.J.Pharmacol. 563: 240-244, 2007.

83. Takahashi Y, Kagawa Y, Izawa K, Ono R, Akagi M, and Kamei C, Effect of histamine H_4 receptor antagonist on allergic rhinitis in mice. Int.Immunopharmacol. 9: 734-738, 2009.

84. Nakano Y, Takahashi Y, Ono R, Kurata Y, Kagawa Y, and Kamei C, Role of histamine H(4) receptor in allergic conjunctivitis in mice. Eur.J.Pharmacol. 608: 71-75, 2009.

85. Nathan C, Metchnikoff's Legacy in 2008. Nat.Immunol. 9: 695-698, 2008.

86. Gordon S and Taylor PR, Monocyte and macrophage heterogeneity. Nat.Rev.Immunol. 5: 953-964, 2005.

87. Geissmann F, Jung S, and Littman DR, Blood monocytes consist of two principal subsets with distinct migratory properties. Immunity. 19: 71-82, 2003.

88. Nahrendorf M, Swirski FK, Aikawa E, Stangenberg L, Wurdinger T, Figueiredo JL, Libby P, Weissleder R, and Pittet MJ, The healing myocardium sequentially mobilizes two monocyte subsets with divergent and complementary functions. J.Exp.Med. 204: 3037-3047, 2007.

89. Strauss-Ayali D, Conrad SM, and Mosser DM, Monocyte subpopulations and their differentiation patterns during infection. J.Leukoc.Biol. 82: 244-252, 2007.

90. Sunderkotter C, Nikolic T, Dillon MJ, Van Rooijen N, Stehling M, Drevets DA, and Leenen PJ, Subpopulations of mouse blood monocytes differ in maturation stage and inflammatory response. J.Immunol. 172: 4410-4417, 2004.

91. Mosser DM and Edwards JP, Exploring the full spectrum of macrophage activation. Nat.Rev.Immunol. 8: 958-969, 2008.

92. Bared SM, Buechler C, Boettcher A, Dayoub R, Sigruener A, Grandl M, Rudolph C, Dada A, and Schmitz G, Association of ABCA1 with syntaxin 13 and flotillin-1 and enhanced phagocytosis in tangier cells. Mol.Biol.Cell 15: 5399-5407, 2004.

93. Lutter D, Ugocsai P, Grandl M, Orso E, Theis F, Lang EW, and Schmitz G, Analyzing M-CSF dependent monocyte/macrophage differentiation: expression modes and meta-modes derived from an independent component analysis. BMC.Bioinformatics. 9: 100, 2008.

94. Eske K, Breitbach K, Kohler J, Wongprompitak P, and Steinmetz I, Generation of murine bone marrow derived macrophages in a standardised serum-free cell culture system. J.Immunol.Methods 342: 13-19, 2009.

95. Kono H and Rock KL, How dying cells alert the immune system to danger. Nat.Rev.Immunol. 8: 279-289, 2008.

96. Chen CJ, Kono H, Golenbock D, Reed G, Akira S, and Rock KL, Identification of a key pathway required for the sterile inflammatory response triggered by dying cells. Nat.Med. 13: 851-856, 2007.

97. Erwig LP and Henson PM, Immunological consequences of apoptotic cell phagocytosis. Am.J.Pathol. 171: 2-8, 2007.

98. O'Shea JJ and Murray PJ, Cytokine signaling modules in inflammatory responses. Immunity. 28: 477-487, 2008.

99. Gordon S, The macrophage: past, present and future. Eur.J.Immunol. 37 Suppl 1: S9-17, 2007.

100. Mackaness GB, Cellular immunity and the parasite. Adv.Exp.Med.Biol. 93: 65-73, 1977.

101. Gordon S, Alternative activation of macrophages. Nat.Rev.Immunol. 3: 23-35, 2003.

102. Brandt E, Woerly G, Younes AB, Loiseau S, and Capron M, IL-4 production by human polymorphonuclear neutrophils. J.Leukoc.Biol. 68: 125-130, 2000.

103. Fadok VA, Bratton DL, Konowal A, Freed PW, Westcott JY, and Henson PM, Macrophages that have ingested apoptotic cells in vitro inhibit proinflammatory cytokine production through autocrine/paracrine mechanisms involving TGF-beta, PGE2, and PAF. J.Clin.Invest 101: 890-898, 1998.

104. Franchimont D, Overview of the actions of glucocorticoids on the immune response: a good model to characterize new pathways of immunosuppression for new treatment strategies. Ann.N.Y.Acad.Sci. 1024: 124-137, 2004.

105. Mosser DM, The many faces of macrophage activation. J.Leukoc.Biol. 73: 209-212, 2003.

106. Hasko G, Pacher P, Deitch EA, and Vizi ES, Shaping of monocyte and macrophage function by adenosine receptors. Pharmacol.Ther. 113: 264-275, 2007.

107. Sirois J, Menard G, Moses AS, and Bissonnette EY, Importance of histamine in the cytokine network in the lung through H_2 and H_3 receptors: stimulation of IL-10 production. J.Immunol. 164: 2964-2970, 2000.

108. Lucas M, Zhang X, Prasanna V, and Mosser DM, ERK activation following macrophage FcgammaR ligation leads to chromatin modifications at the IL-10 locus. J.Immunol. 175: 469-477, 2005.

109. Aderem A and Underhill DM, Mechanisms of phagocytosis in macrophages. Annu.Rev.Immunol. 17: 593-623, 1999.

110. Desjardins M and Griffiths G, Phagocytosis: latex leads the way. Curr.Opin.Cell Biol. 15: 498-503, 2003.

111. Groves E, Dart AE, Covarelli V, and Caron E, Molecular mechanisms of phagocytic uptake in mammalian cells. Cell Mol.Life Sci. 65: 1957-1976, 2008.

112. Russell DG, Vanderven BC, Glennie S, Mwandumba H, and Heyderman RS, The macrophage marches on its phagosome: dynamic assays of phagosome function. Nat.Rev.Immunol. 9: 594-600, 2009.

113. Vachon E, Martin R, Plumb J, Kwok V, Vandivier RW, Glogauer M, Kapus A, Wang X, Chow CW, Grinstein S, and Downey GP, CD44 is a phagocytic receptor. Blood 107: 4149-4158, 2006.

114. Vachon E, Martin R, Kwok V, Cherepanov V, Chow CW, Doerschuk CM, Plumb J, Grinstein S, and Downey GP, CD44-mediated phagocytosis induces inside-out activation of complement receptor-3 in murine macrophages. Blood 110: 4492-4502, 2007.

115. Foxman EF, Campbell JJ, and Butcher EC, Multistep navigation and the combinatorial control of leukocyte chemotaxis. J.Cell Biol. 139: 1349-1360, 1997.

116. Schall TJ, Bacon K, Camp RD, Kaspari JW, and Goeddel DV, Human macrophage inflammatory protein alpha (MIP-1 alpha) and MIP-1 beta chemokines attract distinct populations of lymphocytes. J.Exp.Med. 177: 1821-1826, 1993.

117. Jin T, Zhang N, Long Y, Parent CA, and Devreotes PN, Localization of the G protein betagamma complex in living cells during chemotaxis. Science 287: 1034-1036, 2000.

118. Thelen M, Dancing to the tune of chemokines. Nat.Immunol. 2: 129-134, 2001.

119. Neptune ER, Iiri T, and Bourne HR, Galphai is not required for chemotaxis mediated by Gi-coupled receptors. J.Biol.Chem. 274: 2824-2828, 1999.

120. Hwang JI, Fraser ID, Choi S, Qin XF, and Simon MI, Analysis of C5a-mediated chemotaxis by lentiviral delivery of small interfering RNA. Proc.Natl.Acad.Sci.U.S.A 101: 488-493, 2004.

121. Heit B, Robbins SM, Downey CM, Guan Z, Colarusso P, Miller BJ, Jirik FR, and Kubes P, PTEN functions to 'prioritize' chemotactic cues and prevent 'distraction' in migrating neutrophils. Nat.Immunol. 9: 743-752, 2008.

122. Shortman K and Liu YJ, Mouse and human dendritic cell subtypes. Nat.Rev.Immunol. 2: 151-161, 2002.

123. Shortman K and Caux C, Dendritic cell development: multiple pathways to nature's adjuvants. Stem Cells 15: 409-419, 1997.

124. Kamath AT, Pooley J, O'Keeffe MA, Vremec D, Zhan Y, Lew AM, D'Amico A, Wu L, Tough DF, and Shortman K, The development, maturation, and turnover rate of mouse spleen dendritic cell populations. J.Immunol. 165: 6762-6770, 2000.

125. Shortman K and Naik SH, Steady-state and inflammatory dendritic-cell development. Nat.Rev.Immunol. 7: 19-30, 2007.

126. Naderer T and McConville MJ, The Leishmania-macrophage interaction: a metabolic perspective. Cell Microbiol. 10: 301-308, 2008.

127. van Zandbergen G, Bollinger A, Wenzel A, Kamhawi S, Voll R, Klinger M, Muller A, Holscher C, Herrmann M, Sacks D, Solbach W, and Laskay T, Leishmania disease development depends on the presence of apoptotic promastigotes in the virulent inoculum. Proc.Natl.Acad.Sci.U.S.A 103: 13837-13842, 2006.

128. van Zandbergen G, Klinger M, Mueller A, Dannenberg S, Gebert A, Solbach W, and Laskay T, Cutting edge: neutrophil granulocyte serves as a vector for Leishmania entry into macrophages. J.Immunol. 173: 6521-6525, 2004.

129. Reiner SL and Locksley RM, The regulation of immunity to Leishmania major. Annu.Rev.Immunol. 13: 151-177, 1995.

130. Stenger S, Thuring H, Rollinghoff M, and Bogdan C, Tissue expression of inducible nitric oxide synthase is closely associated with resistance to Leishmania major. J.Exp.Med. 180: 783-793, 1994.

131. Weiss DS, Raupach B, Takeda K, Akira S, and Zychlinsky A, Toll-like receptors are temporally involved in host defense. J.Immunol. 172: 4463-4469, 2004.

132. Rehli M, Sulzbacher S, Pape S, Ravasi T, Wells CA, Heinz S, Sollner L, El Chartouni C, Krause SW, Steingrimsson E, Hume DA, and Andreesen R, Transcription factor Tfec contributes to the IL-4-inducible expression of a small group of genes in mouse macrophages including the granulocyte colony-stimulating factor receptor. J.Immunol. 174: 7111-7122, 2005.

133. Stockinger S, Kastner R, Kernbauer E, Pilz A, Westermayer S, Reutterer B, Soulat D, Stengl G, Vogl C, Frenz T, Waibler Z, Taniguchi T, Rulicke T, Kalinke U, Muller M, and Decker T, Characterization of the interferon-producing cell in mice infected with Listeria monocytogenes. PLoS.Pathog. 5: e1000355, 2009.

134. Bookout AL and Mangelsdorf DJ, Quantitative real-time PCR protocol for analysis of nuclear receptor signaling pathways. Nucl.Recept.Signal. 1: e012, 2003.

135. Notley CA, Inglis JJ, Alzabin S, McCann FE, McNamee KE, and Williams RO, Blockade of tumor necrosis factor in collagen-induced arthritis reveals a novel immunoregulatory pathway for Th1 and Th17 cells. J.Exp.Med. 205: 2491-2497, 2008.

136. Falk W, Tomisawa S, Klimetzek V, and Meltzer MS, Chemotactic activity of bone marrow-derived macrophages changes with time in culture. Infect.Immun. 33: 629-631, 1981.

137. Song DH, Kang JH, Lee GS, Jeung EB, and Yang MP, Upregulation of tumor necrosis factor-alpha expression by trans10-cis12 conjugated linoleic acid enhances phagocytosis of RAW macrophages via a peroxisome proliferator-activated receptor gamma-dependent pathway. Cytokine 37: 227-235, 2007.

138. Pavlinkova G, Yanagawa Y, Kikuchi K, Iwabuchi K, and Onoe K, Effects of histamine on functional maturation of dendritic cells. Immunobiology 207: 315-325, 2003.

139. Idzko M, la Sala A, Ferrari D, Panther E, Herouy Y, Dichmann S, Mockenhaupt M, Di Virgilio F, Girolomoni G, and Norgauer J, Expression and function of histamine receptors in human monocyte-derived dendritic cells. J.Allergy Clin.Immunol. 109: 839-846, 2002.

140. Szeberenyi JB, Pallinger E, Zsinko M, Pos Z, Rothe G, Orso E, Szeberenyi S, Schmitz G, Falus A, and Laszlo V, Inhibition of effects of endogenously synthesized histamine disturbs in vitro human dendritic cell differentiation. Immunol.Lett. 76: 175-182, 2001.

141. Szeberenyi JB, Laszlo V, Pallinger E, Orso E, Rothe G, Schmitz G, and Falus A, Intracellular histamine content increases during in vitro dendritic cell differentiation. Inflamm.Res. 50 Suppl 2: S112-S113, 2001.

142. Morse KL, Behan J, Laz TM, West RE, Jr., Greenfeder SA, Anthes JC, Umland S, Wan Y, Hipkin RW, Gonsiorek W, Shin N, Gustafson EL, Qiao X, Wang S, Hedrick JA, Greene J, Bayne M, and Monsma FJ, Jr., Cloning and characterization of a novel human histamine receptor. J.Pharmacol.Exp.Ther. 296: 1058-1066, 2001.

143. Coge F, Guenin SP, Rique H, Boutin JA, and Galizzi JP, Structure and expression of the human histamine H_4-receptor gene. Biochem.Biophys.Res.Commun. 284: 301-309, 2001.

144. Aoi R, Nakashima I, Kitamura Y, Asai H, and Nakano K, Histamine synthesis by mouse T lymphocytes through induced histidine decarboxylase. Immunology 66: 219-223, 1989.

145. Fadok VA, Savill JS, Haslett C, Bratton DL, Doherty DE, Campbell PA, and Henson PM, Different populations of macrophages use either the vitronectin receptor or the

phosphatidylserine receptor to recognize and remove apoptotic cells. J.Immunol. 149: 4029-4035, 1992.

146. Current Protocols In Immunology. Supplement 11 CPI. 2006. John Wiley & Sons, Inc.

147. Clark RA, Gallin JI, and Kaplan AP, The selective eosinophil chemotactic activity of histamine. J.Exp.Med. 142: 1462-1476, 1975.

148. Faith A, Richards DF, Verhoef A, Lamb JR, Lee TH, and Hawrylowicz CM, Impaired secretion of interleukin-4 and interleukin-13 by allergen-specific T cells correlates with defective nuclear expression of NF-AT2 and jun B: relevance to immunotherapy. Clin.Exp.Allergy 33: 1209-1215, 2003.

149. Nakamura Y and Hoshino M, TH2 cytokines and associated transcription factors as therapeutic targets in asthma. Curr.Drug Targets.Inflamm.Allergy 4: 267-270, 2005.

150. Hartenstein B, Teurich S, Hess J, Schenkel J, Schorpp-Kistner M, and Angel P, Th2 cell-specific cytokine expression and allergen-induced airway inflammation depend on JunB. EMBO J. 21: 6321-6329, 2002.

151. Hu X, Chen J, Wang L, and Ivashkiv LB, Crosstalk among Jak-STAT, Toll-like receptor, and ITAM-dependent pathways in macrophage activation. J.Leukoc.Biol. 82: 237-243, 2007.

152. Wagner EF and Eferl R, Fos/AP-1 proteins in bone and the immune system. Immunol.Rev. 208: 126-140, 2005.

153. Nakayama T, Kato Y, Hieshima K, Nagakubo D, Kunori Y, Fujisawa T, and Yoshie O, Liver-expressed chemokine/CC chemokine ligand 16 attracts eosinophils by interacting with histamine H_4 receptor. J.Immunol. 173: 2078-2083, 2004.

154. Schneider E, Rolli-Derkinderen M, Arock M, and Dy M, Trends in histamine research: new functions during immune responses and hematopoiesis. Trends Immunol. 23: 255-263, 2002.

155. Laszlo V, Stohr J, Hegyesi H, Rothe G, Orso E, Falus A, and Schmitz G, Increase of histidine decarboxylase in human monocytes during macrophage colony stimulating factor induced in vitro phagocytic differentiation. Inflamm.Res. 48 Suppl 1: S85-S86, 1999.

156. Gupta A and Devi LA, The use of receptor-specific antibodies to study G-protein-coupled receptors. Mt.Sinai J.Med. 73: 673-681, 2006.

157. Michel MC, Wieland T, and Tsujimoto G, How reliable are G-protein-coupled receptor antibodies? Naunyn Schmiedebergs Arch.Pharmacol. 379: 385-388, 2009.